Search for supersymmetric particles in hadron-hadron collisions

Sally Dawson
Fermi National Accelerator Laboratory, Batavia, Illinois 60510
and Lawrence Berkeley Laboratory, Berkeley, California 94720

E. Eichten and C. Quigg
Fermi National Accelerator Laboratory, Batavia, Illinois 60510
(Received 9 April 1984; revised manuscript received 21 November 1984)

Elementary cross sections for the production of supersymmetric partners of the known constituents and gauge bosons in collisions of quarks and gluons are calculated in tree approximation. Standard renormalization-group-improved parton-model methods are then used to estimate differential and integrated production cross sections in proton-proton and proton-antiproton collisions. For completeness, some analogous results are presented for electron-positron collisions. Decay modes, experimental signatures, and bounds on masses of supersymmetric partners are surveyed, and prospects for future searches are discussed.

I. INTRODUCTION

The fermion-boson connection known as supersymmetry[1-3] is a far-reaching idea in search of a physical application. In favor of its utility in particle physics stand the evident appeal of linking apparently distinct classes of particles and the widely held conviction that Nature should make use of a fundamental symmetry which can be given a mathematically elegant expression. Moreover, it is easy to identify specific theoretical problems to which supersymmetry might provide solutions.

Although the current paradigm of gauge theories and unification of forces is satisfying in its simplicity and scope, the arbitrariness of the standard model suggests its incompleteness.[4] According to our present understanding, different classes of particles stand on quite different footings in the theory. The gauge bosons are completely specified by the local gauge symmetry. The spin-$\frac{1}{2}$ fermions provide a means toward recognizing the gauge group, but their number and transformation properties are unspecified. The scalars which are introduced to accomplish spontaneous symmetry breaking are constrained only by the general requirement of local gauge invariance. Because the Higgs sector has not yet been thoroughly mapped by experiments, it offers the greatest opportunity for unrestrained model building. It is natural to hope that supersymmetry might reduce or even eliminate the freedom surrounding the fermions and scalars by linking the spinors to the vectors and the scalars to the spinors.

In addition to the arbitrariness of Higgs and fermion representations, the standard model suffers from a multiplicity of apparently free parameters. Leaving aside parameters of the nonperturbative vacuum, these number no less than 18 in the $SU(3)_{color} \otimes SU(2)_L \otimes U(1)_Y$ model and a comparable count in the minimal unified theory based on SU(5). One might wish that an ultimate theory would prescribe the world as we find it, without adjustable parameters. The ambitious supergravity theories make progress in this direction, but the problem remains open.

The Higgs sector of the standard model suffers in addition from a naturalness problem. The origin of the hierarchy of symmetry-breaking scales essential to electronuclear unification is not understood. To maintain the widely separated scales of the $SU(5) \rightarrow SU(3)_c \otimes SU(2)_L \otimes U(1)_Y$ breakdown at 10^{14} GeV and the $SU(2)_L \otimes U(1)_Y \rightarrow U(1)_{EM}$ breakdown at 10^3 GeV requires exceedingly delicate tuning of parameters in the bare Higgs potential which can only be described as contrived. Supersymmetry stabilizes the Higgs-boson masses and couplings against perturbative corrections and thus reduces the sensitivity to heavier scales.

The divergence problems that attend straightforward attempts to quantize gravity are well known.[5] The local gauge theory based upon supersymmetry includes Einstein's gravitation.[6,3] In supergravity, as the resulting theories are known, many of the divergence problems are eliminated so that a finite quantum theory of the gravitational force may be in prospect. Whether this will entail a "superunification" of all the known interactions remains to be seen.

These open issues are representative of the incentives for building theories that incorporate global or local supersymmetry. One may even go so far as to assert that supersymmetry provides the only natural framework for the formulation of spontaneously broken gauge theories with elementary scalars and for the incorporation of gravity into particle physics.

In any such theory, every particle is related to a supersymmetric partner which differs by $\frac{1}{2}$ unit of spin and otherwise carries identical quantum numbers. Among the known particles there are no satisfactory candidates for pairs related by supersymmetry. Consequently we must anticipate doubling the spectrum by associating to every known particle a new superpartner. If supersymmetry were exact, each particle would be degenerate in mass with its superpartner. This is plainly not the case. For theories in which supersymmetry is broken, the mass degeneracy is lifted. The masses acquired by the super-

partners are highly model-dependent. However, if supersymmetry is to contribute to a resolution of the hierarchy problem, supersymmetry should itself be unbroken above the electroweak scale. This suggests that the low-energy artifacts of supersymmetry, including the superpartners, should occur on a scale of ~ 1 TeV or below.

Because any evidence for the validity of supersymmetry would profoundly influence the theoretical outlook, it is important to make a thorough search for superpartners. None has yet been found. However, some useful bounds on superpartner masses have been derived from studies of electron-positron annihilations, from hadronic beam-dump experiments, and from cosmological constraints. In addition, projections have been made for the production rates of the superpartners of the quark and gluon in high-energy collisions.

Because of the uncertainty of theoretical expectations for superparticle masses, we believe it worthwhile to search for all of the expected superpartners. To this end we have calculated the cross sections for hadronic production of all the new particles that appear in a minimal supersymmetric theory, except for those explicitly associated with the Higgs sector. The elementary vertices which occur in these processes are completely determined by the supersymmetry of the Lagrangian. As a consequence, the calculations can be done in generality and will apply, with appropriate mass assignments, to any specific model. Our new results are of value in interpreting existing data, in preparing new experimental searches, and in assessing the capabilities of future accelerators.

Before describing the organization of this article, it is appropriate to acknowledge some of the topics we omit. Insofar as possible, we avoid any mention of and reliance upon specific models for the breaking of supersymmetry. We have thus set aside many questions dealing with the Higgs sector, including the existence and role of the Nambu-Goldstone fermion associated with spontaneous supersymmetry breaking, and relegated the mixing between the fermionic partners of Higgs bosons and those of the $W^\pm$, γ, and Z^0 to an appendix. We have not dealt with the search for superpartners in decays of $W^\pm$ and Z^0. This problem has already received some attention in the literature,[7] and will assume growing importance as the sample of intermediate bosons available for study increases and as the commissioning of Z^0 factories approaches.

The body of this paper is organized as follows. In Sec. II, we review expectations for the minimal spectrum in a supersymmetric theory and for the interactions of superpartners. Using this information, we enumerate possible decay patterns of the superpartners and examine the ensuing constraints on masses. Section III is devoted to the presentation of our results on elementary cross sections for superpartner production in collisions of hadron constituents. Some related results pertaining to electron-positron collisions are obtained as byproducts. These are presented in Appendix A. Numerical results for superpartner production cross sections in hadron-hadron collisions occupy Sec. IV. There we discuss the uncertainties associated with parton distribution functions and consider the prospects for superpartner searches in both fixed-

target and colliding-beam environments. The complications of mixing among spin-$\frac{1}{2}$ superpartners are treated in Appendix B. Summary remarks and general comments on search strategies occupy Sec. V.

II. SUPERPARTNERS AND THEIR INTERACTIONS

In this section we present the general framework of our analysis and enumerate the particles which will be of interest in this work. The class of models we shall examine is the simplest possible supersymmetric extension of the standard $SU(3)_c \otimes SU(2)_L \otimes U(1)_Y$ model of the strong, weak, and electromagnetic interactions. To every known quark or lepton we associate a new scalar superpartner to form a chiral supermultiplet. Similarly, we group a gauge fermion ("gaugino") with each of the gauge bosons of the standard model to form a vector supermultiplet. The couplings in the Lagrangian are then completely specified by the gauge symmetry and the supersymmetry algebra.[3] In anticipation of our later need for Feynman rules, we give below all the relevant portions of the minimal supersymmetric Lagrangian. The bulk of this section is devoted to a discussion of the existing experimental limits on the conjectured supersymmetric partners of the known quarks, leptons, and gauge bosons.

A. General attributes of a supersymmetric model

It is convenient to represent the quarks and leptons by left- and right-handed two-component spinors $\psi_{\chi fg}$, where $\chi = L, R$ is a chirality index, f is a generalized flavor index, and g is a generation index (when required). The scalar partners of these ordinary fermions are denoted by $\phi_{\chi fg}$. The gauge fields are the photon A_μ, the gluons G^a_μ, and the weak bosons $W^\pm_\mu$ and Z_μ, which are paired with the Majorana spinors ψ_A, ψ_G, $\psi_{W^\pm}$, and ψ_Z, respectively.

A large class of renormalizable theories in which supersymmetry is respected at low energies naturally possess a global $U(1)$ invariance, usually called R invariance.[8,2] In such theories there is, in addition to the standard quantum numbers, a new fermionic quantum number R associated with the $U(1)$ symmetry. The quantum-number assignments for the conventional particles and their supersymmetric partners are given in Table I.

We make no assumptions about the nature of the supersymmetry breaking or the Higgs structure of the theory. In any supersymmetric theory at least two scalar doublets are required to give masses to the fermions with weak isospin of both $I_3 = \pm \frac{1}{2}$ (Ref. 9). There will necessarily be charged physical scalars, as well as the familiar neutral Higgs boson. This means that mixing may occur between gauge fermions and the supersymmetric partners of the Higgs bosons (Higgs fermions).[10] In interpreting our results in terms of a specific model, it may be necessary to introduce appropriate mixing angles, and to incorporate the mechanisms for Higgs-fermion production explicitly. This is done explicitly in Appendix B.

In a large class of models, a massless Goldstone fermion $\psi_\mathscr{G}$ appears when the supersymmetry is broken. Although we do not calculate production cross sections for the Goldstone fermion it does appear as a decay product

TABLE I. Supersymmetric partners of $SU(3)_c \otimes SU(2)_L \otimes U(1)_Y$ particles.

Particle	Spin	Color	Charge	R number
g gluon G_μ^a	1	8	0	0
$\tilde{g}$ gluino ψ_G^a	$\frac{1}{2}$	8	0	$\lvert 1 \rvert$
γ photon A_μ	1	0	0	0
$\tilde{\gamma}$ photino ψ_A	$\frac{1}{2}$	0	0	$\lvert 1 \rvert$
$W^\pm, Z^0$ intermediate bosons $W_\mu^\pm, Z_\mu$	1	0	$\pm 1, 0$	0
$\tilde{W}^\pm, \tilde{Z}^0$ W, Z gauginos $\psi_{W^\pm}, \psi_Z$	$\frac{1}{2}$	0	$\pm 1, 0$	$\lvert 1 \rvert$
q quark $\psi_{\chi fg}$	$\frac{1}{2}$	3	$\frac{2}{3}, -\frac{1}{3}$	0
$\tilde{q}$ scalar quark $\phi_{\chi fg}$	0	3	$\frac{2}{3}, -\frac{1}{3}$	$-\chi = \pm 1$
e electron $\psi_{\chi eg}$	$\frac{1}{2}$	0	-1	0
$\tilde{e}$ scalar electron $\phi_{\chi eg}$	0	0	-1	$-\chi = \pm 1$
ν neutrino $\psi_{L\nu g}$	$\frac{1}{2}$	0	0	0
ν scalar neutrino $\phi_{L\nu g}$	0	0	0	1
Higgs bosons H^+ H'^0 H^0 H'^-	0	0	$\pm 1, 0$	0
Higgs fermions $\tilde{H}^+$ $\tilde{H}'^0$ $\tilde{H}^0$ $\tilde{H}'^-$	$\frac{1}{2}$	0	$\pm 1, 0$	$\lvert 1 \rvert$

of other superparticles. For our purposes, the relevant couplings are those of the Goldstone fermion to a gluon or photon and the associated gauge fermion (gluino or photino). These couplings are described by the effective Lagrangian[11]

$$\mathcal{L}_{\text{eff}} = \frac{m_{\tilde{\gamma}}}{2\Lambda_{ss}^2} \bar{\psi}_{\mathcal{G}} F_{\mu\nu} \sigma^\mu \sigma^\nu \psi_A + \frac{m_{\tilde{g}}}{2\Lambda_{ss}^2} \bar{\psi}_{\mathcal{G}} H_{\mu\nu} \sigma^\mu \sigma^\nu \psi_G ,$$

(2.1)

where $m_{\tilde{\gamma}}$ and $m_{\tilde{g}}$ are the masses of the photino and

gluino, $F_{\mu\nu}$ and $H_{\mu\nu}$ are the electromagnetic and chromomagnetic field-strength tensors, Λ_{ss} is the scale at which supersymmetry is broken, and σ^μ is a 2×2 Pauli matrix, with

$$\sigma^0 = \begin{bmatrix} +1 & 0 \\ 0 & +1 \end{bmatrix} .$$

(2.2)

More central to our interests are the interactions between the chiral and vector superfields. The trilinear couplings are

$$\mathcal{L}_{\text{int}}[A] = \sum_{f=\text{quark and lepton flavors}} e\{e_f A^\mu [\bar{\psi}_{Lf} \bar{\sigma}_\mu \psi_{Lf} + \psi_{Rf} \sigma_\mu \bar{\psi}_{Rf}] + ie_f A^\mu [\phi_{Lf}^* \partial_\mu \phi_{Lf} - (\partial_\mu \phi_{Lf}^*)\phi_{Lf} + \phi_{Rf}^* \partial_\mu \phi_{Rf} - (\partial_\mu \phi_{Rf}^*)\phi_{Rf}]$$

$$- ie_f \sqrt{2} [\bar{\psi}_A \phi_{Lf} \bar{\psi}_{Lf} - \psi_A \phi_{Lf}^* \psi_{Lf} + \bar{\psi}_A \phi_{Rf} \bar{\psi}_{Rf} - \psi_A \phi_{Rf}^* \psi_{Rf}]\}$$

(2.3)

and

$$\mathcal{L}_{\text{int}}[G] = \sum_{f=\text{quark flavors}} \{g_s G^{a\mu} [\bar{\psi}_{Lf} \bar{\sigma}_\mu T^a \psi_{Lf} + \psi_{Rf} \sigma_\mu T^{a*} \bar{\psi}_{Rf}]$$

$$+ ig_s G^{a\mu} [\phi_{Lf}^* T^a \partial_\mu \phi_{Lf} - (\partial_\mu \phi_{Lf}^*) T^a \phi_{Lf} + \phi_{Rf}^* T^{a*} \partial_\mu \phi_{Rf} - (\partial_\mu \phi_{Rf}^*) T^{a*} \phi_{Rf}]$$

$$- ig_s \sqrt{2} [\bar{\psi}_G^a \phi_{Lf} T^a \bar{\psi}_{Lf} - \psi_G^a \phi_{Lf}^* T^a \psi_{Lf} + \bar{\psi}_G^a \phi_{Rf} T^{a*} \bar{\psi}_{Rf} - \psi_G^a \phi_{Rf}^* T^{a*} \psi_{Rf}]\} ,$$

(2.4)

where e_f is the electric charge of fermion f in units of the proton charge e and g_s is the strong (color) coupling constant. The SU(3) generator $T^a = \frac{1}{2}\lambda^a$, where λ^a is a Gell-Mann matrix with color index $a = 1, 2, \ldots, 8$. The conjugate Pauli matrix $\bar{\sigma}_\mu$ is given by

$$\bar{\sigma}^{\mu ij} = \epsilon^{ik} \epsilon^{jl} \sigma_{lk}^\mu ,$$

(2.5)

where the antisymmetric tensor ϵ^{ij} takes on the values

$$\epsilon^{12} = \epsilon_{21} = 1 ,$$

$$\epsilon^{21} = \epsilon_{12} = -1 ,$$

(2.6)

$$\epsilon_{11} = \epsilon_{22} = 0 .$$

The effective Lagrangian for the weak interactions requires more notation. We write the charge $\frac{2}{3}$ and $-\frac{1}{3}$

quarks as $\psi_{\chi ug}$ and $\psi_{\chi dg}$, respectively, and denote the leptons by $\psi_{\chi vg}$ and $\psi_{\chi eg}$. An analogous notation, $\phi_{\chi fg}$, is used for their scalar partners, which we call scalar quarks and scalar leptons. Mixing among the n_g quark and scalar-quark generations is described by a $2n_g \times 2n_g$ extended Cabibbo-Kobayashi-Maskawa matrix,

$$Q = \begin{bmatrix} U & V \\ V' & \hat{U} \end{bmatrix} \qquad (2.7)$$

built up of four unitary $n_g \times n_g$ matrices. These are the standard quark mixing matrix U, a corresponding scalar-quark mixing matrix $\hat{U}$, and two matrices V and V' describing the quark—scalar-quark couplings.

Intergeneration mixing may also arise, in principle, in the lepton sector. We write the lepton—scalar-lepton mixing matrix in terms of $n_g \times n_g$ unitary matrices as

$$L = \begin{bmatrix} M & N \\ N' & \hat{M} \end{bmatrix} . \qquad (2.8)$$

On current evidence, there is no lepton mixing so that the matrix M can be replaced by the identity. All the new mixing matrices $(\hat{U}, V, V', \hat{M}, N, N')$ are *a priori* completely unknown. In particular, there is no general theoretical reason to expect any of the elements to be small.

The effective charged-current weak-interaction Lagrangian is

$$\mathcal{L}_{int}[W] = \sum_{g,g'} \left[\frac{g_W}{\sqrt{2}} W^{+\mu} \overline{\psi}_{Lug} \overline{\sigma}_\mu U_{gg'} \psi_{Ldg'} + \frac{ig_W}{\sqrt{2}} W^{+\mu} [\phi^*_{Lug} \hat{U}_{gg'} \partial_\mu \phi_{Ldg'} - (\partial_\mu \phi^*_{Lug}) \hat{U}_{gg'} \phi_{Ldg'}] \right.$$

$$- ig_W [\overline{\psi}_{W+} \phi_{Lug} V'^*_{gg'} \overline{\psi}_{Ldg'} - \overline{\psi}_{W-} \phi_{Ldg} V_{g'g} \overline{\psi}_{Lug'}] + \frac{g_W}{\sqrt{2}} W^{+\mu} \overline{\psi}_{Lvg} \overline{\sigma}_\mu M_{gg'} \psi_{Leg'}$$

$$+ \frac{ig_W}{\sqrt{2}} W^{+\mu} [\phi^*_{Lvg} \hat{M}_{gg'} \partial_\mu \phi_{Leg'} - (\partial_\mu \phi^*_{Lvg}) \hat{M}_{gg'} \phi_{Leg'}]$$

$$\left. - ig_W [\overline{\psi}_{W+} \phi_{Lvg} N'^*_{gg'} \overline{\psi}_{Leg'} - \overline{\psi}_{W-} \phi_{Leg} N_{g'g} \overline{\psi}_{Lvg'}] \right] + \text{H.c.} , \qquad (2.9)$$

while the neutral-current Lagrangian is[7]

$$\mathcal{L}_{int}[Z] = \sum_{f = \text{quark and lepton flavors}} \left[\frac{g_W}{2\cos\theta_W} Z^\mu [L_f \overline{\psi}_{Lf} \overline{\sigma}_\mu \psi_{Lf} + R_f \psi_{Rf} \sigma_\mu \overline{\psi}_{Rf}] \right.$$

$$+ \frac{ig_W}{2\cos\theta_W} Z^\mu \{ L_f [\phi^*_{Lf} \partial_\mu \phi_{Lf} - (\partial_\mu \phi^*_{Lf}) \phi_{Lf}] + R_f [\phi^*_{Rf} \partial_\mu \phi_{Rf} - (\partial_\mu \phi^*_{Rf}) \phi_{Rf}] \}$$

$$\left. - \frac{ig_W}{\cos\theta_W \sqrt{2}} \{ L_f [\overline{\psi}_Z \phi_{Lf} \overline{\psi}_{Lf} - \psi_Z \phi^*_{Lf} \psi_{Lf}] + R_f [\overline{\psi}_Z \phi_{Rf} \overline{\psi}_{Rf} - \psi_Z \phi^*_{Rf} \psi_{Rf}] \} \right] . \qquad (2.10)$$

Here the weak coupling constant is

$$g_W = e / \sin\theta_W , \qquad (2.11a)$$

where θ_W is the weak mixing angle, and the neutral-current parameters are

$$L_f = \tau_f^{(3)} - 2e_f \sin^2\theta_W , \quad R_f = -2e_f \sin^2\theta_W , \qquad (2.11b)$$

where $\tau_f^{(3)}$ is twice the (left-handed) weak isospin I_3 of fermion f.

The quartic couplings of two gauge bosons and two scalars are given by

$$\mathcal{L}_{quartic} = \sum_{f = \text{quark flavors}} \left[\left\{ \phi^*_{Lf} \left[g_s^2 T^a T^b G^a_\mu G^{b\mu} + 2g_s T^a G^a_\mu \left[ee_f A^\mu + \frac{g_W L_f Z^\mu}{2\cos\theta_W} \right] \right] \phi_{Lf} \right\} + \{L \rightarrow R\} \right]$$

$$+ \sum_{f = \text{quark and lepton flavors}} \left[\left\{ \left[\phi^*_{Lf} \left[ee_f A^\mu + \frac{g_W L_f Z^\mu}{2\cos\theta_W} \right]^2 \phi_{Lf} \right] + [L \rightarrow R] \right\} + (g_W^2/2)\phi^*_{Lf} W^+_\mu W^{-\mu} \phi_{Lf} \right]$$

$$+ \sum_{gg'} (g_W/\sqrt{2}) \left\{ \left[\phi^*_{Lug} \left[\frac{eA^\mu}{3} + \frac{g_W(L_u + L_d)Z^\mu}{2\cos\theta_W} + 2g_s G^{a\mu} T^a \right] \hat{U}_{gg'} \phi_{Ldg'} \right. \right.$$

$$\left. \left. + \phi^*_{Lvg} \left[-eA^\mu + \frac{g_W(L_v + L_l)Z^\mu}{2\cos\theta_W} \right] \hat{M}_{gg'} \phi_{Llg'} \right] W^+_\mu + \text{H.c.} \right\} . \qquad (2.12)$$

The kinetic interaction terms for the vector superfields give rise to couplings between the gauge fermions and gauge bosons. The relevant portion of the effective Lagrangian is

$$\mathcal{L}_{\text{eff}}(\text{kinetic}) = e\,(A_\mu + Z_\mu \cot\theta_W)(\bar{\psi}_{W+}\bar{\sigma}^\mu\psi_{W+} - \bar{\psi}_{W-}\bar{\sigma}^\mu\psi_{W-})$$
$$- e\{W_\mu^+[\bar{\psi}_{W+}\bar{\sigma}^\mu(\psi_A + \psi_Z\cot\theta_W) - (\bar{\psi}_A + \bar{\psi}_Z\cot\theta_W)\bar{\sigma}^\mu\psi_{W-}] + \text{H.c.}\} - ig_s f_{abc} G_\mu^a(\bar{\psi}_{G_b}\bar{\sigma}^\mu\psi_{G_c})\ . \qquad (2.13)$$

Although the interactions of superpartners with ordinary matter and with gauge bosons are completely defined by the supersymmetry, the mass spectrum of the superpartners is not similarly specified. Indeed, the masses of the superparticles are extremely model-dependent and many different mass hierarchies are allowed in various theoretical schemes. In the absence of a compelling model, it is necessary to turn to experiment for restrictions on the spectrum. This we now do at some length.

B. Experimental constraints on the spectrum of superpartners

We now consider in turn the experimental bounds on the masses of the minimal set of superpartners. Although we shall not rely on any specific model, this does not mean that all the results are in a strict sense model-independent. In most cases it is necessary to entertain several different possibilities for the decay of a superparticle. We state carefully the assumptions upon which each limit depends, and caution the reader that in the present state of model building, few categorical statements are reliable.

1. Photinos

At the moment, the most restrictive bounds on the mass of the supersymmetric partner of the photon are derived from astrophysical arguments. Three cases must be considered.

(a) The photino is the lightest superparticle, with a mass less than 1 MeV/c^2, the scale set by the decoupling temperature of weakly interacting particles. This is the favored case in many models in which supersymmetry is broken spontaneously.[12]

(b) The photino is the lightest superparticle, but its mass exceeds 1 MeV/c^2. This occurs naturally in models in which the photino acquires a mass through radiative corrections.[13]

(c) The photino decays into a photon and a Goldstone fermion. Although a light Goldstone fermion arises when global supersymmetry is spontaneously broken, the Goldstone fermion becomes the spinor component of a massive gravitino in supergravity models.[14]

Scenario (a) was first considered[15] for the case of light relic neutrinos. A limit on the photino mass follows from the observed bounds on the cosmological mass density. As the early Universe expanded and cooled, such light photinos would have survived without annihilation. Their contribution to the present mass density of the Universe is

$$\rho_{\tilde{\gamma}} = \tfrac{3}{22} g_{\tilde{\gamma}} m_{\tilde{\gamma}} n_\gamma\ , \qquad (2.14)$$

where $g_{\tilde{\gamma}} = 2$ is the effective number of photino degrees of freedom, $m_{\tilde{\gamma}}$ is the photino mass, and the present number density of photons in the Universe is

$$n_\gamma \approx 400\ \text{cm}^{-3} \qquad (2.15)$$

for the 2.7-K cosmic microwave background. This implies that

$$\rho_{\tilde{\gamma}} \approx 109 m_{\tilde{\gamma}}\ \text{cm}^{-3}\ . \qquad (2.16)$$

What is believed[16] to be a generous upper limit on the current mass density of the Universe is the closure density

$$\rho_{\text{crit}} = 3H_0^2/8\pi G_N\ , \qquad (2.17)$$

where the gravitational constant is

$$G_N = 1.19 \times 10^{-40}(\text{cm}^3/\text{sec}^2)/(\text{eV}/c^2) \qquad (2.18)$$

and the Hubble constant is known within a factor of two as

$$H_0 = (1.8 - 3.2) \times 10^{-18}\ \text{sec}^{-1}\ , \qquad (2.19)$$

whereupon

$$\rho_{\text{crit}} = (3.2 - 10.3)\ (\text{keV}/c^2)\ \text{cm}^{-3}\ . \qquad (2.20)$$

The requirement that $\rho_{\tilde{\gamma}} < \rho_{\text{crit}}$ then leads at once to the bound

$$m_{\tilde{\gamma}} < (32 - 94)\ \text{eV}/c^2 \lesssim 100\ \text{eV}/c^2\ . \qquad (2.21)$$

In this case, all supersymmetric particles would eventually decay to the nearly massless photino.

For case (b) in which the photino is heavy enough to annihilate into light fermions, the astrophysical limit on the photino mass has been deduced by Goldberg.[17] Goldberg calculates the cross section for the annihilation of two photinos into light fermions, which proceeds by the exchange of the supersymmetric partner of the products as shown in Fig. 1, and then integrates the rate equation
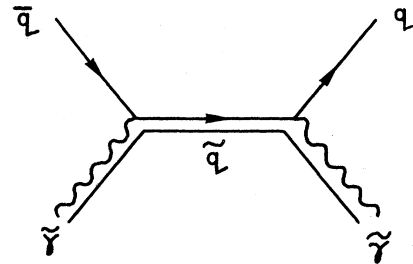

FIG. 1. Feynman diagram for the process photino + photino → $q\bar{q}$. The exchanged particle is a scalar quark.

numerically to obtain an estimate of the present photino density. The annihilation cross section and hence the conclusion depend upon the masses $m_{\tilde{f}}$ of the light superpartners of the produced fermions, which are all set equal in this calculation. The results may be summarized as follows.

(i) If the photino is lighter than the τ lepton, then the allowed region is

$$m_{\tilde{\gamma}} > (28 \text{ GeV}/c^2) \left[\frac{m_{\tilde{f}}}{100 \text{ GeV}/c^2} \right]^2 , \qquad (2.22)$$

which is only consistent with the assumption for $m_{\tilde{f}} < 25$ GeV/c^2.

(ii) If the photino is heavier than the τ lepton and $m_{\tilde{f}} < 45$ GeV/c^2, then the limit becomes simply

$$m_{\tilde{\gamma}} > m_\tau . \qquad (2.23)$$

(iii) If the photino is heavier than the τ lepton and $45 < m_{\tilde{f}} \lesssim 100$ GeV/c^2, then the limit is

$$m_{\tilde{\gamma}} \gtrsim m_{\tilde{f}}/5 . \qquad (2.24)$$

These limits are summarized in Fig. 2. Clearly a large range of stable photino masses is compatible with the cosmological constraints.

The final case (c) we consider is that of an unstable photino decaying into a photon and a massless Goldstone fermion. Cabibbo, Farrar, and Maiani[18] have noted that any photons produced by photino decays in the early Universe must have thermalized with the cosmic microwave background. This requires a photino lifetime shorter than 10^3 sec. The lifetime for the decay $\tilde{\gamma} \to \gamma \mathcal{G}$ is given by

$$\tau = 8\pi \Lambda_{ss}^4/m_{\tilde{\gamma}}^5 , \qquad (2.25)$$

STABLE PHOTINO (GOLDBERG)
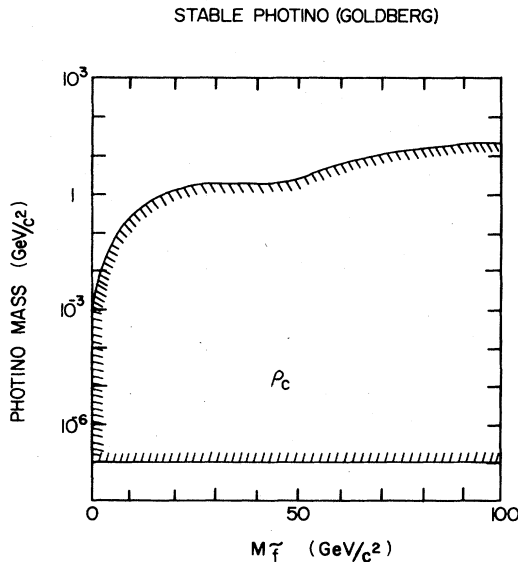
FIG. 2. Cosmological limits on the allowed photino mass as a function mass of the lightest scalar partner of a fermion (Ref. 17). This figure assumes that the photino is stable and is the lightest supersymmetric particle.

which is consistent with the black-body bound so long as

$$m_{\tilde{\gamma}} > 1.75 \text{ MeV}/c^2 \left[\frac{\Lambda_{ss}}{1 \text{ TeV}/c^2} \right]^{4/5} . \qquad (2.26)$$

There are also a number of particle-physics experiments which may be reinterpreted to give limits on $m_{\tilde{\gamma}}$ and Λ_{ss} (Ref. 19). These experiments involve detecting the photon from the photino decay. They include axion searches in channels such as $(\psi$ or $\Upsilon) \to \gamma + $neutrals, heavy-lepton searches in reactions such as[20]

$$pp \to l^+l^- + \text{anything} \qquad (2.27)$$
$$\quad \vdash \gamma + X^+ ,$$

and searches[21] for the reactions

$$e^+e^- \to \tilde{\gamma}\tilde{\gamma} \to \gamma\gamma \mathcal{G} \mathcal{G} \qquad (2.28a)$$

or[22]

$$e^+e^- \to \gamma\tilde{\gamma}\tilde{\gamma} . \qquad (2.28b)$$

The available limits are displayed in Fig. 3.

Although it is not central to our analysis, we remark parenthetically that there is a lower limit on Λ_{ss} from the decays $\psi \to$unobserved neutrals,[23] interpreted as a massless photino and massless Goldstone fermion. The experimental results then require $\Lambda_{ss} \geq 10$ GeV for light photinos, as shown in Fig. 3. This result can undoubtedly be extended to larger photino masses in studies of Υ decays.

A stronger limit of $\Lambda_{ss} \gtrsim 50$ GeV can be inferred from constraints on the emission of photinos and gravitinos or Goldstone fermions from white dwarf or red giant
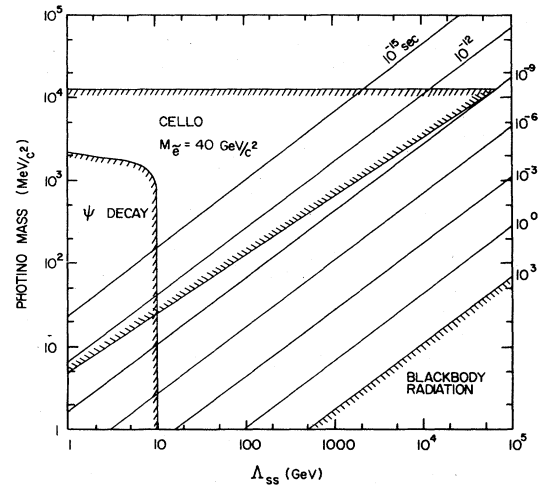

FIG. 3. Limits on the allowed photino mass as a function of the supersymmetry-breaking scale Λ_{ss}. This figure assumes that the photino decays to a photon and a massless Goldstone fermion. The limits are from ψ decay (Ref. 23), where the limit on $\psi \to$unobserved neutrals is interpreted as a bound on $\psi \to \tilde{\gamma} \mathcal{G}$; from a search in the CELLO detector for $e^+e^- \to \tilde{\gamma}\tilde{\gamma} \to \gamma\gamma \mathcal{G} \mathcal{G}$ (Ref. 21); and from blackbody radiation in the early Universe (Ref. 18). The CELLO limit assumes a scalar-electron mass of 40 GeV/c^2. The corresponding photino lifetimes are shown on the right vertical scale.

stars,[24-26] but this applies only if the masses of both the photino and the Goldstone fermion or gravitino are less than about 10 keV/c^2 (Ref. 27). Pagels and Primack[28] and Bouquet and Vayonakis[26] have deduced a plausible upper bound on Λ_{ss} from the limit ($m_{\text{gravitino}} \lesssim 100$ eV/c^2) on the mass of light relic gravitinos. The relation[29]

$$m_{\text{gravitino}} = \left[\frac{4\pi G_N}{3} \right]^{1/2} \Lambda_{ss}^2 , \qquad (2.29)$$

where G_N is the Newton's gravitational constant (2.18), leads to the restriction $\Lambda_{ss} \lesssim 1.2 \times 10^6$ GeV. Weinberg[30] has remarked that massive, unstable gravitinos which would have decayed before the time of helium synthesis are permitted and would allow values of Λ_{ss} in excess of 10^{11} to 10^{16} GeV.

We shall see below that hadron beam-dump experiments place complicated constraints on the relationship among the gluino and photino masses and the scale Λ_{ss} of supersymmetric breaking.

2. Gluinos

We next review the existing limits on gluino masses. Many of these can be strengthened by a more detailed analysis, and we present our new results in Sec. IV. The discussion of bounds on gluino masses is complicated by the fact that diverse patterns of gluino decay are allowed by current observations. We consider three cases.

(a) The gluino is stable or long-lived, with $\tau_{\tilde{g}} \gtrsim 10^{-8}$ sec.

(b) The gluino decays into a photino and a quark-antiquark pair.

(c) The gluino decays into a gluon and a Goldstone fermion.

Quite stringent limits may be derived under the assumption that the gluino is stable and is confined in stable "R hadrons."[31] If the gluino is confined in the same manner as quarks and gluons are, it will combine with quark-antiquark pairs to form hadrons with charges 0 and ± 1. MIT-bag-model calculations suggest[32] that these states should have masses near 1 GeV/c^2 if the gluino is massless, and that their masses should approach the gluino mass if the gluino is heavy. While these estimates appear sensible, it is appropriate to remark that the bag model is untested with regard to gluonic degrees of freedom. In any R-invariant theory, there will be at least one R hadron which is stable with respect to strong and electromagnetic decays. We shall show in Sec. IV that, charged-stable-particle searches[33] rule out the existence of R hadrons with lifetimes greater than 10^{-8} sec in the mass range between 1.5 and 9 GeV/c^2.

To restrict the properties of gluinos bound into neutral hadrons, or of unconfined gluinos, we reanalyze neutral-particle-search experiments.[34] We shall show in Sec. IV that only unconfined gluinos with masses between 2 and 4 GeV/c^2 and lifetimes exceeding 10^{-7} sec are excluded. This limit does not depend on assumptions about the masses of scalar quarks or other particles. It is remarkable that light ($m_{\tilde{g}} \lesssim 1.5$ GeV/c^2), stable ($\tau_{\tilde{g}} \gtrsim 10^{-8}$ sec) gluinos could have escaped detection.

If the gluino decays into a photino and a $q\bar{q}$ pair by the mechanism shown in Fig. 4, then its mass and lifetime are
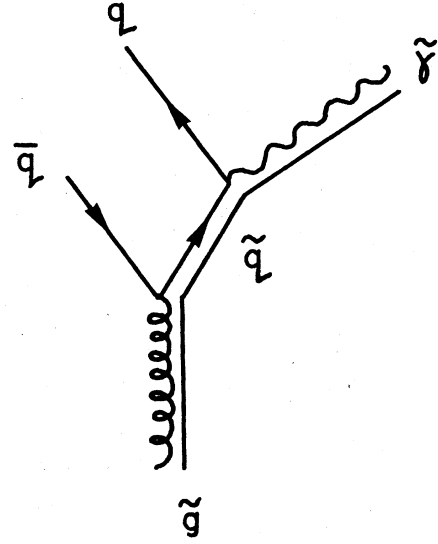

FIG. 4. Feynman diagram for gluino decay into a $q\bar{q}$ pair and a photino.

severely constrained by hadron-beam-dump experiments carried out at Fermilab[35] and CERN.[36] The primary aim of these experiments is to search for the production and subsequent interaction of prompt neutrinos, but they have some sensitivity to any short-lived particle whose neutral penetrating decay products interact in the target calorimeter.

The data may be examined in several different ways, depending on the assumed decay mode of the gluino and the subsequent behavior of the photino and gluino decay products. The partial lifetime for the decay

$$\tilde{g} \to q\bar{q}\tilde{\gamma} , \qquad (2.30)$$

where the photino mass is negligible, is[37]

$$\tau(\tilde{g} \to q\bar{q}\tilde{\gamma}) = \frac{48\pi m_{\tilde{q}}^4}{\alpha \alpha_s e_q^2 m_{\tilde{g}}^5} , \qquad (2.31)$$

where $m_{\tilde{q}}$ is the scalar-quark mass. Summing over up, down, and strange quark pairs, we find

$$\tau(\tilde{g} \to q\bar{q}\tilde{\gamma}) \approx \frac{2 \times 10^{-20} \text{ sec}}{\alpha_s} \left[\frac{m_{\tilde{q}}}{1 \text{ GeV}/c^2} \right]^4$$
$$\times \left[\frac{1 \text{ GeV}/c^2}{m_{\tilde{g}}} \right]^5 . \qquad (2.32)$$

With the somewhat arbitrary choice $\alpha_s = 0.5$, which seems plausible for gluinos in the few-GeV/c^2 range, this becomes

$$\tau(\tilde{g} \to q\bar{q}\tilde{\gamma}) \approx 4 \times 10^{-20} \text{ sec} \left[\frac{m_{\tilde{q}}}{1 \text{ GeV}/c^2} \right]^4 \left[\frac{1 \text{ GeV}/c^2}{m_{\tilde{g}}} \right]^5 .$$
$$(2.33)$$

(This estimate is a factor of two larger than that given by Kane and Leveille;[37] the difference is unimportant.) Here and in all of the phenomenological analysis carried out in

this paper, we assume for simplicity that the supersymmetric partners of left-handed and right-handed quarks are degenerate in mass.

Under the assumption that the photino is stable, the two beam-dump experiments search for the following chain of events: (i) $pN \rightarrow \tilde{g}\tilde{g} +$ anything; (ii) the decay $\tilde{g} \rightarrow q\bar{q}\tilde{\gamma}$ in the target; (iii) the reaction $\tilde{\gamma}q \rightarrow \tilde{g}q$ in the calorimeter. Prompt neutrino interactions in the calorimeter are accounted for by charm production in the target at $p_\perp < 1.5$ GeV/c. Events at larger transverse momentum are attributed to gluino production. Fermilab experiment E-613 is sensitive to gluinos with $\tau_{\tilde{g}} < 10^{-11}$ sec, whereas the CERN-Hamburg-Amsterdam-Rome-Moscow (CHARM) experiment at CERN is sensitive to gluino lifetimes shorter than 10^{-10} sec. Longer-lived gluinos would interact and be degraded in the target. The resulting constraints, which depend upon model assumptions for the gluino production mechanisms and upon the scalar-quark mass, are indicated in Fig. 5.

Farrar and Fayet[38] have considered the use of calorimetry experiments to exclude light gluinos which decay to massless photinos. The experimental results they analyze do not improve the bounds summarized here.

In principle, light gluinos with lifetimes between about 10^{-12} and 10^{-14} sec may also be detected in emulsions and other high-resolution devices constructed for the study of charm and b flavor. For gluinos decaying to $q\bar{q}\tilde{\gamma}$, the characteristic signature is missing energy without an accompanying charged lepton. This should allow discrimination against the conventional decay modes of heavy quarks.

Note that for certain values of scalar-quark masses, corresponding to 10^{-10} sec $< \tau_{\tilde{g}} < 10^{-8}$ sec, gluino masses less than 1 GeV/c^2 are consistent with the experimental restrictions.

The authors of the Fermilab beam-dump experiment[35] have also analyzed their data under the assumption that the gluino decays according to the chain

$$\tilde{g} \rightarrow q\bar{q}\tilde{\gamma} \atop \searrow \gamma \mathscr{G} , \qquad (2.34)$$

wherein a light photino decays into a photon and a (nearly) massless Goldstone fermion. As before, the analysis requires that the gluino lifetime be less than 10^{-11} sec, so the gluino decays in the target before interacting. There are now two possibilities for detection: (i) to observe anomalous "neutral-current" interactions of the Goldstone fermion in the calorimeter, for which the cross section is[39]

$$\sigma(\mathscr{G}N) = \frac{8\alpha_s M_N E}{9\Lambda_{ss}{}^4}$$

$$\approx 1.5 \times 10^{-40} \text{ cm}^2 \left[\frac{1 \text{ TeV}}{\Lambda_{ss}}\right]^4 \left[\frac{E}{1 \text{ GeV}}\right] , \qquad (2.35)$$

where E is the Goldstone-fermion energy and we have chosen $\alpha_s = 0.5$; and (ii) to detect the electromagnetic shower from the decay $\tilde{\gamma} \rightarrow \gamma \mathscr{G}$ occurring in the calorimeter.

The first method leads to the relationship between the gluino mass and the supersymmetry-breaking scale displayed in Fig. 6. The second method leads to a relation between the photino and gluino masses and the scale of supersymmetry breaking because of its sensitivity to the photino lifetime, given by (2.25). This is indicated in Fig. 7. Comparing with the constraints on $m_{\tilde{\gamma}}$ and Λ_{ss} displayed earlier in Fig. 3, we find that the beam-dump results imply important new restrictions on the photino mass, provided that the gluino mass is no more than a few GeV/c^2.
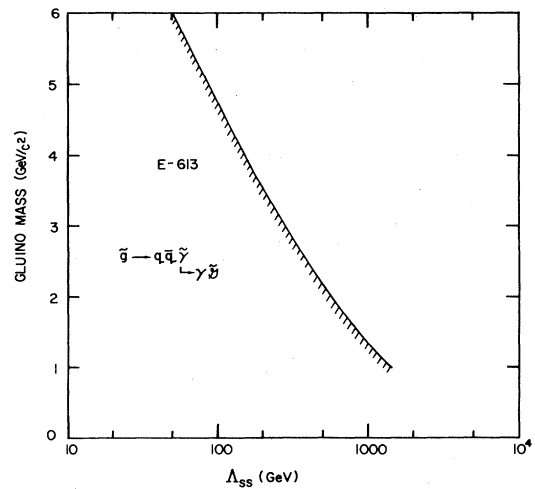

FIG. 5. Limits on the gluino mass as a function of the lightest scalar-quark mass. The gluino is assumed to decay to a $q\bar{q}$ pair and a massless photino. The limits are from beam-dump experiments (Refs. 35 and 36) and stable-particle searches (Ref. 33). The corresponding gluino lifetimes are also shown.

FIG. 6. Limits on the gluino mass as a function of the supersymmetry-breaking scale Λ_{ss} from Ref. 35. This figure is based on the decay chain $\tilde{g} \rightarrow q\bar{q}\tilde{\gamma} \rightarrow q\bar{q}\gamma\mathscr{G}$, where both the photino and the Goldstone fermion are massless, and it is also assumed that the gluino lifetime is much less than the photino lifetime.
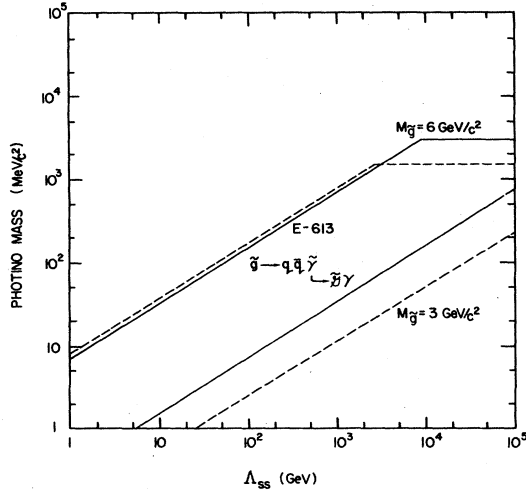
FIG. 7. Limits on the photino mass as a function of the supersymmetry breaking scale Λ_{ss} for assumed gluino masses of 3 and 6 GeV/c^2, from Ref. 35. This figure assumes the decay chain $\tilde{g} \to q\bar{q}\,\tilde{\gamma} \to q\bar{q}\gamma\,\tilde{\mathscr{G}}$, where the Goldstone fermion is massless.

The final possibility we consider is the decay of a gluino into a gluon and a massless Goldstone fermion, for which the partial lifetime is

$$\tau(\tilde{g} \to g\,\tilde{\mathscr{G}}) = 8\pi\Lambda_{ss}^{\,4}/m_{\tilde{g}}^{\,5}$$

$$\approx 1.65 \times 10^{-23}\ \text{sec}\ \left[\frac{\Lambda_{ss}}{1\ \text{GeV}/c^2}\right]^4$$

$$\times \left[\frac{1\ \text{GeV}/c^2}{m_{\tilde{g}}}\right]^5 . \tag{2.36}$$
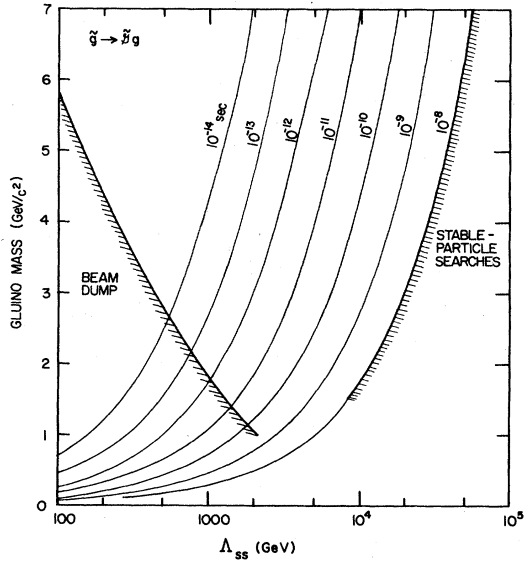
FIG. 8. Limits on the gluino mass as a function of the supersymmetry breaking scale Λ_{ss}. The limits are from the Fermilab beam-dump experiment (Ref. 35) and stable-particle searches (Ref. 33) and assume that the gluino decays to a gluon and a massless Goldstone fermion. The corresponding gluino lifetimes are also shown.
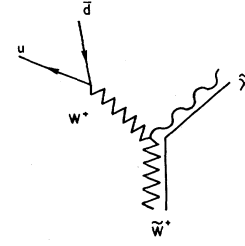
FIG. 9. Feynman diagram for the decay of a W gaugino into a quark-antiquark pair and a photino.

The relationship between $m_{\tilde{\gamma}}$ and Λ_{ss} is also constrained by the Fermilab beam-dump experiment,[35] as shown by the left-hand curve in Fig. 8. We note that for this decay mode there remains a region between $\Lambda_{ss} = 1$ and 10 TeV, where there is no experimental restriction on the existence of light gluinos.

The key result of this summary of constraints on gluino masses is that in *all* scenarios for gluino decay it is possible to find ranges of parameters for which light (~ 1 GeV/c^2) gluinos are allowed by experiment.[40] This corresponds to a gap in experimental technique for lifetimes between about 10^{-8} and 10^{-10} or 10^{-11} sec in hadron-initiated experiments.

3. Supersymmetric partners of intermediate bosons

The W gaugino $\tilde{W}$ can decay into two-body final states such as $\tilde{W} \to \mu\tilde{\nu}$ or $\tilde{\mu}\nu$, or into three-body final states via the transition $\tilde{W} \to \tilde{\gamma}W$ and subsequent decay of the (real or virtual) W. The decays mediated by W exchange have the same kinematic structure as heavy-lepton decays, as suggested in Fig. 9. Heavy-lepton searches[41] using the JADE detector at DESY PETRA look for the event chain

$$e^+e^- \to l^+l^-$$
$$\searrow \text{(hadrons)}^- + \nu_l$$
$$\text{(hadrons)}^+ + \bar{\nu}_l . \tag{2.37}$$

This decay has the same signature as $\tilde{W}$ decay: two acoplanar jets plus missing energy. For the case of a sequential heavy lepton, JADE finds a lower bound of

$$m_{l^\pm} \geq 20.6\ \text{GeV}/c^2 , \tag{2.38}$$

based on the absence of the signal (2.37). Some caution must be exercised in interpreting this figure as a bound on the $\tilde{W}$ mass. The $W\tilde{W}\tilde{\gamma}$ vertex entails a vector coupling, whereas the $Wl\nu_l$ coupling is taken to be $V - A$ in the Monte Carlo acceptance calculations leading to (2.38). It nevertheless seems clear that a reanalysis of the experiment will provide a limit $m_{\tilde{W}} \geq 20$ GeV/c^2, provided that the photino is (essentially) massless. An analysis of Mark J data[42] that considers both two-body and three-body channels leads to the limit $m_{\tilde{W}} \geq 25$ GeV/c^2, assuming the scalar neutrino and photino are massless.

Searches for neutral heavy leptons can in principle place limits on the mass of the Z gaugino $\tilde{Z}$ since the production and decay chains are entirely analogous, as shown

in Fig. 10. Because the $\widetilde{Z}$ limits depend upon the selectron mass, while neutral-heavy-lepton limits depend on the intermediate-boson mass, it is not entirely trivial to reinterpret old limits in the new setting. We present the cross section for $e^+e^- \to \widetilde{\gamma}\widetilde{Z}$ in Appendix A. The JADE Collaboration[43] has recently placed a lower limit of 41 GeV/c^2 on the $\widetilde{Z}$ mass, assuming the photino to be massless and $m_{\widetilde{e}}=22$ GeV/c^2. Similar results have been obtained by the Mark-J Collaboration.[42]

4. Supersymmetric partners of quarks

There are four sources of restrictive limits on scalar-quark masses: (i) free-quark searches; (ii) searches for narrow resonances in e^+e^- annihilations; (iii) heavy-lepton searches; and (iv) stable-hadron searches. We shall look in turn at the various pieces of evidence.

Both the JADE experiment at PETRA[44] and the free-quark search at SLAC PEP[45] place limits on long-lived, fractionally charged objects Q by measuring

$$R_Q = \frac{\sigma(e^+e^- \to Q\overline{Q})}{\sigma(e^+e^- \to \mu^+\mu^-)} . \qquad (2.39)$$

For production of scalar quarks associated with either chirality, the ratio is

$$R_Q = \frac{3e_Q^2}{4}(1 - 4m_{\widetilde{q}}^2/s)^{3/2} . \qquad (2.40)$$

This production rate is doubled if $\widetilde{q}_L$ and $\widetilde{q}_R$ are degenerate in mass.

The PEP experiment is sensitive to scalar quarks with lifetimes exceeding 10^{-8} sec. In running at $E_{\text{c.m.}}=29$ GeV, they find

$$R < \begin{cases} 7.7 \times 10^{-3}, & |e_Q| = \tfrac{2}{3}, \ M_Q < 13.8 \ \text{GeV}/c^2 , \\[2mm] 9.7 \times 10^{-3}, & |e_Q| = \tfrac{1}{3}, \ M_Q < 14.1 \ \text{GeV}/c^2 \end{cases} \qquad (2.41)$$

for pair production, and slightly less restrictive limits for inclusive pair production. These upper limits imply, through (2.40), that unconfined scalar quarks with lifetimes greater than 10^{-8} sec must have masses exceeding about 14 GeV/c^2. These conclusions are unfortunately not free from assumptions about the nature of scalar-quark–matter interactions, because the scalar quark must penetrate approximately 0.3 hadronic interaction lengths
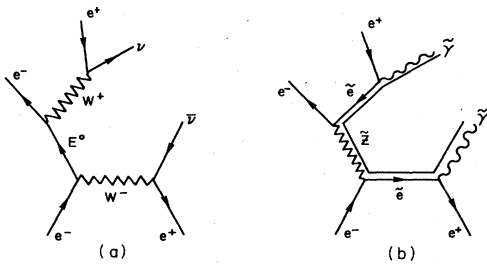
of material to be detected. The JADE search sets slightly stronger limits ($R \lesssim 6 \times 10^{-3}$) on the exclusive production of charge $\tfrac{2}{3}$ quarks with $M_Q < 12$ GeV/c^2 and lifetimes exceeding about 10^{-8} sec.

Stable, or long-lived, scalar quarks confined within integrally charged hadrons would have escaped detection in the free-quark searches. In this instance, however, stable-hadron searches are relevant. The experiments of Ref. 33 were searches for charged particles with lifetimes greater than 5×10^{-8} sec produced in high-energy pN collisions. We shall show in Sec. IV that these searches exclude scalar-quark-bearing hadrons with masses between 1.5 and 7 GeV/c^2. It is natural to assume that the mass of a hadron containing a scalar quark is approximately equal to the mass of the scalar quark itself. This would be the case in the MIT bag model, for example.

A recent search by the JADE collaboration[46] is sensitive to both charged and neutral hadrons containing scalar quarks produced in the elementary reaction

$$e^+e^- \to \widetilde{q}\,\widetilde{q}^* . \qquad (2.42)$$

Their analysis excludes stable scalar quarks with charge $\tfrac{2}{3}$ and masses between 2.5 and 15.0 GeV/c^2 and with charge $-\tfrac{1}{3}$ and masses between 2.5 and 13.5 GeV/c^2. The JADE results assume $\widetilde{q}_L$ and $\widetilde{q}_R$ are degenerate in mass.

Restrictions on short-lived scalar quarks are implied by searches for narrow resonances in e^+e^- annihilations into hadrons. The hadronic and leptonic decay widths of scalar-scalar bound states have been calculated in a potential model by Nappi.[47] Detection is made difficult by the fact that the vector particles are p-wave bound states with correspondingly small leptonic widths. Despite this, it is possible to rule out charge $\tfrac{2}{3}$ scalar quarks with masses less than 3 GeV/c^2. There are no meaningful limits from narrow resonance searches on scalar quarks with charge $-\tfrac{1}{3}$.

Although we cannot cite any specific strong-interaction experiment that limits the mass of unstable scalar quarks, it seems unlikely that the decay patterns under consideration would have escaped notice in bubble chamber experiments if $m_{\widetilde{q}} \lesssim$ a few GeV/c^2.

The JADE Collaboration has recently obtained a limit on the production of scalar quarks in e^+e^- interactions using a method similar to that used for heavy-lepton searches.[46] In this analysis it is assumed that the scalar quark decays into a quark and a massless photino. The expected signature for this decay mode is two acoplanar jets plus missing energy. An analysis of the distribution in acoplanarity angle leads to the exclusion at 95% confidence of charge $\tfrac{2}{3}$ scalar quarks in the interval $3.1 < m_{\widetilde{q}} < 17.8$ GeV/c^2 and of charge $-\tfrac{1}{3}$ in the interval $7.4 < m_{\widetilde{q}} < 16.0$ GeV/c^2.

The conclusion from various scalar-quark-search experiments is that stable scalar quarks, whether confined or free, must have masses exceeding about 14 GeV/c^2. If the photino is (nearly) massless, unstable, charge $\tfrac{2}{3}$ scalar quarks are ruled out for masses less than 17.8 GeV/c^2. For unstable scalar quarks of charge $-\tfrac{1}{3}$, a window exists below 7.4 GeV/c^2; otherwise, the mass must exceed 16 GeV/c^2. If the photino is massive, all that can be said on

FIG. 10. (a) Feynman diagram for the production and subsequent decay of a heavy lepton E^0 in e^+e^- annihilation. (b) Feynman diagram for the production of a Z gaugino and its decay into e^+e^- + photino in e^+e^- annihilation. The particle exchanged in the t channel is a scalar electron.

the basis of present analyses is that the mass of an unstable charge $\frac{2}{3}$ scalar quark must exceed 3 GeV/c^2 if the scalar-quark lifetime is less than 5×10^{-8} sec.

The limits we have cited are derived from direct experimental searches for scalar quarks or from scalar-quark-bearing hadrons. Less direct constraints in the form of restrictions upon the scalar-quark mass matrix may be deduced from theoretical analyses of other observables. Two examples will illustrate this possibility. With specific assumptions about the scalar-quark mixing matrix $\hat{U}$, one may use the measured K^0-$\bar{K}^0$ transition amplitude to bound scalar-quark mass splittings within a generation. Similarly, Haber and Kane[19] have observed that if the gluino is light, the goodness of SU(2)$_{\text{isospin}}$ symmetry in the strong interactions will limit the mass difference between up and down scalar quarks. In practice, this restriction will not apply with the same force to other scalar-quark flavors, and so cannot be interpreted as giving a model-independent lower bound on the mass of the lighest scalar quark of charge $-\frac{1}{3}$.

5. Supersymmetric partners of leptons

The most stringent limits on scalar-lepton masses are derived from experiments on electron-positron annihilations. Direct searches for pair production of stable or unstable scalar leptons have been carried out using several detectors. For stable particles, recent JADE results[46] require

$$m_{\tilde{e}} > 16.6 \text{ GeV}/c^2 \ ,$$
$$m_{\tilde{\mu}} > 16.6 \text{ GeV}/c^2 \ . \tag{2.43}$$

Unstable scalar leptons decaying into a lepton and a massless photino are similarly constrained by measurements at SLAC SPEAR,[48] PETRA,[46,49] and PEP.[50] Taken together, these limits imply

$$m_{\tilde{e}} > 17.8 \text{ GeV}/c^2 \ ,$$
$$m_{\tilde{\mu}} > 16.9 \text{ GeV}/c^2 \ , \tag{2.44}$$
$$m_{\tilde{\tau}} > 15.3 \text{ GeV}/c^2 \ .$$

These limits are considerably weakened if the photino is not massless, and collapse entirely if the photino mass exceeds about 7 GeV/c^2.

Improved limits on the scalar-electron mass may be obtained[51] from the process

$$e^+ e^- \rightarrow e^{\pm} \tilde{e}^{\mp} \tilde{\gamma}$$
$$\quad\quad\quad \rightarrow e^{\mp} \tilde{\gamma} \ . \tag{2.45}$$

The Mark-II group at PEP[52] has placed a limit of

$$m_{\tilde{e}} > 22.2 \text{ GeV}/c^2$$

for the case of a massless photino, and $\tilde{e}$ lifetimes shorter than about 10^{-8} sec.

F. Summary

The bounds summarized in this section set the context for our calculations of superpartner production cross sections and for future searches. We caution again that each limit depends on specific assumptions about the spectrum of other superpartners and decay modes.

III. FEYNMAN RULES AND CROSS SECTIONS

In this section we present the Feynman rules for the interactions among ordinary particles and their superpartners introduced in Sec. II. We shall then present the results of our calculations of the differential and total cross sections for the pair production of superpartners in collisions of quarks and gluons. Similar results for $e^+ e^-$ collisions are collected in Appendix A. Some of the processes we treat have been considered before in the literature. Where appropriate, we comment on the comparison between our results and earlier work. Our goal is to present a comprehensive and uniform treatment of the reactions of principal interest in the search for superpartners in hadron-hadron collisions.

A. Feynman rules and other preliminaries

We begin by listing the Feynman rules used in this work. We use two-component Weyl notation,[3] adopt Bjorken and Drell metric conventions,[53] and work in the Feynman gauge. Our graphical notation for the propagators is given in Fig. 11. Superparticle propagators are denoted by two lines, one of which is the same as the corresponding ordinary particle, and the other is a solid straight line. This provides a simple mnemonic for the spin of the superparticle as the minimum spin which results from combining the spin of its ordinary partner with a spin-$\frac{1}{2}$ particle.

The rules for vertices can be derived from the interaction Lagrangians given in Eqs. (2.1), (2.3), (2.4), (2.9), (2.10), (2.12), and (2.13). The three-point couplings of a gauge boson to two gauginos are given in Fig. 12. The three-point vertices which describe the couplings of a gauge boson to two scalar superpartners of fermions or of a gaugino to a fermion and its superpartner are shown in Fig. 13. Note that we have been careful to distinguish the chirality indices of the fermions and their superpartners. The definitions of the flavor mixing matrices have been given in Sec. II A. The only other vertex we require is the four-point interaction involving two gluons and two scalar quarks, which is given in Fig. 14.

Two special properties of the theories with broken supersymmetry are relevant to the calculations we carry out and thus deserve explicit mention. First, the fermionic partners of the gauge bosons (the gauginos) are Majorana fields, so care must be exercised in obtaining the statistical symmetry factors for cross sections. Second, the R invariance reviewed in Sec. II A is undoubtedly broken by the vacuum expectation values of the Higgs scalars which break the electroweak SU(2)$_L \otimes$ U(1)$_Y$ symmetry and endow the $W^{\pm}$ and Z^0 with masses. The residual R' invariance which remains in many models after electroweak symmetry breaking may itself by explicitly but softly broken. The phenomenological consequences of these possibilities have been analyzed by Farrar and Weinberg,[54] to whom we refer the reader for further details.

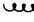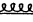In view of the theoretical uncertainties, we have calculated cross sections for both the R'-invariant and R'-
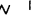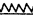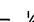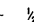
FIG. 11. Notation used in all of our Feynman diagrams. Superparticle propagators are denoted by two lines, one of which is the same as for the corresponding ordinary particle and the other is a solid straight line.

noninvariant classes of models. The difference resides entirely in gaugino mass terms. Gauginos are massless if R' invariance holds and the gaugino has a nonzero R' quantum number, and are massive if R' invariance is broken or the R' quantum number of the gaugino is zero.

For the purposes of our calculations we shall consider the masses of all the gauginos, scalar quarks, and scalar leptons as free parameters within the boundaries set by experiment. In writing the cross sections we have, for brevity, supposed the masses of the left- and right-handed scalar quark (or scalar lepton) to be equal and that there is no mass mixing between left- and right-handed scalar quarks. It is, however, straightforward to generalize our results to the unequal-mass case. How this may be done is explained below for each class of reactions.

B. Cross sections for supersymmetric-particle pair production

Here we summarize our results for the pair production of various superpartners in collisions of quarks and
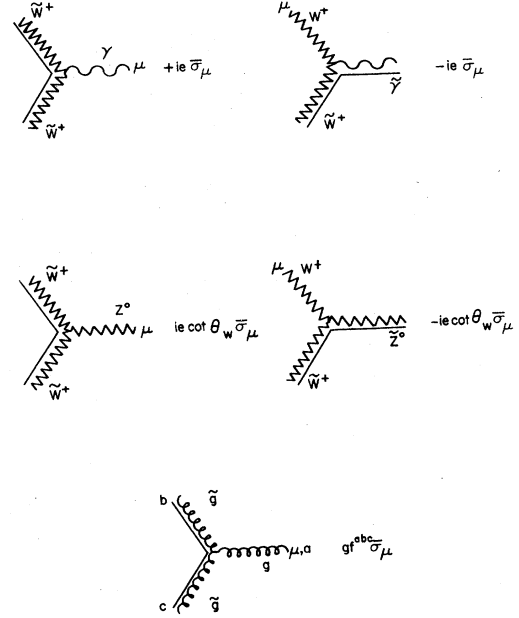
FIG. 12. Feynman rules for the three-point couplings of a gauge boson to two gauginos. The gauginos are two-component Majorana spinors.

gluons. The cross sections we quote are averaged over initial-state spins and colors and summed over final-state spins and colors. The connection between the elementary partonic cross sections and observable cross sections in hadron collisions involves a discussion of structure functions and other practical matters, which will be taken up in Sec. IV.

1. Production of gaugino pairs in quark-antiquark collisions

The differential cross section for pair production of gauge fermions in $q\bar{q}'$ collisions, which proceeds by the diagrams shown generically in Fig. 15, is given by

$$\frac{d\sigma}{dt}(q\bar{q}' \to \text{gauginos}) = \frac{\pi}{s^2}\left[A_s \frac{[(t-m_1^2)(t-m_2^2)+(u-m_1^2)(u-m_2^2)+2m_1m_2s]}{(s-M_s^2)^2} \right.$$
$$+ A_t \frac{(t-m_1^2)(t-m_2^2)}{(t-M_t^2)^2} + A_u \frac{(u-m_1^2)(u-m_2^2)}{(u-M_u^2)^2}$$
$$+ A_{st} \frac{[(t-m_1^2)(t-m_2^2)+m_1m_2s]}{(s-M_s^2)(t-M_t^2)} + A_{tu} \frac{m_1m_2s}{(t-M_t^2)(u-M_u^2)}$$
$$\left. + A_{su} \frac{[(u-m_1^2)(u-m_2^2)+m_1m_2s]}{(s-M_s^2)(u-M_u^2)} \right],$$

(3.1)

where m_1 and m_2 are the masses of the produced gauginos and M_s, M_t, and M_u are the masses of the particles exchanged in the s, t, and u channels, respectively. The coefficients A_x are collected in Table II for all possible pairs of gauginos. In theories with a surviving R' invari-

ance, the t-u interference contribution is absent, since in this case a gaugino ψ_i and an antigaugino $\bar{\psi}_i$ are distinguished by different R' quantum numbers.

The case of $\widetilde{W}^+\widetilde{W}^-$, $\widetilde{W}^{\pm}\widetilde{Z}$, and $\widetilde{Z}\widetilde{Z}$ production deserves some additional comments. In our discussions
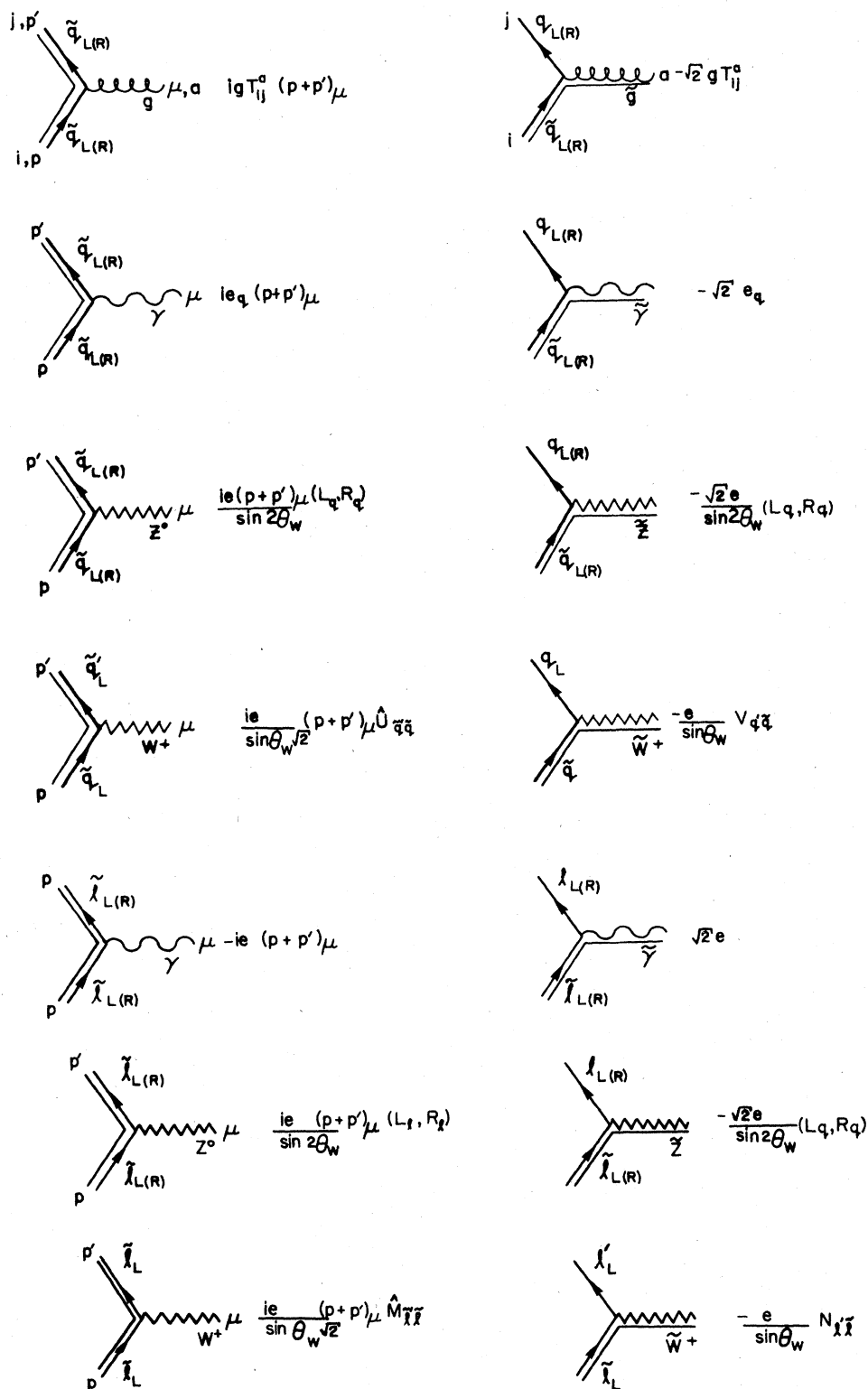
FIG. 13. Feynman rules for the three-point couplings of a gauge boson to two scalar quarks or scalar leptons and for the couplings of a gaugino to a quark and a scalar quark (or lepton and scalar lepton). The factors L_i and R_i are defined in Eq. (2.11b) and the mixing matrices $\hat{U}$, V, and $\hat{M}$ in Eqs. (2.7) and (2.8). The quarks are two-component Weyl spinors, while the gauginos are two-component Majorana spinors.
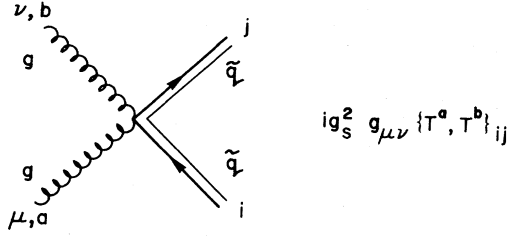
FIG. 14. Feynman rule for the four-point coupling of two gluons and two scalar quarks.

we have ignored Higgs-fermion couplings and mixing with gauginos. Since the couplings of Higgs fermions to light quarks are determined by small Yukawa coefficients, it is certainly generally justifiable to ignore direct production of Higgs fermions in hadron machines. However, in any supersymmetric model there must be a coupling between Higgs fermions and the electroweak gauginos $\widetilde{W}^{\pm}$, $\widetilde{Z}$, and $\widetilde{\gamma}$, which results from the supersymmetric generalization of the Higgs-boson gauge couplings. The two-point couplings are

$$im_W(\psi_{\widetilde{W}^-}\psi_{H^+}+\psi_{\widetilde{W}^+}\psi_{H'^-})+\frac{im_Z}{\sqrt{2}}\psi_{\widetilde{Z}}(\psi_{H^0}+\psi_{H'^0})+\text{H.c.}$$

(3.2)

This effectively mixes the $(\widetilde{W}^+,\widetilde{H}^+)$, $(\widetilde{W}^-,\widetilde{H}'^-)$, and $[\widetilde{Z}^0,(\widetilde{H}^0+\widetilde{H}'^0)/\sqrt{2}]$ pairs to form massive four-component Dirac fields. Mixing is discussed in detail in Appendix B, where the more general case, including possible explicit supersymmetry-breaking mass terms is considered and the resulting modifications to cross sections are derived.
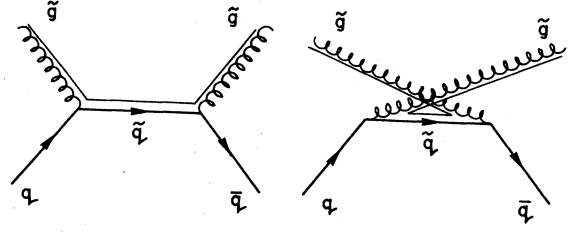
Defining the convenient quantities

FIG. 15. Feynman diagrams for gluino production in $q\bar{q}$ scattering.

$$\mathcal{S}=[s-(m_1+m_2)^2]^{1/2}[s-(m_1-m_2)^2]^{1/2} ,$$

(3.3)

$$\Delta_{ai}=M_a^2-m_i^2 ,$$

(3.4)

and

$$\Lambda_a=\ln\left[\frac{s+\Delta_{a1}+\Delta_{a2}-\mathcal{S}}{s+\Delta_{a1}+\Delta_{a2}+\mathcal{S}}\right] ,$$

(3.5)

we may express the total cross section as

$$\sigma(q\bar{q}'\rightarrow\text{gauginos})=\frac{\pi}{(1+I)s^2}\left[\frac{A_s\mathcal{S}}{3(s-M_s^2)^2}\{2s^2+s[6m_1m_2-(m_1^2+m_2^2)]-(m_1^2-m_2^2)^2\}\right.$$

$$+\left\{A_t\left[\mathcal{S}+(\Delta_{t1}+\Delta_{t2})\Lambda_t+\frac{\mathcal{S}\Delta_{t1}\Delta_{t2}}{M_t^4+m_1^2m_2^2+M_t^2(s-m_1^2-m_2^2)}\right]\right.$$

$$+\frac{A_{st}}{(s-M_s^2)}\left[\mathcal{S}\left[M_t^2-\frac{(s+m_1^2+m_2^2)}{2}\right]+(\Delta_{t1}\Delta_{t2}+m_1m_2s)\Lambda_t\right]+(t\leftrightarrow u)\right\}$$

$$\left.-A_{tu}\frac{m_1m_2s}{(s+\Delta_{t1}+\Delta_{u2})}(\Lambda_t+\Lambda_u)\right] .$$

(3.6)

The quantity $1/(1+I)$ is the symmetry factor. $I=1$ for identical gauginos $\widetilde{g}\widetilde{g}$, $\widetilde{\gamma}\widetilde{\gamma}$, and $\widetilde{Z}\widetilde{Z}$ in an R'-noninvariant theory or when the gaugino has zero R' charge in an R'-invariant theory. In all other cases $I=0$.

If the left-handed and right-handed scalar quarks have different masses

$$m_{\widetilde{q}_L}\neq m_{\widetilde{q}_R} ,$$

(3.7)

then the differential cross section (3.1) becomes simply

$$\frac{d\sigma}{dt}\bigg|_{m_{\widetilde{q}_L}\neq m_{\widetilde{q}_R}}=\frac{d\sigma}{dt}(A_L;M_t=m_{\widetilde{q}_L};M_u=m_{\widetilde{q}_L})$$

$$+\frac{d\sigma}{dt}(A_R;M_t=m_{\widetilde{q}_R};M_u=m_{\widetilde{q}_R}) ,$$

(3.8)

TABLE II. Coefficients for the reaction $q_i\bar{q}_j \to$ gaugino$_1$ + gaugino$_2$. Here $x_W = \sin^2\theta_W$. The neutral-current couplings are defined in Eq. (2.11b) and e_q is the quark charge in units of the proton charge e.

gaugino$_1$	gaugino$_2$	s	t	u	A_s	A_t	A_u	A_{st}	A_{su}	A_{tu}
$\tilde{\gamma}$	$\tilde{\gamma}$	—	$\tilde{q}$	$\tilde{q}$	0	$\dfrac{2\alpha^2 e_q^4}{3}\delta_{qq'}$	A_t	0	0	$-2A_t$
$\tilde{\gamma}$	$\tilde{g}$	—	$\tilde{q}$	$\tilde{q}$	0	$\dfrac{8\alpha_s \alpha e_q^2}{9}\delta_{qq'}$	A_t	0	0	$-2A_t$
$\tilde{\gamma}$	$\tilde{Z}$	—	$\tilde{q}$	$\tilde{q}$	0	$\dfrac{\alpha^2 e_q^2}{12 x_W}\left(\dfrac{L^2+R^2}{1-x_W}\right)\delta_{qq'}$	A_t	0	0	$-2A_t$
$\tilde{Z}$	$\tilde{Z}$	—	$\tilde{q}$	$\tilde{q}$	0	$\dfrac{\alpha^2}{48 x_W^2}\left(\dfrac{L^4+R^4}{(1-x_W)^2}\right)\delta_{qq'}$	A_t	0	0	$-2A_t$
$\tilde{Z}$	$\tilde{g}$	—	$\tilde{q}$	$\tilde{q}$	0	$\dfrac{\alpha_s \alpha}{9 x_W}\left(\dfrac{L^2+R^2}{1-x_W}\right)\delta_{qq'}$	A_t	0	0	$-2A_t$
$\tilde{g}$	$\tilde{g}$	g	$\tilde{q}$	$\tilde{q}$	$\dfrac{8\alpha_s^2}{3}\delta_{qq'}$	$\dfrac{32\alpha_s^2}{27}\delta_{qq'}$	A_t	$\dfrac{8\alpha_s^2}{3}\delta_{qq'}$	A_{st}	$\dfrac{8\alpha_s^2}{27}\delta_{qq'}$
$\tilde{W}^-$	$\tilde{W}^-$	γ AND Z	$\tilde{q}''$	$\tilde{q}''$	$\dfrac{2\alpha^2}{3}\left[e_q^2+\dfrac{e_q(L_q+R_q)}{2x_W\left(1-\frac{M_Z^2}{s}\right)}\right]$ $+\dfrac{(L_q^2+R_q^2)}{8x_W^2\left(1-\frac{M_Z^2}{s}\right)^2}\delta_{qq'}$	$\dfrac{\alpha^2}{12x_W^2}\left|V_{\tilde{q}''q}^* V_{\tilde{q}q''}\right|^2 \delta_{qu}$	$\dfrac{\alpha^2}{12x_W^2}\left|V'_{\tilde{q}''q}V'^*_{\tilde{q}''q'}\right|^2 \delta_{qd}$	$\dfrac{\alpha^2}{3x_W}\left[e_q+\dfrac{L_q}{2x_W\left(1-\frac{M_Z^2}{s}\right)}\right]$ $\text{Re}\left(V^*_{\tilde{q}q'}V_{\tilde{q}q''}\right)$ $\times\delta_{qq'}\times\delta_{qu}$	$\dfrac{\alpha^2}{3x_W}\left[e_q+\dfrac{L_q}{2x_W\left(1-\frac{M_Z^2}{s}\right)}\right]$ $\text{Re}\left(V'_{\tilde{q}''q}V^*_{\tilde{q}q'}\right)$ $\times\delta_{qq'}\times\delta_{qd}$	0
$\tilde{W}^+$	$\tilde{Z}$	W	$\tilde{q}'$	$\tilde{q}'$	$\dfrac{\alpha^2(1-x_W)}{6x_W^2}\left|U_{qq'}\right|^2$	$\dfrac{\alpha^2}{24x_W^2}\left(\dfrac{L_q^2}{1-x_W}\right)\left|V_{\tilde{q}q'}\right|^2$	$\dfrac{\alpha^2}{24x_W^2}\left(\dfrac{L_q^2}{1-x_W}\right)\left|V'_{\tilde{q}q'}\right|^2$	$\dfrac{-\alpha^2 L_q'}{6x_W^2}\text{Re}\left(V^*_{\tilde{q}q'}U_{qq'}\right)$	$\dfrac{\alpha^2 L_q}{6x_W^2}\text{Re}\left(V'_{\tilde{q}q'}U^*_{qq'}\right)$	$\dfrac{-\alpha^2}{12x_W^2}\dfrac{L_q'L_q}{(1-x_W)}$ $\text{Re}\left(V^*_{\tilde{q}q'}V'_{\tilde{q}q'}\right)$
$\tilde{W}^+$	$\tilde{\gamma}$	W	$\tilde{q}'$	$\tilde{q}'$	$\dfrac{\alpha^2}{6x_W}\left|U_{qq'}\right|^2$	$\dfrac{\alpha^2 e_q^2}{6x_W}\left|V_{\tilde{q}q'}\right|^2$	$\dfrac{\alpha^2 e_q^2}{6x_W}\left|V'_{\tilde{q}q'}\right|^2$	$\dfrac{-\alpha^2 e_q}{3x_W}\text{Re}\left(V^*_{\tilde{q}q'}U_{qq'}\right)$	$\dfrac{\alpha^2 e_q}{3x_W}\text{Re}\left(V'_{\tilde{q}q'}U^*_{qq'}\right)$	$\dfrac{-\alpha^2 e_q e_q'}{3x_W}\text{Re}$ $\left(V^*_{\tilde{q}q'}V'_{\tilde{q}q'}\right)$
$\tilde{W}^+$	$\tilde{g}$	—	$\tilde{q}'$	$\tilde{q}'$	0	$\dfrac{2\alpha_s\alpha}{9x_W}\left|V_{\tilde{q}q'}\right|^2$	$\dfrac{2\alpha_s\alpha}{9x_W}\left|V'_{\tilde{q}q'}\right|^2$	0	0	$\dfrac{-4\alpha_s\alpha}{9x_W}\text{Re}$ $\left(V^*_{\tilde{q}q'}V'_{\tilde{q}q'}\right)$

where A_L and A_R are (respectively) the contribution from left- and right-handed quark initial states to the coefficients A given in Table II. For the $\tilde{\gamma}\tilde{\gamma}$, $\tilde{\gamma}\tilde{g}$, and $\tilde{g}\tilde{g}$ cross sections, $A_L = A_R = A/2$. For $\tilde{W}^{\pm}\tilde{\gamma}$, $\tilde{W}^{\pm}\tilde{g}$, and $\tilde{W}^{\pm}\tilde{Z}$ production $A_L = A$ and $A_R = 0$. For $\tilde{\gamma}\tilde{Z}$, $\tilde{g}\tilde{Z}$, and $\tilde{Z}\tilde{Z}$ production which involve both left- (L_q) and right- (R_q) handed $\tilde{Z}$ couplings we can express the A coefficients in Table II as $A = A(L_q, R_q)$. Then the coefficients for left- and right-handed scalar quarks are $A_L = A(L_q, 0)$ and $A_R = A(0, R_q)$. Finally, for $\tilde{W}^+\tilde{W}^-$ production the direct s-channel couplings are

$$A_L^{(s)} = \frac{\alpha^2}{3}\left[e_q^2 + \frac{e_q L_q}{x_W(1 - M_Z^2/s)}\right.$$
$$\left. + \frac{L_q^2}{4x_W^2(1 - M_Z^2/s)^2}\right]\delta_{qq'},$$

$$A_R^{(s)} = \frac{\alpha^2}{3}\left[e_q^2 + \frac{e_q R_q}{x_W(1 - M_Z^2/s)}\right.$$
$$\left. + \frac{R_q^2}{4x_W^2(1 - M_Z^2/s)^2}\right]\delta_{qq'},$$

while for all other channels in $\tilde{W}^+\tilde{W}^-$ production, $A_L = A$ and $A_R = 0$.

The total cross section (3.6) is replaced by

$$\sigma \big|_{m_{\tilde{q}_L} \neq m_{\tilde{q}_R}} = \sigma(A_L; M_t = m_{\tilde{q}_L}; M_u = m_{\tilde{q}_L})$$
$$+ \sigma(A_R; M_t = m_{\tilde{q}_R}; M_u = m_{\tilde{q}_R}). \quad (3.9)$$

FIG. 16. Feynman diagrams for gluino production in gluon-gluon scattering.

Some of these cross sections have appeared previously in the literature. Leveille[55] has calculated the s-channel contributions to $q\bar{q} \to \tilde{g}\tilde{g}$ and we agree with his results. Harrison and Llewellyn Smith[56] have calculated all terms in $q\bar{q} \to \tilde{g}\tilde{g}$. We agree with their results. Barger, Robinett, Keung, and Phillips[57] have calculated the cross sections for $q\bar{q} \to \tilde{W}^+\tilde{W}^-$ and $q\bar{q} \to \tilde{W}^+\tilde{\gamma}$; we agree with their results.

2. Production of gluino pairs in gluon-gluon collisions

Of the possible pairs of gauge fermions, only gluinos can be produced at lowest order in gluon-gluon collisions. The Feynman diagrams for this process are shown in Fig. 16. The differential cross section

$$\frac{d\sigma}{dt}(gg \to \tilde{g}\tilde{g}) = \frac{9\pi\alpha_s^2}{4s^2}\left\{\frac{2(t - m_{\tilde{g}}^2)(u - m_{\tilde{g}}^2)}{s^2} + \left[\left[\frac{(t - m_{\tilde{g}}^2)(u - m_{\tilde{g}}^2) - 2m_{\tilde{g}}^2(t + m_{\tilde{g}}^2)}{(t - m_{\tilde{g}}^2)^2}\right.\right.\right.$$

$$\left. + \frac{(t - m_{\tilde{g}}^2)(u - m_{\tilde{g}}^2) + m_{\tilde{g}}^2(u - t)}{s(t - m_{\tilde{g}}^2)}\right]$$

$$+ (t \leftrightarrow u)\bigg] + \frac{m_{\tilde{g}}^2(s - 4m_{\tilde{g}}^2)}{(t - m_{\tilde{g}}^2)(u - m_{\tilde{g}}^2)}\bigg\}, \quad (3.10)$$

where $m_{\tilde{g}}$ is the gluino mass. An elementary integration gives the total cross section

$$\sigma(gg \to \tilde{g}\tilde{g}) = \frac{3\pi\alpha_s^2}{4s}\left\{3\left[1 + \frac{4m_{\tilde{g}}^2}{s} - \frac{4m_{\tilde{g}}^4}{s^2}\right]\ln\left[\frac{s + \mathcal{S}}{s - \mathcal{S}}\right]\right.$$

$$\left. - \left[4 + \frac{17m_{\tilde{g}}^2}{s}\right]\frac{\mathcal{S}}{s}\right\}. \quad (3.11)$$

Our result is twice the result of Ref. 37 and agrees with that of Ref. 56.

3. Pair production of superpartners of fermions

The production of scalar-quark pairs in hadron collisions can occur from quark-quark, quark-antiquark, or gluon-gluon initial states.

Consider first the reaction

$$q_i q_j \rightarrow \tilde{q}_i \tilde{q}_j \; , \tag{3.12}$$

for which the Feynman diagrams are shown in Fig. 17. We consider only the contribution due to gluino exchange, and neglect photino and Z-gaugino exchange diagrams. The differential cross section is

FIG. 17. Feynman diagrams for scalar-quark—scalar-quark production in qq scattering.

$$\frac{d\sigma}{dt}(q_i q_j \rightarrow \tilde{q}_i \tilde{q}_j) = \frac{4\pi\alpha_s^2}{9s^2} \left\{ -\frac{(t-m_i^2)(t-m_j^2)+st}{(t-m_{\tilde{g}}^2)^2} - \delta_{ij} \frac{(u-m_i^2)(u-m_j^2)+su}{(u-m_{\tilde{g}}^2)^2} \right.$$
$$\left. + \frac{sm_{\tilde{g}}^2}{(t-m_{\tilde{g}}^2)^2} + \frac{sm_{\tilde{g}}^2}{(u-m_{\tilde{g}}^2)^2}\delta_{ij} - \frac{2sm_{\tilde{g}}^2}{3(t-m_{\tilde{g}}^2)(u-m_{\tilde{g}}^2)}\delta_{ij} \right\} , \tag{3.13}$$

where m_i and m_j are the masses of the produced scalar quarks and $m_{\tilde{g}}$ is the gluino mass. The contribution of the $\tilde{q}_{iL}\tilde{q}_{jL} + \tilde{q}_{iR}\tilde{q}_{jR}$ final states is proportional to $m_{\tilde{g}}^2$, and therefore is absent in an R'-invariant theory. The remaining piece corresponds to $\tilde{q}_{iL}\tilde{q}_{jR} + \tilde{q}_{iR}\tilde{q}_{jL}$ final states. The total cross section is then

$$\sigma(q_i q_j \rightarrow \tilde{q}_i \tilde{q}_j) = \frac{4\pi\alpha_s^2}{9s^2} \left[\left[-2\mathscr{S} - (s+\Delta_{ti}+\Delta_{tj})\Lambda_t + \frac{1}{1+\delta_{ij}} \frac{\mathscr{S}sm_{\tilde{g}}^2}{\Delta_{ti}\Delta_{tj}+sm_{\tilde{g}}^2} + \frac{1}{3}\delta_{ij} \frac{sm_{\tilde{g}}^2}{s+\Delta_{ti}+\Delta_{tj}}\Lambda_t \right] + \delta_{ij}(t\rightarrow u) \right] .$$
$$\tag{3.14}$$

We have assumed that $\tilde{q}_{iL}$ and $\tilde{q}_{iR}$ are distinguishable.

The generalization to unequal-mass scalar quarks is slightly involved here. We first recast the differential cross section as

$$\frac{d\sigma}{dt}(q_i q_j \rightarrow \tilde{q}_i \tilde{q}_j) = \frac{d\sigma}{dt}(q_i q_j \rightarrow \tilde{q}_{iL}\tilde{q}_{jR} + \tilde{q}_{iR}\tilde{q}_{jL}) + \frac{d\sigma}{dt}(q_i q_j \rightarrow \tilde{q}_{iL}\tilde{q}_{jL} + \tilde{q}_{iR}\tilde{q}_{jR})$$
$$= \mathscr{A}(m_i,m_j) + \mathscr{B}(m_i,m_j) . \tag{3.15}$$

Note that $\mathscr{B}(m_i,m_j)$ is proportional to the gluino mass. The unequal-mass form is then

$$\mathscr{A}(m_i,m_j) = \tfrac{1}{2}[\mathscr{A}(m_L,m_R) + \mathscr{A}(m_R,m_L)] ,$$
$$\tag{3.16}$$
$$\mathscr{B}(m_i,m_j) = \tfrac{1}{2}[\mathscr{B}(m_L,m_L) + \mathscr{B}(m_R,m_R)] .$$

A similar procedure applies for the total cross section.

For quark-antiquark collisions, the differential cross section for the reaction

$$q_i \bar{q}_j \rightarrow \tilde{q}_i \tilde{q}_j^* \tag{3.17}$$

receives contributions from the diagrams of Fig. 18. It is given by

$$\frac{d\sigma}{dt}(q_i \bar{q}_j \rightarrow \tilde{q}_i \tilde{q}_j^*) = \frac{4\pi\alpha_s^2}{9s^2} \left\{ \left[\frac{ut-m_i^2 m_j^2}{s^2} \right] \left[\delta_{ij}\left(2 - \frac{2}{3}\frac{s}{(t-m_{\tilde{g}}^2)}\right) + \frac{s^2}{(t-m_{\tilde{g}}^2)^2} \right] + \frac{m_{\tilde{g}}^2 s}{(t-m_{\tilde{g}}^2)^2} \right\} . \tag{3.18}$$
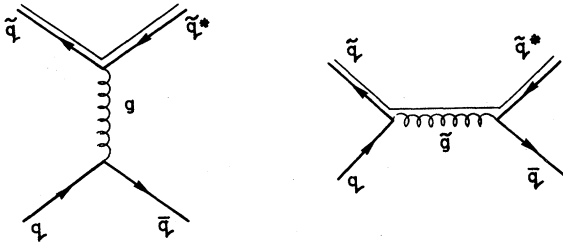

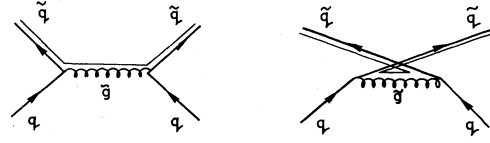FIG. 18. Feynman diagrams for scalar-quark—scalar-antiquark production in $q\bar{q}$ scattering.
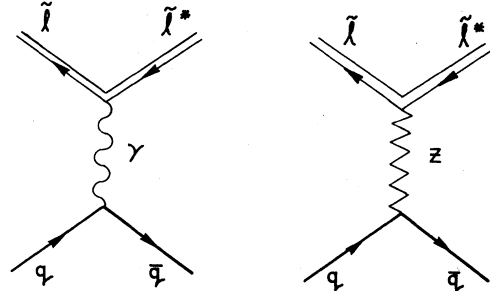

FIG. 19. Feynman diagrams for scalar-lepton—scalar-antilepton production in $q\bar{q}$ scattering.

As above, we have calculated the cross section to produce scalar quarks belonging to both chiral supermultiplets. In an R'-invariant theory (or for massless gluinos), the cross section for $q_i \bar{q}_j \rightarrow \tilde{q}_{iR} \tilde{q}_{jL}^* + \tilde{q}_{iL} \tilde{q}_{jR}^*$ vanishes. The total cross section is

$$\sigma(q_i \bar{q}_j \rightarrow \tilde{q}_i \tilde{q}_j^*) = \frac{4\pi\alpha_s^2}{27s^2} \left\{ \delta_{ij} \left[\frac{\mathscr{S}^3}{s^2} + \frac{\mathscr{S}(s + \Delta_{ti} + \Delta_{tj})}{s} + \frac{2(\Delta_{ti}\Delta_{tj} + m_{\tilde{g}}^2 s)}{s} \Lambda_t \right] \right.$$
$$\left. + 3 \left[-2\mathscr{S} - (s + \Delta_{ti} + \Delta_{tj})\Lambda_t + \frac{\mathscr{S} s m_{\tilde{g}}^2}{s m_{\tilde{g}}^2 + \Delta_{ti}\Delta_{tj}} \right] \right\} . \tag{3.19}$$

The generalization to unequal-mass scalar quarks follows the procedure outlined for $q_i q_j \rightarrow \tilde{q}_i \tilde{q}_j$.

In the special case of the initial state $q_i \bar{q}_i$ there are other possible superpartner final states accessible through the s-channel gauge-boson exchange. For the reaction

$$q_i \bar{q}_i \rightarrow \tilde{q}_j \tilde{q}_j^*, \quad i \neq j , \tag{3.20}$$

the differential cross section is

$$\frac{d\sigma}{dt}(q_i \bar{q}_i \rightarrow \tilde{q}_j \tilde{q}_j^*) = \frac{8\pi\alpha_s^2}{9s^2} \frac{(ut - m_j^4)}{s^2}, \quad i \neq j , \tag{3.21}$$

which does not depend on the R'-invariance properties of the theory. In this case, the final state is purely of the form $\tilde{q}_L \tilde{q}_L^* + \tilde{q}_R \tilde{q}_R^*$. The total cross section is

$$\sigma(q_i \bar{q}_i \rightarrow \tilde{q}_j \tilde{q}_j^*) = \frac{4\pi\alpha_s^2}{27s^4} \mathscr{S}^3, \quad i \neq j . \tag{3.22}$$

Scalar-lepton pair production proceeds via the s-channel γ and Z^0 exchanges shown in Fig. 19 which lead to the $\tilde{l}_L \tilde{l}_L^* + \tilde{l}_R \tilde{l}_R^*$ final state. The differential cross section is

$$\frac{d\sigma}{dt}(q\bar{q} \rightarrow \tilde{l}\tilde{l}^*) = \frac{4\pi\alpha^2}{3s^2} \left[e_q^2 e_l^2 + \frac{e_q e_l(L_q + R_q)(L_l + R_l)}{8x_W(1-x_W)(1-M_Z^2/s)} + \frac{(L_q^2 + R_q^2)(L_l^2 + R_l^2)}{64x_W^2(1-x_W)^2(1-M_Z^2/s)^2} \right] \left[\frac{ut - m_{\tilde{l}}^4}{s^2} \right] , \tag{3.23}$$

where $m_{\tilde{l}}$ is the scalar-lepton mass, and the total cross section is

$$\sigma(q\bar{q} \rightarrow \tilde{l}\tilde{l}^*) = \frac{2\pi\alpha^2 \mathscr{S}^3}{9s^4} \left[e_q^2 e_l^2 + \frac{e_q e_l(L_q + R_q)(L_l + R_l)}{8x_W(1-x_W)(1-M_Z^2/s)} + \frac{(L_q^2 + R_q^2)(L_l^2 + R_l^2)}{64x_W^2(1-x_W)^2(1-M_Z^2/s)^2} \right] . \tag{3.24}$$

The final mechanism we shall consider for scalar-quark pair production is gluon fusion, for which the Feynman diagrams are shown in Fig. 20. The final state reached in this process is

$$gg \rightarrow \tilde{q}_{iL} \tilde{q}_{iL}^* + \tilde{q}_{iR} \tilde{q}_{iR}^* , \tag{3.25}$$

because the gluon does not couple states of opposite chirality. The differential cross section is given by

$$\frac{d\sigma}{dt}(gg \rightarrow \tilde{q}_i \tilde{q}_i^*) = \frac{\pi\alpha_s^2}{s^2} \left[\frac{7}{48} + \frac{3(u-t)^2}{16s^2} \right] \left[1 + \frac{2m^2 t}{(t-m^2)^2} + \frac{2m^2 u}{(u-m^2)^2} + \frac{4m^4}{(t-m^2)(u-m^2)} \right] , \tag{3.26}$$

where m is the scalar-quark mass. The total cross section is then

$$\sigma(gg \rightarrow \tilde{q}_i \tilde{q}_i^*) = \frac{\pi\alpha_s^2}{3s^2} \left[\left[\frac{5}{8} + \frac{31}{4}\frac{m^2}{s} \right] \mathscr{S} + \left[4 + \frac{m^2}{s} \right] m^2 \ln \left[\frac{s - \mathscr{S}}{s + \mathscr{S}} \right] \right] . \tag{3.27}$$

For the cross sections (3.21), (3.24), and (3.26), the effect of unequal scalar-quark (or scalar-lepton) masses is simply to replace

$$\frac{d\sigma}{dt}(m) \rightarrow \frac{1}{2}\frac{d\sigma}{dt}(m_L) + \frac{1}{2}\frac{d\sigma}{dt}(m_R) . \tag{3.28}$$

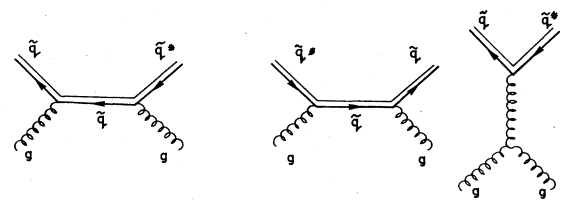The total cross sections are modified in an identical manner.

FIG. 20. Feynman diagrams for scalar-quark–scalar-antiquark production in gluon-gluon scattering.

Scalar-quark pair production in qq collisions has previously been calculated in Ref. 48. We agree with this result. The result (3.17), (3.19), (3.21), and (3.22) for scalar-quark pair production in $q\bar{q}$ collisions agree with results given by Harrison and Llewellyn Smith[56] and by Antoniadis, Baulieu, and Delduc.[58] Our results for $gg \to \tilde{q}\,\tilde{q}^*$ agree with those of Grifols and Mendez[59] and Refs. 64 and 66.

FIG. 21. Feynman diagrams for gluino—scalar-quark production in gluon-quark scattering.

4. Associated production of scalar quarks and gauginos

The last class of reactions we consider is the production of scalar quarks and gauge fermions in gluon-quark collisions, for which the reaction mechanisms are indicated generically in Fig. 21. The general form of the differential cross section is

$$
\frac{d\sigma}{dt}(gq_j \to \text{gaugino} + \tilde{q}_i) = \frac{\pi}{s^2}\left[B_s \frac{(\mu^2 - t)}{s} + B_t \frac{[(\mu^2 - t)s + 2\mu^2(m_i^2 - t)]}{(t - \mu^2)^2} \right.
$$
$$
+ \frac{B_u(u - \mu^2)(u + m_i^2)}{(u - m_i^2)^2} + \frac{B_{st}[(s - m_i^2 + \mu^2)(t - m_i^2) - \mu^2 s]}{s(t - \mu^2)}
$$
$$
+ B_{su}\frac{[s(u + \mu^2) + 2(m_i^2 - \mu^2)(\mu^2 - u)]}{s(u - m_i^2)}
$$
$$
\left. + B_{tu}\frac{[(m_i^2 - t)(t + 2u + \mu^2) + (t - \mu^2)(s + 2t - 2m_i^2) + (u - \mu^2)(t + \mu^2 + 2m_i^2)]}{2(t - \mu^2)(u - m_i^2)} \right],
$$

$$(3.29)$$

where μ is the mass of the gauge fermion and m_i is the mass of the scalar quark. The coefficients B_x for each of the final states are tabulated in Table III. Upon integration we obtain the total cross section

$$
\sigma(gq_j \to \text{gaugino} + \tilde{q}_i) = \frac{\pi}{s^2}\left[B_s \frac{\mathscr{S}}{2}(1 - \Delta/s) + B_t[2\Delta\mathscr{S}/s + (s + 2\mu^2)\tilde{\Lambda}] + B_u[\mathscr{S}(1 + 2\Delta/s) + (3m^2 - \mu^2)\Lambda] \right.
$$

$$
+ B_{st}[\mathscr{S}(1 - \Delta/s) + (m^2 - \Delta^2/s)\tilde{\Lambda}] + B_{su}[\mathscr{S}(1 - 2\Delta/s) + (\mu^2 + m^2 - 2\Delta^2/s)\Lambda]
$$

$$
\left. + B_{tu}[-(m^2 + \mu^2 + 2(m^4 - \mu^4)/s)\Lambda + (-2m^2 + 2(m^4 - \mu^4)/s)\tilde{\Lambda} - \mathscr{S}] \right],
$$

$$(3.30)$$

where

$$
\Delta = m_i^2 - \mu^2 ,
$$

$$(3.31)$$

$$
\Lambda = \ln\left| \frac{\Delta + s - \mathscr{S}}{\Delta + s + \mathscr{S}} \right| ,
$$

$$(3.32)$$

and

$$
\tilde{\Lambda} = \ln\left| \frac{\Delta - s - \mathscr{S}}{\Delta - s + \mathscr{S}} \right| .
$$

$$(3.33)$$

The unequal-mass case for the left-handed and right-handed scalar quarks is again easily dealt with. We simply replace

$$
\frac{d\sigma}{dt}(m_i) \to \frac{1}{2}\frac{d\sigma}{dt}(m_{L_i}) + \frac{1}{2}\frac{d\sigma}{dt}(m_{R_i}) ,
$$

$$(3.34)$$

and similarly for the total cross section.

The cross section for producing a scalar quark and gluino has been given in Refs. 55, 56, and 58. We agree with these results.

We turn next to the task of computing superpartner production cross sections in hadron-hadron collisions.

IV. PRODUCTION CROSS SECTIONS AND DETECTION PROSPECTS

In this section we present the numerical results for the associated production of the superpartners of the ordinary

TABLE III. Coefficients for the reaction $gq_j \rightarrow \text{gaugino} + \tilde{q}_i$. Here $x_W = \sin^2\theta_W$. The neutral-current couplings are defined in Eq. (2.11b), and e_q is the quark charge in units of the proton charge e.

Gaugino	s	Exchanged particle t	u	B_s	B_t	B_u	B_{st}	B_{su}	B_{tu}
$\tilde{\gamma}$	q		$\tilde{q}$	$\dfrac{\alpha_s \alpha e_q^2}{3}\delta_{ij}$	0	B_s	0	$-B_s$	0
$\tilde{W}^+$	q		$\tilde{q}$	$\dfrac{\alpha_s \alpha}{12 x_W}\|V_{q\bar{q}}\|^2$	0	B_s	0	$-B_s$	0
$\tilde{Z}$	q		$\tilde{q}$	$\dfrac{\alpha_s \alpha}{24 x_W}\left[\dfrac{L_q^2 + R_q^2}{1 - x_W}\right]\delta_{ij}$	0	B_s	0	$-B_s$	0
$\tilde{g}$	q	$\tilde{g}$	$\tilde{q}$	$\dfrac{4\alpha_s^2}{9}\delta_{ij}$	$\alpha_s^2 \delta_{ij}$	$\dfrac{4\alpha_s^2}{9}\delta_{ij}$	$-\alpha_s^2 \delta_{ij}$	$\dfrac{\alpha_s^2}{18}\delta_{ij}$	$\dfrac{\alpha_s^2}{2}\delta_{ij}$

fermions and gauge bosons in pp and $p\bar{p}$ collisions. We will make use of the lowest-order elementary cross sections calculated in Sec. III.

We begin with a discussion of the assumptions associated with using the Born diagrams for the quark and gluon subprocesses and the uncertainties in the distribution functions of quarks, antiquarks, and gluons in the proton and antiproton.

A. Parton model and kinematics

The basic assumption of the parton model is that a physical hadron can be described at high energies in terms of quasifree pointlike substructures called partons. Thus we envision a hadron of momentum P as being made of partons carrying longitudinal momenta $x_i P$ where the momentum fractions x_i satisfy

$$0 \le x_i \le 1 \tag{4.1}$$

and

$$\sum_{\text{partons } i} x_i = 1 . \tag{4.2}$$

The idealization that partons carry negligible transverse momentum will be adequate for our purposes.

The cross section for the hadronic reaction

$$a + b \rightarrow c + \text{anything} \tag{4.3}$$

is given by

$$d\sigma(a + b \rightarrow c + X) = \sum_{\text{parton species } i,j} f_i^{(a)}(x_a) f_j^{(b)}(x_b)$$
$$\times d\hat{\sigma}(i + j \rightarrow c + X'), \tag{4.4}$$

where the probability of finding a parton of type i with momentum fraction x_a in hadron a is denoted $f_i^{(a)}(x_a)$ and $d\hat{\sigma}$ is the parton cross section. The parton distributions satisfy

$$\sum_i \int_0^1 dx \, x f_i(x) = 1 .$$

The summation in Eq. (4.4) runs over all contributing parton configurations. Denoting the invariant mass of the parton-parton system as $(\hat{s})^{1/2}$, we can define a variable τ by

$$(\hat{s})^{1/2} = \sqrt{s\tau} , \tag{4.5}$$

and denoting the longitudinal momentum of c in the hadron-hadron c.m. frame by $p_{||}$, we may define the Feynman variable x by

$$x = 2p_{||}/\sqrt{s} . \tag{4.6}$$

Then the kinematic variables x_a and x_b of the elementary process are related to those of the hadronic process by

$$x_{a,b} = \tfrac{1}{2}[(x^2 + 4\tau)^{1/2} \pm x] . \tag{4.7}$$

These parton momentum fractions satisfy the obvious requirements

$$x_a x_b = \tau , \tag{4.8}$$
$$x_a - x_b = x .$$

The general ideas of the parton model are thoroughly explained in the book by Feynman.[60] Many interesting applications of the parton-model philosophy to hadronic interactions were introduced by Berman, Bjorken, and Kogut.[61]

All the specific processes we considered in Sec. III are two-body scattering cross sections; hence it is appropriate to develop the kinematics for this process in some detail here.

Consider the process

$$a + b \rightarrow c + d + \text{anything} , \tag{4.9}$$

where the masses of the final-state particles are M_c and M_d. Then if particle c is produced at center-of-mass angle θ with transverse momentum $p_\perp$, with $x_\perp$ given by

$$x_\perp = 2p_\perp/\sqrt{s} , \tag{4.10}$$

the invariant cross section for the reaction (4.9) is

$$E\frac{d\sigma}{d^3p}=\frac{1}{\pi}\sum_{\substack{\text{parton species } i,j}}\int_{x_{\min}}^{1}\frac{dx_a}{x_a-x_\perp\left[\dfrac{\chi+\cos\theta}{2\sin\theta}\right]}\left[x_ax_bf_i^{(a)}(x_a)f_j^{(b)}(x_b)\frac{d\hat\sigma}{d\hat t}(\hat s,\hat t,\hat u)\right]. \tag{4.11}$$

The kinematic invariants of the elementary reaction

$$i+j\to c+d$$

are given by

$$\hat s=x_ax_bs , \tag{4.12a}$$

$$\hat t=M_c^{2}-x_ax_\perp s\left[\frac{\chi-\cos\theta}{2\sin\theta}\right] , \tag{4.12b}$$

$$\hat u=M_c^{2}-x_bx_\perp s\left[\frac{\chi+\cos\theta}{2\sin\theta}\right] . \tag{4.12c}$$

Here

$$x_b=\frac{2\Delta+x_ax_\perp s\left[\dfrac{\chi-\cos\theta}{\sin\theta}\right]}{2x_as-x_\perp s\left[\dfrac{\chi+\cos\theta}{\sin\theta}\right]} , \tag{4.13}$$

$$x_{\min}=\frac{2\Delta+x_\perp s\left[\dfrac{\chi+\cos\theta}{\sin\theta}\right]}{2s-x_\perp s\left[\dfrac{\chi-\cos\theta}{\sin\theta}\right]} , \tag{4.14}$$

$$\chi=\left[1+\frac{4M_c^{2}\sin^2\theta}{x_\perp^{2}s}\right]^{1/2} , \tag{4.15}$$

and

$$\Delta=M_d^{2}-M_c^{2} . \tag{4.16}$$

B. Distribution functions and QCD corrections

Within QCD the partons are identified as quarks and gluons. The asymptotic freedom of QCD provides the theoretical framework for the parton-model assumption of quasifree partons. The most important modification of the elementary parton model picture is due to the strong-interaction (QCD) corrections to the parton distribution functions. In leading-logarithmic approximation these corrections are process independent, and can be incorporated by the replacement

$$f_i^{(a)}(x_a)\to f_i^{(a)}(x_a,Q^2) , \tag{4.17}$$

where Q^2 is a characteristic momentum scale of the particular subprocess. Typically $Q^2\approx\hat s$.

We will neglect higher-order strong-interaction corrections to the elementary cross sections. Experience has shown that this is reliable within roughly a factor of 2 at least for $Q^2\geq30$ GeV^2.

The actual distribution functions for quarks and gluons in the proton (and antiproton) cannot presently be calculated directly from QCD. It is necessary to determine these distributions from experiment. The specific distribution functions we require for the proton are the gluon distribution $g(x,Q^2)$, valence-up-quark distribution $u_V(x,Q^2)$, valence-down-quark distribution $d_V(x,Q^2)$, antiup-quark distribution $u_s(x,Q^2)$, strange-quark distribution $s_s(x,Q^2)$, and finally the charmed-quark distribution $c_s(x,Q^2)$. Using the strong-interaction symmetries we know that the antidown-quark distribution equals the antiup-quark distribution, and that for strange and charmed quarks the particle and antiparticle distributions are identical.

The total up-quark distribution in the proton is given by $u_V(x,Q^2)+u_s(x,Q^2)$ and for the down quark $d_V(x,Q^2)+u_s(x,Q^2)$. The distribution functions for the antiproton can be trivially obtained from the proton case by exchanging quark and antiquark distributions.

For the numerical results we will present in the rest of this section, we will adopt the distribution functions of Eichten, Hinchliffe, Lane, and Quigg.[62] In order to obtain some measure of the uncertainty of our results due to incomplete experimental knowledge of the distribution functions, we employ two different sets of distributions consistent with present experimental data. The two sets we have chosen from the analysis of Ref. 62 are given at $Q^2=Q_0^2=5$ GeV^2 by the following.

Set 1: $\Lambda=0.20$ GeV,

$$xg(x,Q_0^2)=(2.62+9.17x)(1-x)^{5.90} ,$$

$$xu_V(x,Q_0^2)=1.78x^{0.5}(1-x^{1.51})^{3.5} ,$$

$$xd_V(x,Q_0^2)=0.67x^{0.4}(1-x^{1.51})^{4.5} ,$$

$$xu_s(x,Q_0^2)=0.182(1-x)^{8.54} , \tag{4.18}$$

$$xs_s(x,Q_0^2)=0.081(1-x)^{8.54} ,$$

$$xc_s(x,Q_0^2)=0 .$$

Set 2: $\Lambda=0.29$ GeV,

$$xg(x,Q_0^2)=(1.75+15.575x)(1-x)^{6.03} ,$$

$$xu_V(x,Q_0^2)=1.78x^{0.5}(1-x^{1.51})^{3.5} ,$$

$$xd_V(x,Q_0^2)=0.67x^{0.4}(1-x^{1.51})^{4.5} ,$$

$$xu_s(x,Q_0^2)=0.185(1-x)^{7.12} , \tag{4.19}$$

$$xs_s(x,Q_0^2)=0.0795(1-x)^{7.12} ,$$

$$xc_s(x,Q_0^2)=0 ,$$

where Λ is the QCD scale parameter. The evolution of the structure functions, i.e., the behavior of $f_i(x,Q^2)$ for $Q^2>Q_0^2$, was determined from QCD by integrating the Altarelli-Parisi[63] equations. We refer the interested reader to Ref. 62 for more details of this method and for explicit parametrizations of the distribution functions for all $Q^2\leq(10\text{ TeV})^2$.

The principal uncertainties in the experimental determination of the distribution functions are in extracting the gluon distribution functions, and to a lesser extent the antiquark distribution functions. The appropriate variable for describing the Q^2 dependence of the distribution functions in QCD is the ratio

$$\frac{\ln(Q^2/\Lambda^2)}{\ln(Q_0{}^2/\Lambda^2)} \,. \tag{4.20}$$

Set 2 of Eq. (4.19) is associated with a larger QCD scale parameter ($\Lambda = 0.29$ GeV), and hence has more rapid variation with Q^2 than set 1, Eq. (4.18), which has $\Lambda = 0.2$ GeV. Set 2 has a harder gluon distribution at $Q^2 = Q_0{}^2$ than set 1. That is, the gluon distribution for set 2 is larger at large x ($x \gtrsim 0.2$) than that of set 1. Hence those cross sections which are particularly sensitive to the gluon distribution function might show some significant variation between using set 1 and set 2. Wherever such uncertainty might exist, we will display our numerical results for both sets of distribution functions.

We now turn to our numerical results for pair production of the gaugino-gaugino, scalar-quark—gaugino, and scalar-quark—scalar-quark final states. All cross sections are plotted assuming a theory without R' invariance, and with all quark—scalar-quark mixing angles set to zero, and assuming that $\tilde{q}_{L_i}$ and $\tilde{q}_{R_i}$ are degenerate in mass for all scalar-quark flavors.

C. Gaugino pair production

The total cross sections for $pp \rightarrow \text{gaugino}_1 + \text{gaugino}_2$ are presented in Figs. 22—32. The cross sections for $p\bar{p} \rightarrow \text{gaugino}_1 + \text{gaugino}_2$ are presented in Figs. 33—43. We have taken the following sets of values for the masses of the produced supersymmetric partners:

Spectrum 1:

$$m_{\tilde{g}} = 3 \text{ GeV}/c^2, \quad m_{\tilde{Z}} = m_{\tilde{W}} = 20 \text{ GeV}/c^2\,,$$

$$m_{\tilde{\gamma}} = 10^{-7} \text{ GeV}/c^2, \quad m_{\tilde{q}} = 20 \text{ GeV}/c^2\,.$$

Spectrum 2:

$$m_{\tilde{g}} = m_{\tilde{\gamma}} = m_{\tilde{Z}} = m_{\tilde{W}} = 50 \text{ GeV}/c^2\,,$$

$$m_{\tilde{q}} = 50 \text{ GeV}/c^2\,.$$

Spectrum 3:

$$m_{\tilde{g}} = m_{\tilde{\gamma}} = m_{\tilde{Z}} = m_{\tilde{W}} = 100 \text{ GeV}/c^2\,,$$

$$m_{\tilde{q}} = 100 \text{ GeV}/c^2\,.$$

The first spectrum entails typical light masses which are consistent with present experimental limits described in Sec. II, while spectra 2 and 3 are representative of the
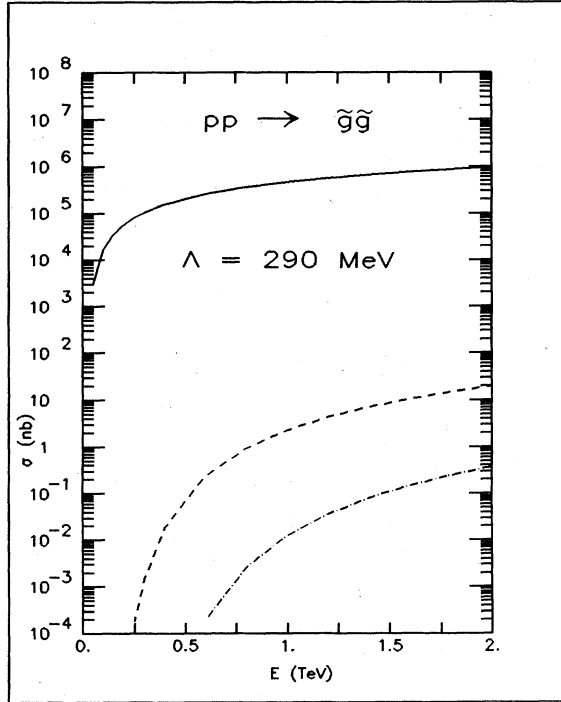
FIG. 22. Total cross section for $pp \rightarrow \tilde{g}\tilde{g}$. The masses of the supersymmetric particles are as follows. Spectrum 1: $m_{\tilde{g}} = 3$ GeV/c^2, $m_{\tilde{\gamma}} = 100$ eV/c^2, $m_{\tilde{q}} = m_{\tilde{Z}} = m_{\tilde{W}} = 20$ GeV/c^2 (solid curve). Spectrum 2: $m_{\tilde{g}} = m_{\tilde{\gamma}} = m_{\tilde{q}} = m_{\tilde{Z}} = m_{\tilde{W}} = 50$ GeV/c^2 (dashed curve). Spectrum 3: $m_{\tilde{g}} = m_{\tilde{\gamma}} = m_{\tilde{q}} = m_{\tilde{Z}} = m_{\tilde{W}} = 100$ GeV/c^2 (dot-dashed curve). Figures 22 to 31 all use parton distribution set 2.
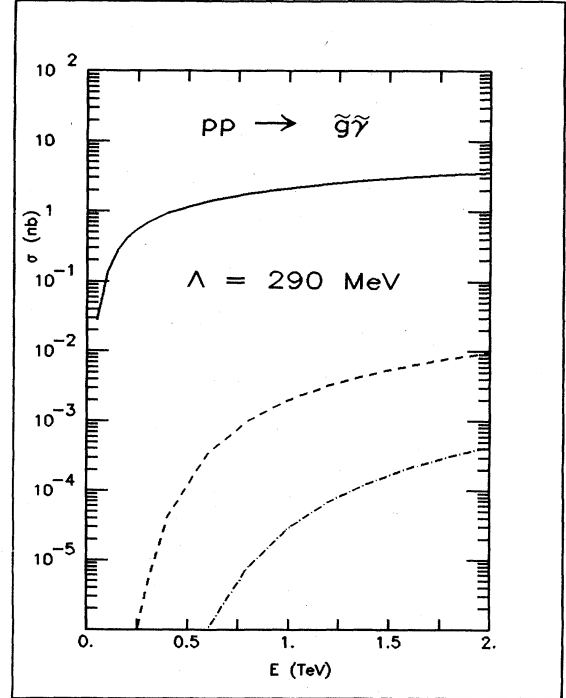
FIG. 23. Total cross section for $pp \rightarrow \tilde{g}\tilde{\gamma}$. The supersymmetric-particle masses are as in Fig. 22.
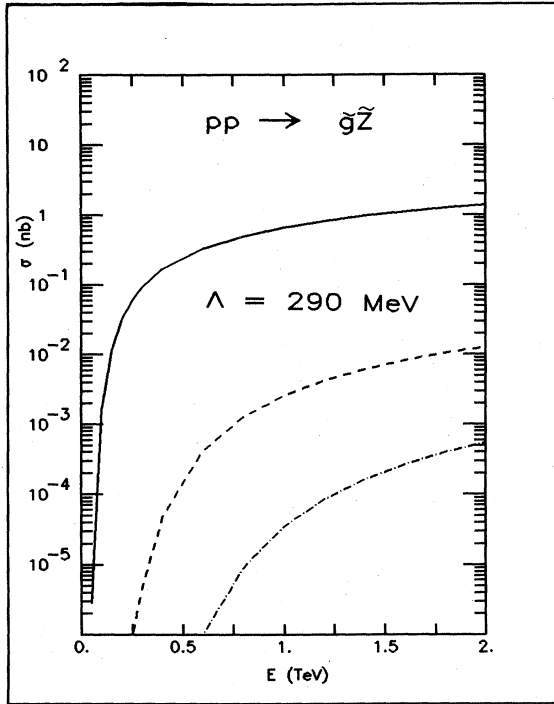
FIG. 24. Total cross section for $pp \rightarrow \tilde{g}\tilde{Z}$. The supersymmetric-particle masses are as in Fig. 22.
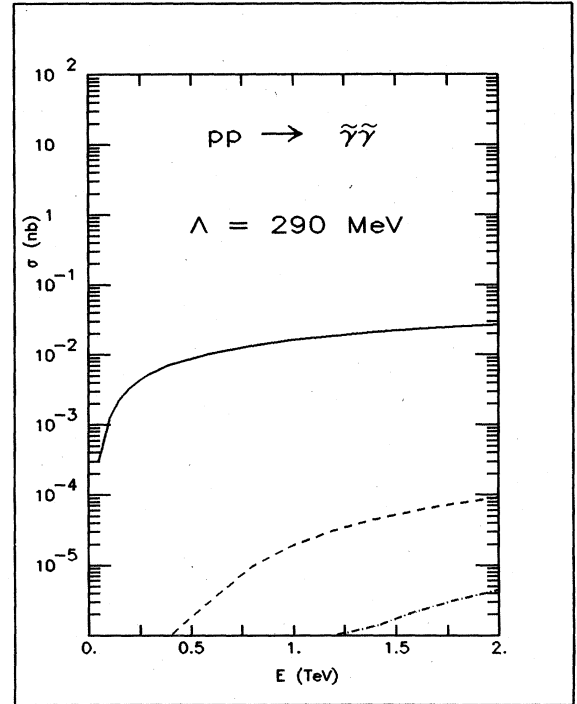

FIG. 26. Total cross section for $pp \rightarrow \tilde{\gamma}\tilde{\gamma}$. The supersymmetric-particle masses are as in Fig. 22.
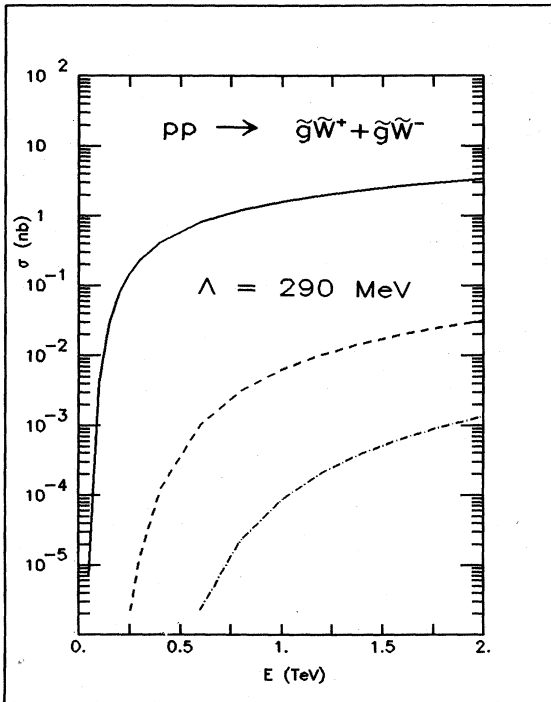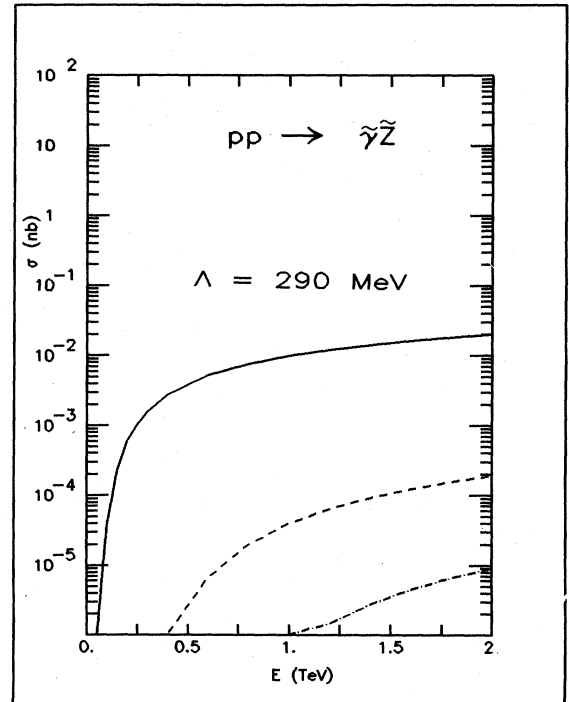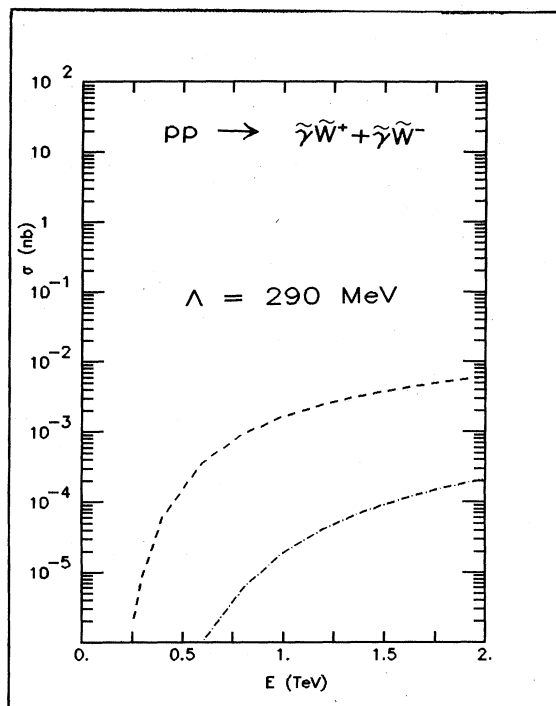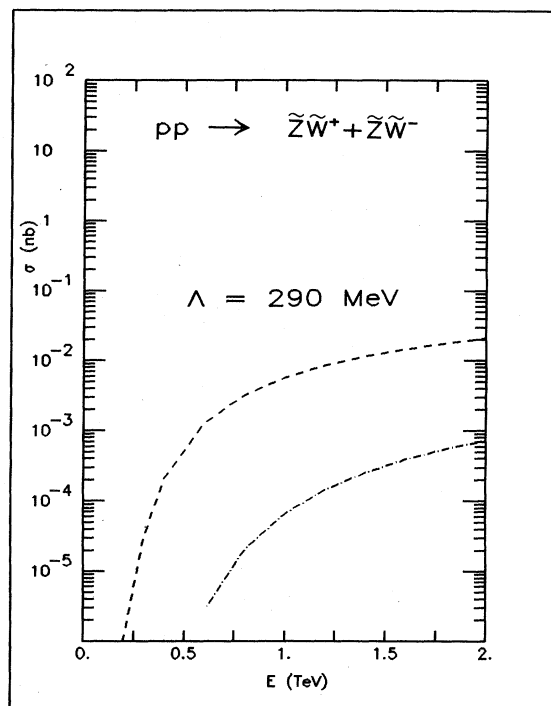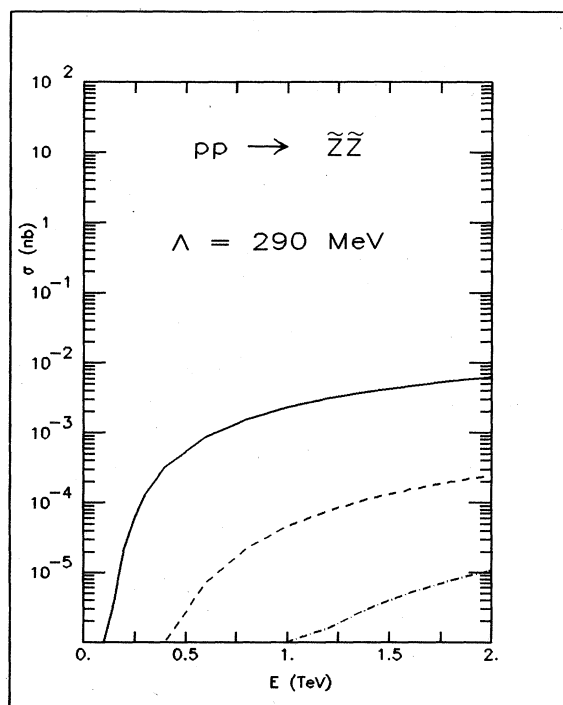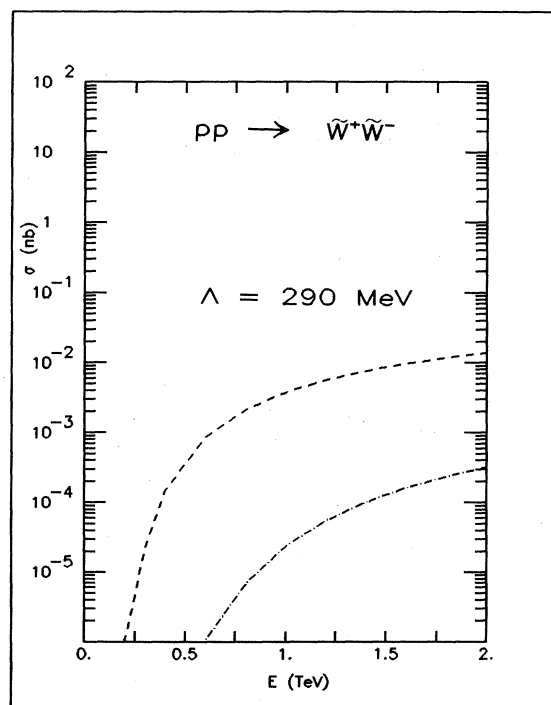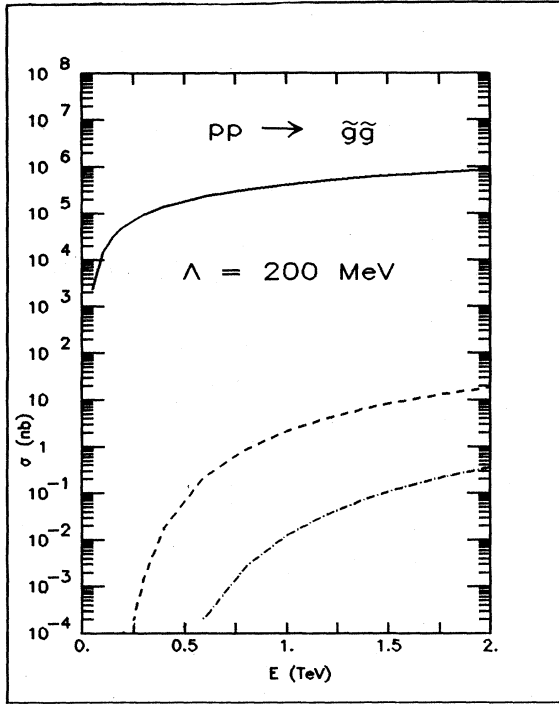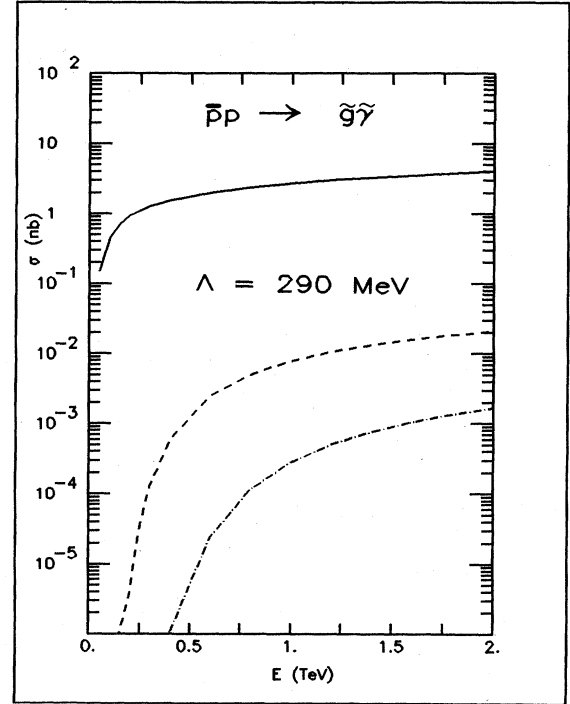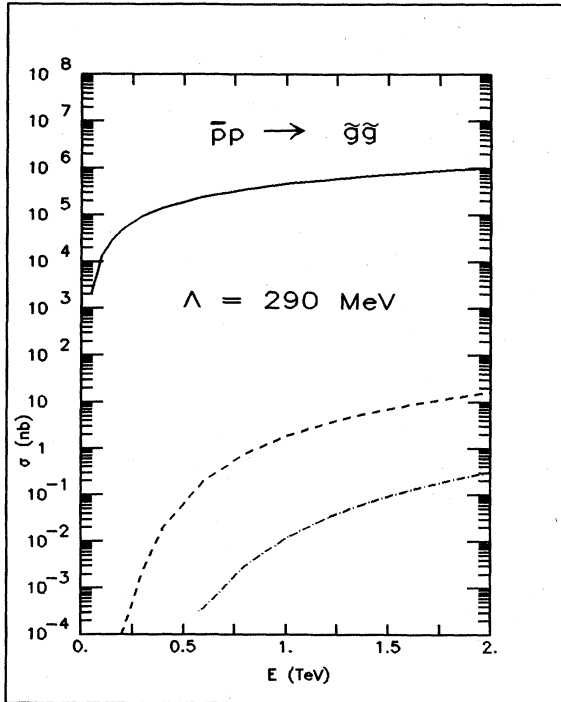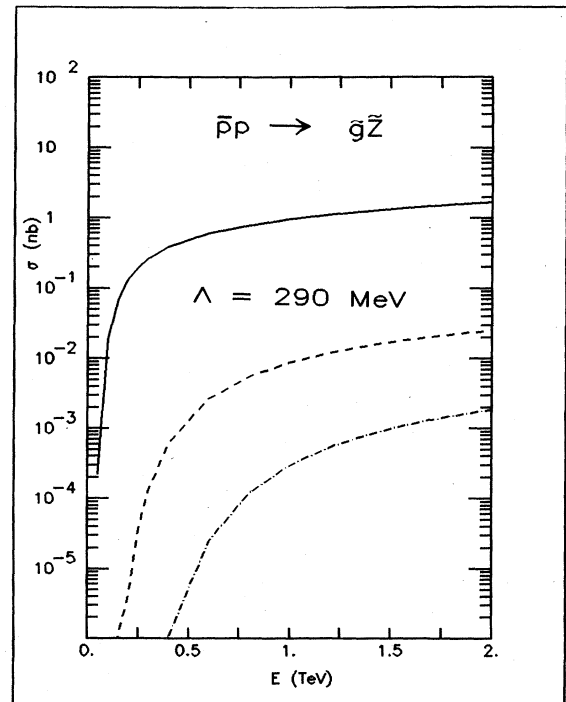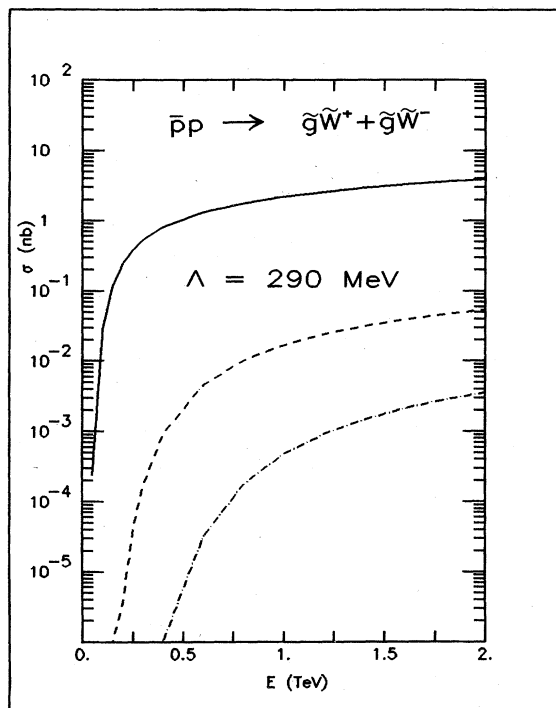

FIG. 25. Total cross section for $pp \rightarrow \tilde{g}\tilde{W}^+ + pp \rightarrow \tilde{g}\tilde{W}^-$. The supersymmetric-particle masses are as in Fig. 22.

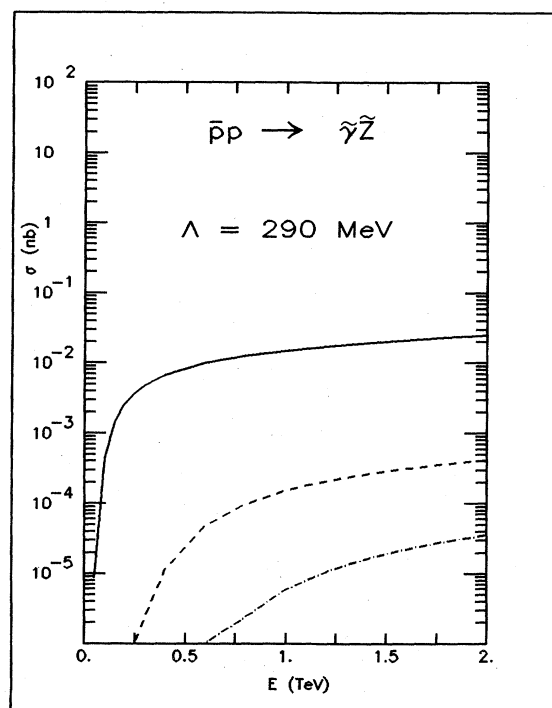FIG. 27. Total cross section $pp \rightarrow \tilde{\gamma}\tilde{Z}$. The supersymmetric-particle masses are as in Fig. 22.

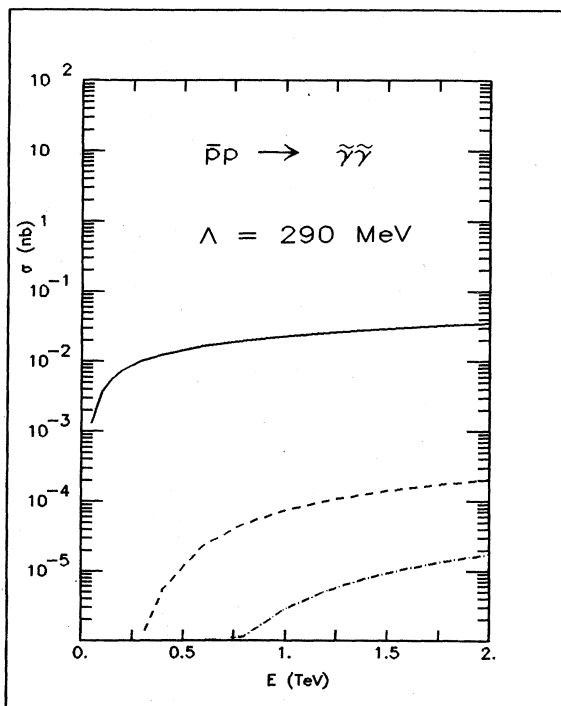FIG. 28. Total cross section for $pp \rightarrow \widetilde{\gamma} \widetilde{W}^+ + pp \rightarrow \widetilde{\gamma} \widetilde{W}^-$. The supersymmetric-particle masses are as in Fig. 22.

FIG. 30. Total cross section for $pp \rightarrow \widetilde{Z}\widetilde{W}^+ + pp \rightarrow \widetilde{Z}\widetilde{W}^-$. The supersymmetric-particle masses are as in Fig. 22.

FIG. 29. Total cross section for $pp \rightarrow \widetilde{Z}\widetilde{Z}$. The supersymmetric-particle masses are as in Fig. 22.

FIG. 31. Total cross section for $pp \rightarrow \widetilde{W}^+ \widetilde{W}^-$. The supersymmetric-particle masses are as in Fig. 22.

FIG. 32. Total cross section for $pp \rightarrow \tilde{g}\tilde{g}$ using parton distribution set 1. The supersymmetric-particle masses are as in Fig. 22.

FIG. 34. Total cross section for $p\bar{p} \rightarrow \tilde{g}\tilde{\gamma}$. The supersymmetric-particle masses are as in Fig. 22.
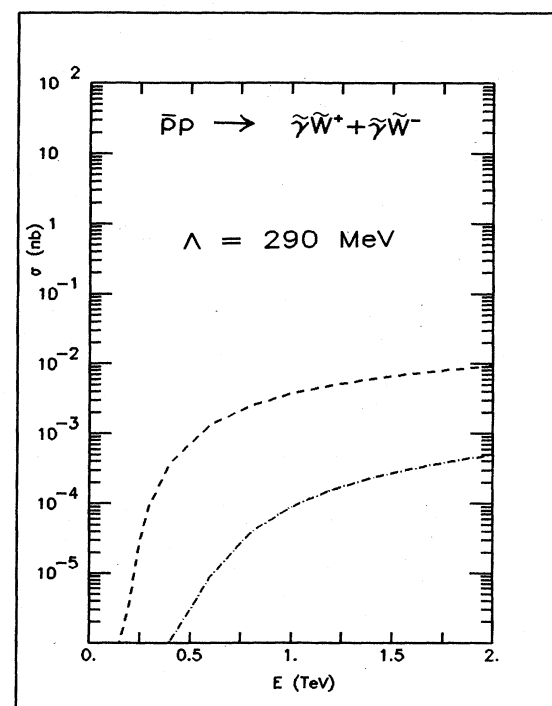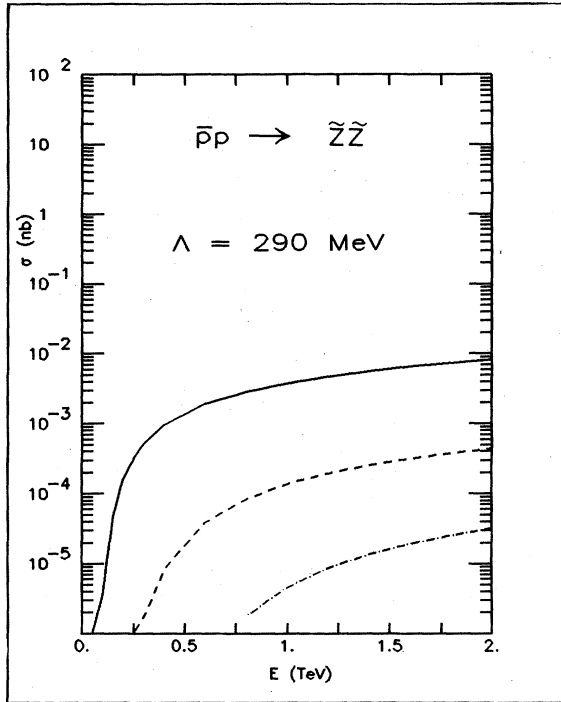

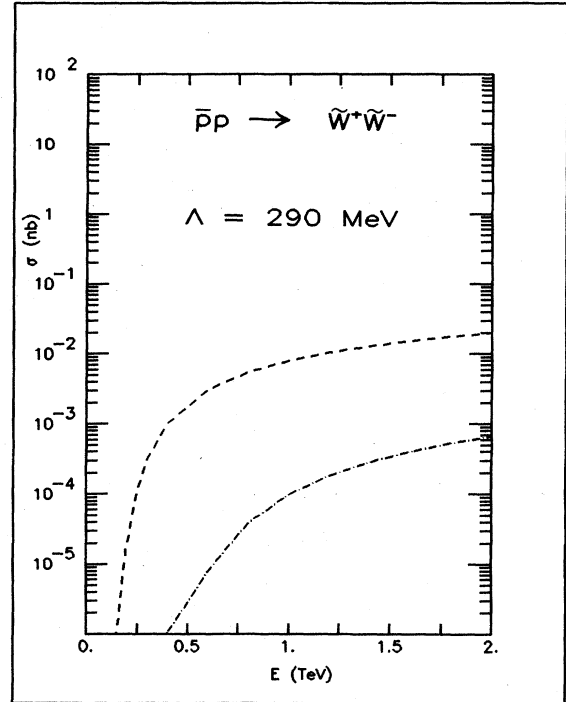FIG. 33. Total cross section for $p\bar{p} \rightarrow \tilde{g}\tilde{g}$. The supersymmetric-particle masses are as in Fig. 22. Figures 33 to 42 all use parton distribution set 2.

FIG. 35. Total cross section for $p\bar{p} \rightarrow \tilde{g}\tilde{Z}$. The supersymmetric-particle masses are as in Fig. 22.

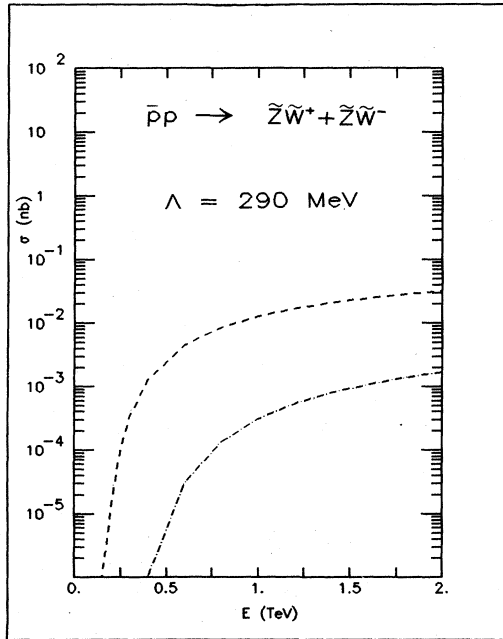FIG. 36. Total cross section for $p\bar{p}\to\tilde{g}\widetilde{W}^+ + p\bar{p}\to\tilde{g}\widetilde{W}^-$. The supersymmetric-particle masses are as in Fig. 22.

FIG. 38. Total cross section for $p\bar{p}\to\tilde{\gamma}\widetilde{Z}$. The supersymmetric-particle masses are as in Fig. 22.

FIG. 37. Total cross section for $p\bar{p}\to\tilde{\gamma}\tilde{\gamma}$. The supersymmetric-particle masses are as in Fig. 22.

FIG. 39. Total cross section for $p\bar{p}\to\tilde{\gamma}\widetilde{W}^- + p\bar{p}\to\tilde{\gamma}\widetilde{W}^+$. The supersymmetric-particle masses are as in Fig. 22.

FIG. 40. Total cross section for $p\bar{p}\rightarrow\tilde{Z}\tilde{Z}$. The supersymmetric-particle masses are as in Fig. 22.

FIG. 42. Total cross section for $p\bar{p}\rightarrow\tilde{W}^{+}\tilde{W}^{-}$. The supersymmetric-particle masses are as in Fig. 22.

FIG. 41. Total cross section for $p\bar{p}\rightarrow\tilde{Z}\tilde{W}^{+}+p\bar{p}\rightarrow\tilde{Z}\tilde{W}^{-}$. The supersymmetric-particle masses are as in Fig. 22.
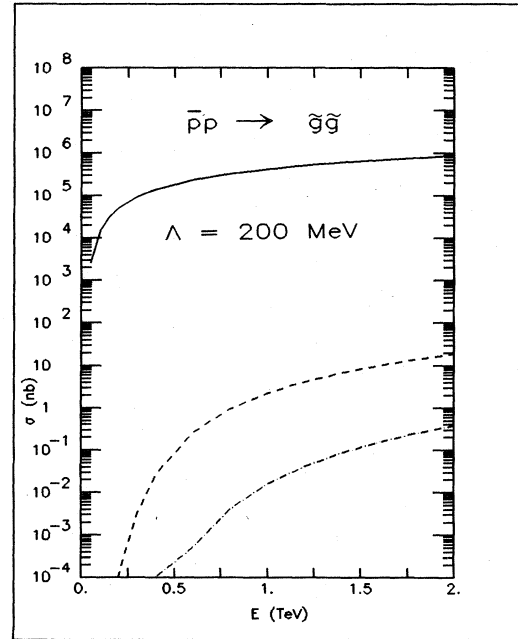
FIG. 43. Total cross section for $p\bar{p}\rightarrow\tilde{g}\tilde{g}$ using parton distribution set 1. The supersymmetric-particle masses are as in Fig. 22.

expectations for larger-mass supersymmetric partners. We make the idealization that all scalar-quark flavors are degenerate in mass.

The associated production of gluinos has the largest cross section among the processes we have considered. For example, from Fig. 22, $\sigma(pp \rightarrow \widetilde{g}\widetilde{g})$ is 2.2 nb at $\sqrt{s} = 1000$ GeV for spectrum 2 ($m_{\widetilde{g}} = 50$ GeV/c^2). A measure of the sensitivity of our results to the gluon distribution can be obtained by comparing the results for distribution set 2 [Eq. (4.19)] shown in Fig. 22 with those for distribution set 1 [Eq. (4.18)] depicted in Fig. 32. The differences are typically 10–15%. In particular, using set 1, $\sigma(pp \rightarrow \widetilde{g}\widetilde{g}) = 2.1$ nb at $\sqrt{s} = 1000$ GeV for spectrum 2 ($m_{\widetilde{g}} = 50$ GeV/c^2).

At Fermilab Tevatron collider energies, $\sqrt{s} = 2000$ GeV, the cross section $\sigma(p\bar{p} \rightarrow \widetilde{g}\widetilde{g}) = 0.31$ nb for spectrum 3 ($m_{\widetilde{g}} = 100$ GeV/c^2). Hence, with an assumed machine luminosity of 10^{30} cm^{-2} sec^{-1}, an experiment running 10^7 sec could accumulate 3×10^3 events. Such heavy gluinos will yield one or two jets in each hemisphere, with unbalanced transverse momentum. The potential backgrounds are from heavy-quark ($t\bar{t}$) pairs or from the evolution of high-$p_\perp$ jets into heavy quarks. For gluino masses above the top-quark mass, the background from direct $t\bar{t}$ production falls much more rapidly with increasing gluino mass than does the signal from gluino pair production. For relatively small gluino masses, these events have a characteristic structure with one broad jet in each hemisphere and a small $p_\perp$ imbalance if the gluino decays to a $q\bar{q}$ pair and a (nearly) massless photino. Unfortunately the background is severe and it may require many events to distinguish these $\widetilde{g} + \widetilde{g}$ events. The major background comes from events in which a pair of light constituents (g, u, d, s) are produced at high $p_\perp$ and then one constituent emits a hard gluon. The gluon subsequently produces a $b\bar{b}$ or $c\bar{c}$ pair which has a semileptonic decay. This background has broad jets and large missing $p_\perp$ (in the neutrino). Here the ability to detect the charged lepton with high efficiency is crucial for separating out the background. This and other backgrounds have been investigated in detail at existing collider energies by Aronson et al.[64] and by Savoy-Navarro.[64] Beam-dump experiments will also be sensitive to the gluino decay pattern described above.

The cross sections for pp (or $p\bar{p}$) $\rightarrow \widetilde{g}\widetilde{Z}$ and $\widetilde{g}\widetilde{W}$ are more than two orders of magnitude smaller than the $\widetilde{g}\widetilde{g}$ cross section for the same masses. For example, for spectrum 2 ($m_{\widetilde{g}} = m_{\widetilde{Z}} = m_{\widetilde{W}} = 50$ GeV/c^2) at $\sqrt{s} = 1000$ GeV, $\sigma(pp \rightarrow \widetilde{g}\widetilde{Z}) = 2.6 \times 10^{-3}$ nb and $\sigma(pp \rightarrow \widetilde{g}\widetilde{W}) = 6.3 \times 10^{-3}$ nb. Furthermore, these events probably do not have a recognizable signature. If the $\widetilde{W}$ (or $\widetilde{Z}$) is lighter than the W boson (or Z boson) it will presumably decay to $q\bar{q}\widetilde{\gamma}$ and $l\bar{\nu}\widetilde{\gamma}$ (or $l\bar{l}\widetilde{\gamma}$ and $\nu\bar{\nu}\widetilde{\gamma}$). In the first case the $\widetilde{g}\widetilde{W}$ (or $\widetilde{g}\widetilde{Z}$) events have a signature which is indistinguishable from the $\widetilde{g}\widetilde{g}$ events: a broad jet in each hemisphere with missing $p_\perp$. Since the background was already significant for this event signature in the case of $\widetilde{g}\widetilde{g}$ production, the signal-to-noise ratio is hopelessly small for $\widetilde{W}\widetilde{g}$ (or $\widetilde{Z}\widetilde{g}$) production with $m_{\widetilde{W}}$ ($m_{\widetilde{Z}}$) $\gtrsim 20$ GeV/c^2 in the absence of a convincing signal for $\widetilde{W}$ (or $\widetilde{Z}$) production.

In the second case the $\widetilde{W}$ (or $\widetilde{Z}$) decays to a lepton pair and a photino. For the $\widetilde{W}$ the result is a charged lepton and missing transverse momentum (from both the neutrino and photino) and possibly a hard photon. Unfortunately, for the $\widetilde{W}$ masses accessible at energies and machine luminosities up to the Tevatron collider, the lepton will be relatively low in energy (10–20 GeV) and hence hard to clearly identify. Also heavy-quark decays and $W + $ jet events will be a significant background to this process. Similar comments apply to $\widetilde{Z}$ production.

The cross section for the reaction pp (or $p\bar{p}$) $\rightarrow \widetilde{\gamma}\widetilde{g}$ depicted in Fig. 23 (or Fig. 34) is of the same order of magnitude as the cross section for $\widetilde{g}\widetilde{Z}$ or $\widetilde{g}\widetilde{W}$ production. However the experimental signature may be different and hence there is a good possibility of observing these final states. If the photino decays quickly into a photon and Goldstone fermion, the hard photon can be used as a trigger. If, on the other hand the photino is stable, it will escape undetected and so for the final states $\widetilde{\gamma}\widetilde{g}$ the events will have large missing energy in one hemisphere and a broad jet in the other. These events have been discussed by many authors.[65] For example, for spectrum 2 ($m_{\widetilde{g}} = m_{\widetilde{\gamma}} = 50$ GeV/c^2) the cross section $\sigma(pp \rightarrow \widetilde{g}\widetilde{\gamma}) = 2 \times 10^{-3}$ nb at $\sqrt{s} = 1000$ GeV, and $\sigma(pp \rightarrow \widetilde{g}\widetilde{\gamma}) = 2.1 \times 10^{-2}$ nb at $\sqrt{s} = 2000$ GeV. Using standard running time and luminosity assumptions, this corresponds to 200 events/yr at the Tevatron collider. A potential background to this signature arises from the decay $W \rightarrow \tau\nu_\tau$, followed by the decay of $\tau \rightarrow \nu_\tau + $ hadrons. This may result in a low-multiplicity monojet. The monojet background from $Z + $ jet production, with $Z \rightarrow \nu\bar{\nu}$, cannot be eliminated by a lepton veto. This is probably most severe for relatively heavy photinos, and light gluinos.

The other cross sections involving a single photino in the final state are $\widetilde{\gamma}\widetilde{W}$ and $\widetilde{\gamma}\widetilde{Z}$. These cross sections have the same signatures as $\widetilde{\gamma}\widetilde{g}$ if the $\widetilde{W}$ (or $\widetilde{Z}$) is lighter than the W boson (or Z boson). However, the cross sections are typically one to two orders of magnitude smaller than the corresponding $\widetilde{g}\widetilde{\gamma}$ cross section. For spectrum 2 ($m_{\widetilde{Z}} = m_{\widetilde{\gamma}} = 50$ GeV/c^2), $\sigma(pp \rightarrow \widetilde{\gamma}\widetilde{Z}) = 3.9 \times 10^{-5}$ nb and $\sigma(pp \rightarrow \widetilde{\gamma}\widetilde{W}^+ + \widetilde{\gamma}\widetilde{W}^-) = 1.6 \times 10^{-3}$ nb at $\sqrt{s} = 1000$ GeV. Thus the limits which can be obtained on masses for $\widetilde{\gamma}$, $\widetilde{Z}$, and $\widetilde{W}$ are not very strong. Using the minimum experimentally acceptable masses of spectrum 1 for $\widetilde{Z}$ ($m_{\widetilde{Z}} \geq 20$ GeV/c^2) and $\widetilde{W}$ ($m_{\widetilde{W}} \geq 20$ GeV/c^2) and a light $\widetilde{\gamma}$ ($m_{\widetilde{\gamma}} = 100$ eV/c^2), we find a cross section of $\sigma(p\bar{p} \rightarrow \widetilde{\gamma}\widetilde{Z}) = 2.4 \times 10^{-2}$ nb at $\sqrt{s} = 2000$ GeV. The cross section for $\widetilde{\gamma}\widetilde{W}$ has the additional enhancement associated with the W pole in the s channel.

Finally, we consider the cross section for photino pair production. For light photinos, this process is observable only if the photino is unstable and decays into a photon and a Goldstone fermion, or if 4π calorimetry can be made truly hermetic. The signature is then two hard photons and missing $p_\perp$, or missing energy. The cross section $\sigma(p\bar{p} \rightarrow \widetilde{\gamma}\widetilde{\gamma})$ for spectrum 2 ($m_{\widetilde{\gamma}} = 50$ GeV/c^2) is $\sigma(p\bar{p} \rightarrow \widetilde{\gamma}\widetilde{\gamma}) = 2.0 \times 10^{-4}$ nb at $\sqrt{s} = 2000$ GeV. The remaining cross sections pp (or $p\bar{p}$) $\rightarrow \widetilde{Z}\widetilde{Z}$, $\widetilde{Z}\widetilde{W}$, or $\widetilde{W}\widetilde{W}$ are relatively small. For spectrum 2 ($m_{\widetilde{Z}} = m_{\widetilde{W}} = 50$

GeV/c^2), $\sigma(p\bar{p}\rightarrow\tilde{Z}\,\tilde{Z})=4.4\times10^{-4}$ nb, $\sigma(p\bar{p}\rightarrow\tilde{Z}\,\tilde{W})$ $=3.2\times10^{-2}$ nb, and $\sigma(p\bar{p}\rightarrow\tilde{W}\,\tilde{W})=2.0\times10^{-2}$ nb at $\sqrt{s}=2000$ GeV. The most favorable process is $\tilde{W}$ pair production, which is enhanced by the s-channel photon and Z^0 exchanges. For $\tilde{W}$ and $\tilde{Z}$ masses ≥30 GeV/c^2, the $\tilde{W}^{\pm}\tilde{Z}$ process is substantially enhanced by the s-channel $W^{\pm}$ exchange. Unfortunately, we have not been able to find a recognizable signature for these processes, for light W and Z gauginos.

We have plotted in Figs. 44—57 the differential cross section $E\,d\sigma/d^3p$ for those processes which seem most likely to be observable; i.e., for $\tilde{g}$, $\tilde{\gamma}$, and $\tilde{W}^{\pm}$ inclusive production. We have taken the center-of-mass scattering angle $\theta=90°$, 45°, and 30° and used the most favorable spectrum 1 of gaugino masses ($m_{\tilde{g}}=3$ GeV/c^2, $m_{\tilde{\gamma}}=100$ eV/c^2, $m_{\tilde{Z}}=20$ GeV/c^2, $m_{\tilde{W}}=20$ GeV/c^2, and $m_{\tilde{q}}=20$ GeV/c^2).

D. Gaugino—scalar-quark production

The total cross sections for producing a scalar quark (or scalar antiquark) and a gaugino are shown in Figs. 58—61, where we have summed over scalar-quark flavors. Since we have summed over scalar-quark and scalar-antiquark

FIG. 45. Differential cross section $E\,d\sigma/d^3p$ for inclusive $\tilde{g}$ production for pp collisions at $\sqrt{s}=43$ GeV. All other parameters are as in Fig. 44.
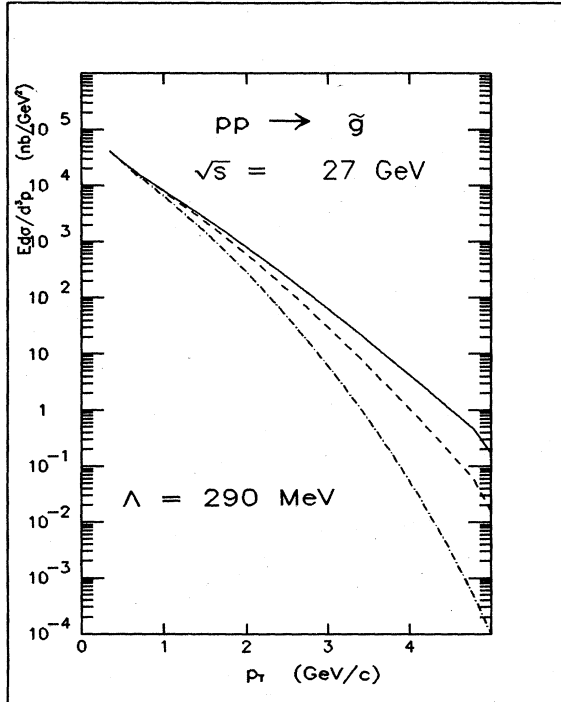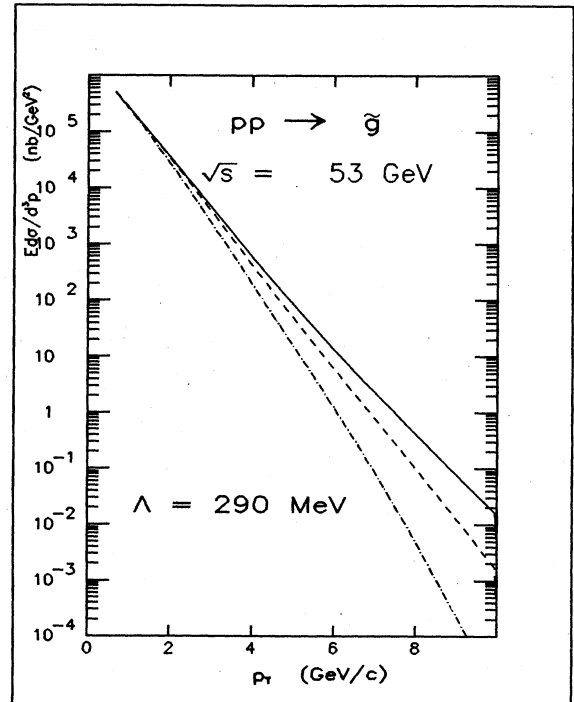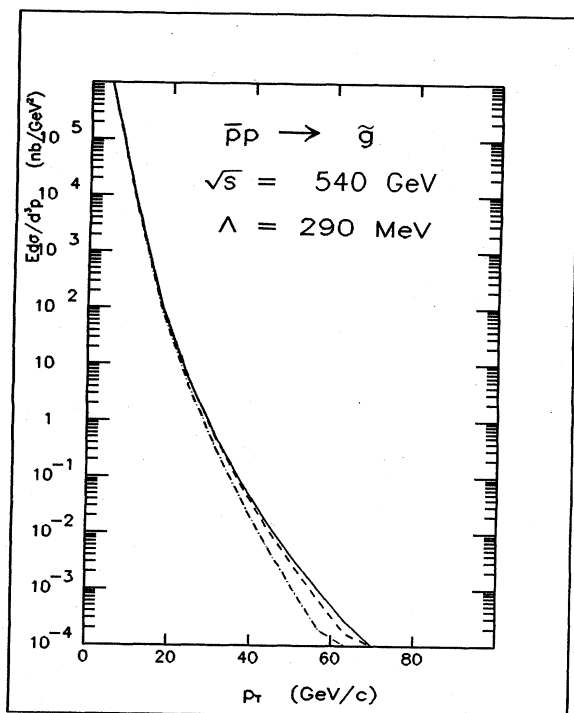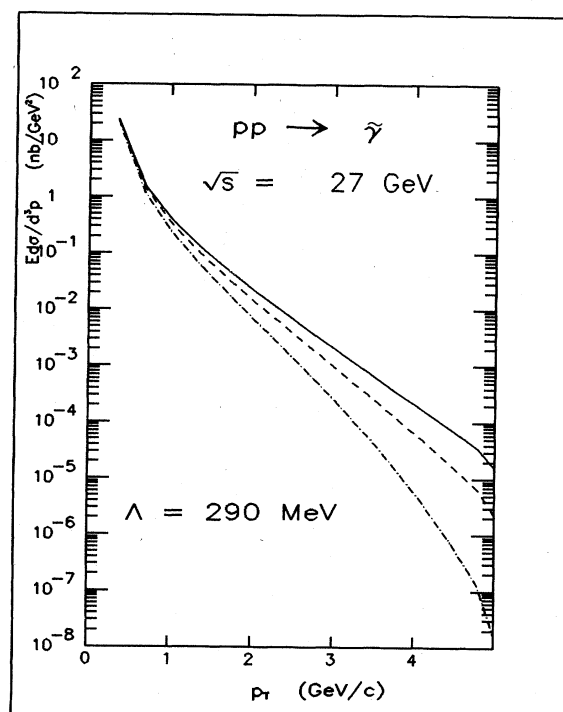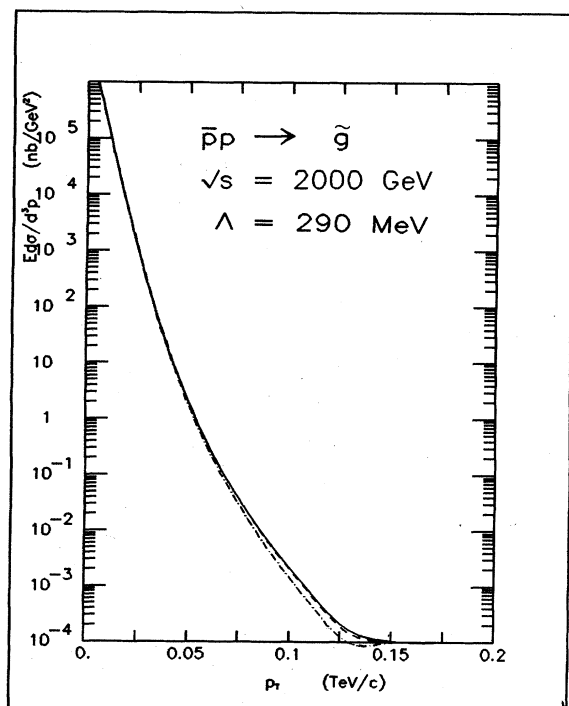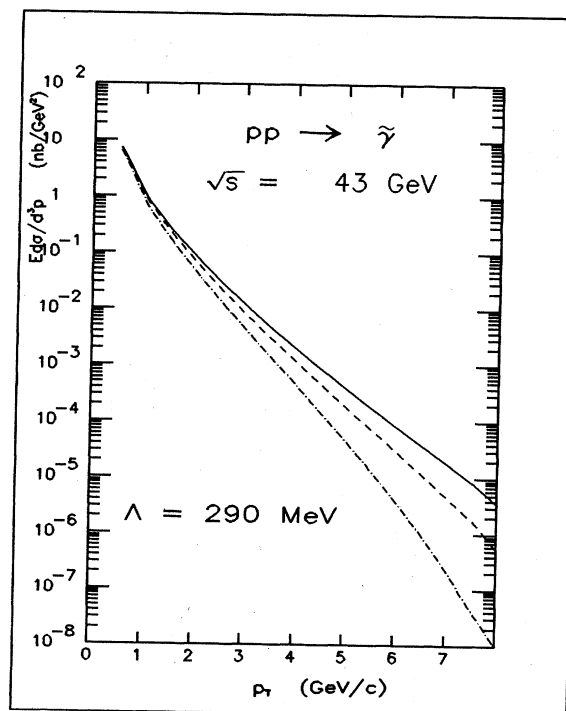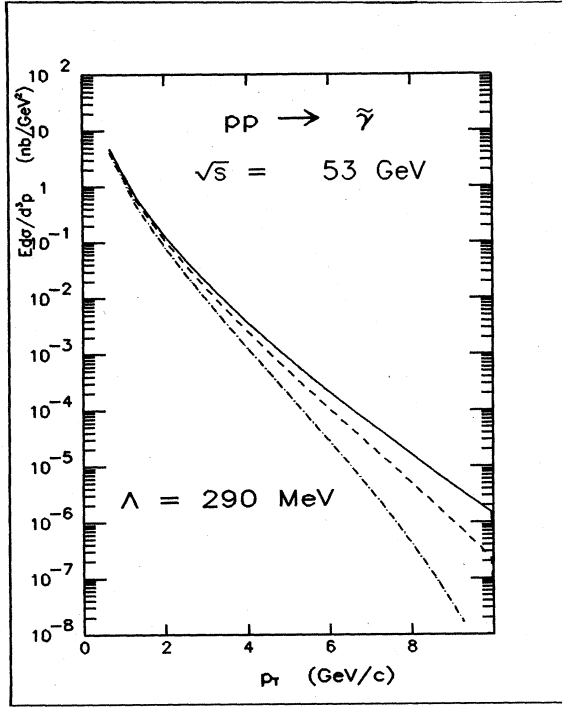

FIG. 44. Differential cross section $E\,d\sigma/d^3p$ for inclusive $\tilde{g}$ production at center-of-mass angle $\theta=90°$, 45°, and 30° for pp collisions at $\sqrt{s}=27$ GeV. The contributions from all reactions with gaugino pairs in the final state are included. The supersymmetric-particle masses are those of spectrum 1. Parton distribution is set 2. The production at center-of-mass angles 90°, 45°, and 30° is represented by solid, dashed, and dot-dashed curves, respectively.
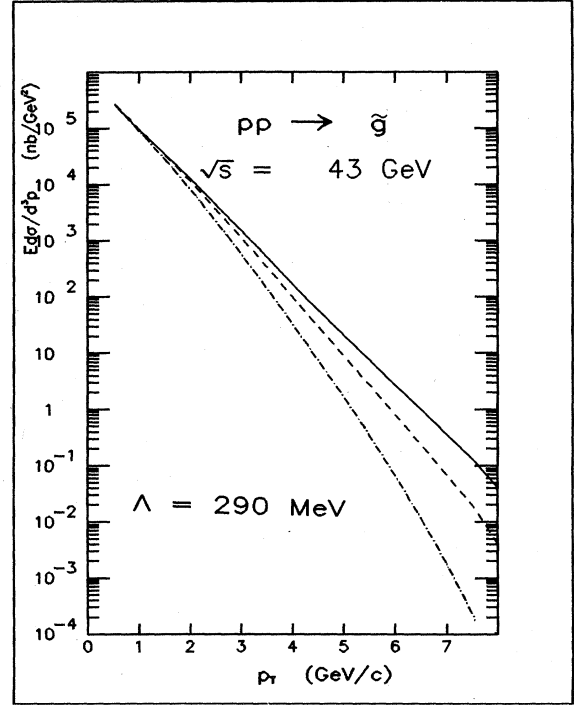
FIG. 46. Differential cross section $E\,d\sigma/d^3p$ for inclusive $\tilde{g}$ production for pp collisions at $\sqrt{s}=53$ GeV. All other parameters are as in Fig. 44.
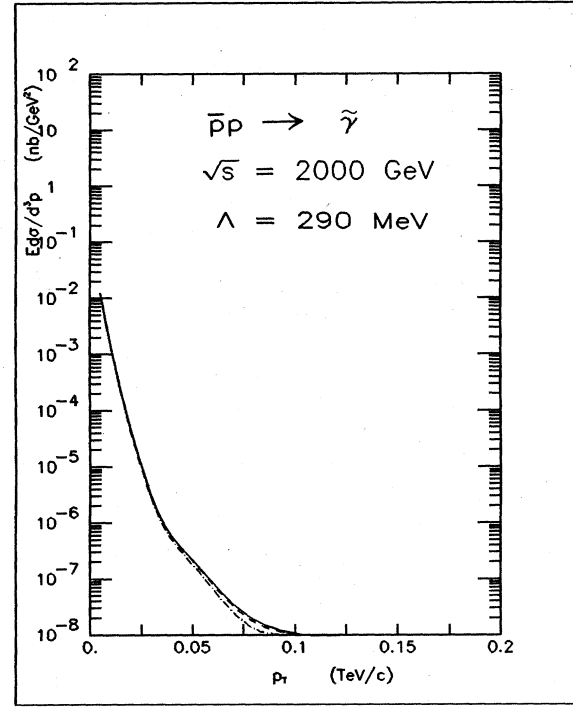
FIG. 47. Differential cross section $E\,d\sigma/d^3p$ for inclusive $\tilde{g}$ production for $p\bar{p}$ collisions at $\sqrt{s}=540$ GeV. All other parameters are as in Fig. 44.

FIG. 49. Differential cross section $E\,d\sigma/d^3p$ for inclusive $\tilde{\gamma}$ production for pp collisions at $\sqrt{s}=27$ GeV. All other parameters are as in Fig. 44.

FIG. 48. Differential cross section $E\,d\sigma/d^3p$ for inclusive $\tilde{g}$ production for $p\bar{p}$ collisions at $\sqrt{s}=2000$ GeV. All other parameters are as in Fig. 44.
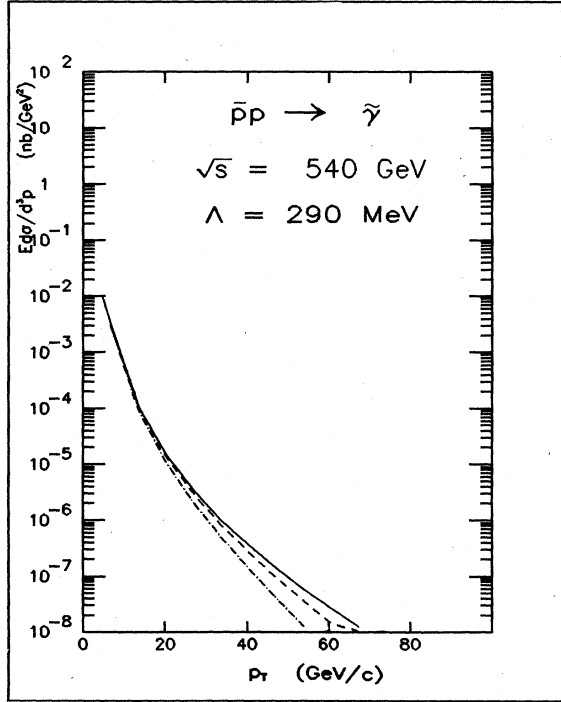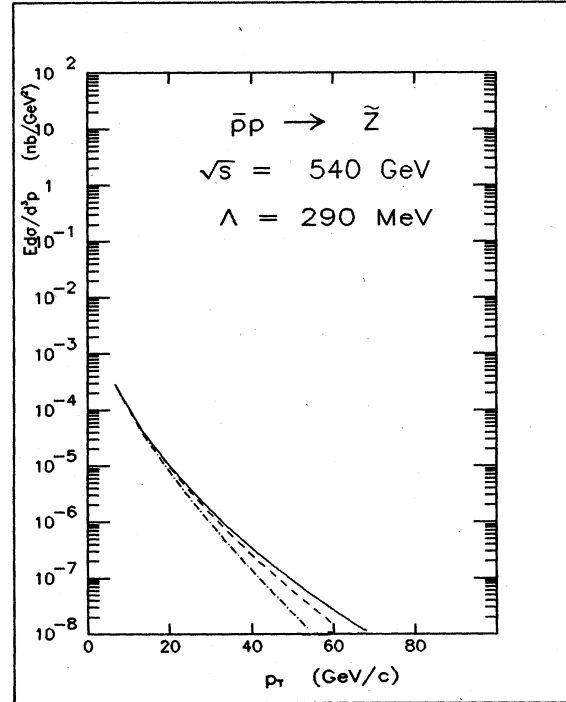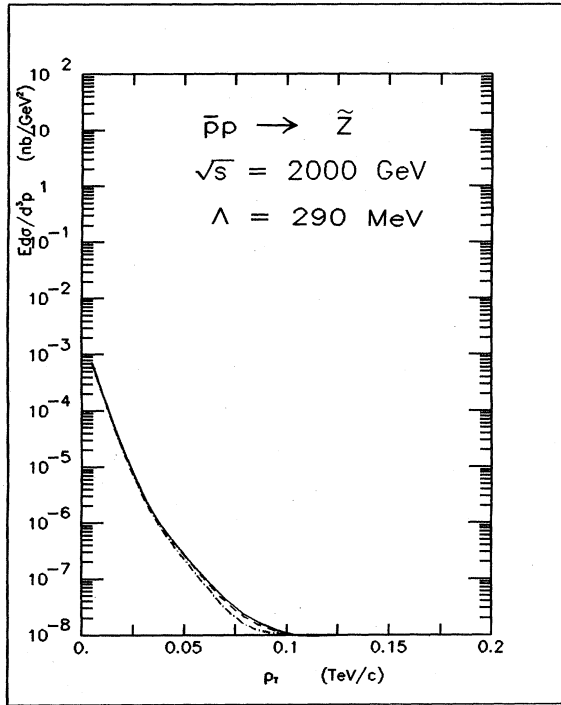
FIG. 50. Differential cross section $E\,d\sigma/d^3p$ for inclusive $\tilde{\gamma}$ production for pp collisions at $\sqrt{s}=43$ GeV. All other parameters are as in Fig. 44.

FIG. 51. Differential cross section $E \, d\sigma/d^3p$ for inclusive $\tilde{\gamma}$ production for pp collisions at $\sqrt{s} = 53$ GeV. All other parameters are as in Fig. 44.

FIG. 53. Differential cross section $E \, d\sigma/d^3p$ for inclusive $\tilde{\gamma}$ production for $p\bar{p}$ collisions at $\sqrt{s} = 2000$ GeV. All other parameters are as in Fig. 44.

FIG. 52. Differential cross section $E \, d\sigma/d^3p$ for inclusive $\tilde{\gamma}$ production for $p\bar{p}$ collisions at $\sqrt{s} = 540$ GeV. All other parameters are as in Fig. 44.

FIG. 54. Differential cross section $E \, d\sigma/d^3p$ for inclusive $\tilde{Z}$ production for $p\bar{p}$ collisions at $\sqrt{s} = 540$ GeV. All other parameters are as in Fig. 44.

FIG. 55. Differential cross section $E\, d\sigma/d^3p$ for inclusive production of $\tilde{Z}$ for $p\bar{p}$ collisions at $\sqrt{s} = 2000$ GeV. All other parameters are as in Fig. 44.
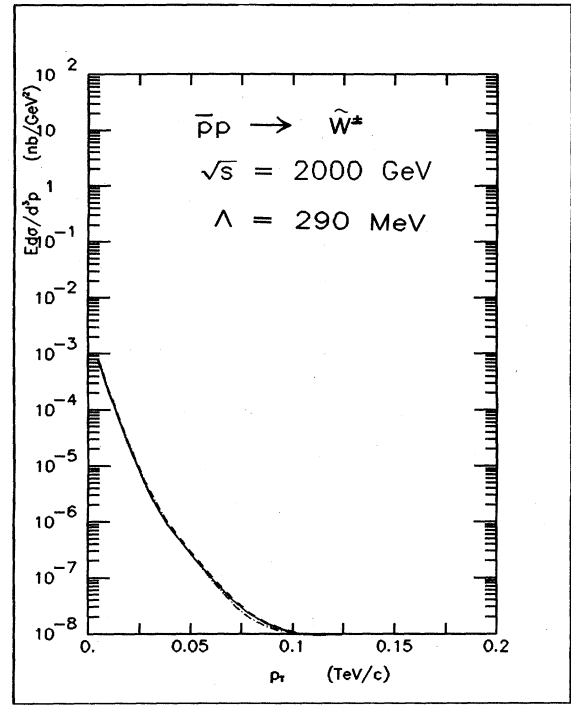

FIG. 57. Differential cross section $E\, d\sigma/d^3p$ for inclusive production of $\tilde{W}^+$ or $\tilde{W}^-$ for $p\bar{p}$ collisions at $\sqrt{s} = 2000$ GeV. All other parameters are as in Fig. 44.
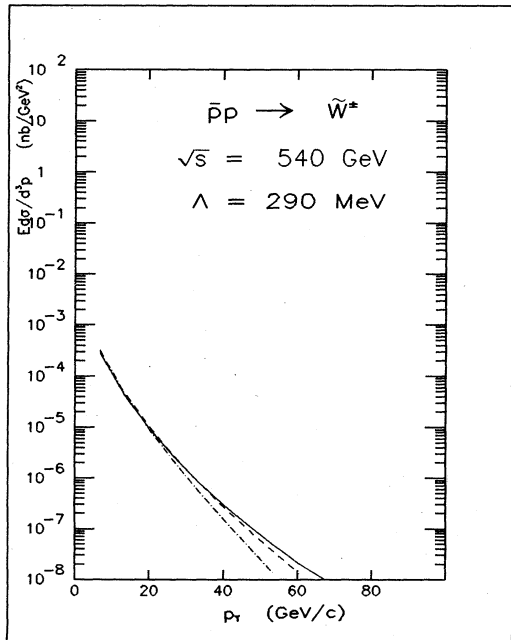

FIG. 56. Differential cross section $E\, d\sigma/d^3p$ for inclusive production of $\tilde{W}^+$ or $\tilde{W}^-$ for $p\bar{p}$ collisions at $\sqrt{s} = 540$ GeV. All other parameters are as in Fig. 44.
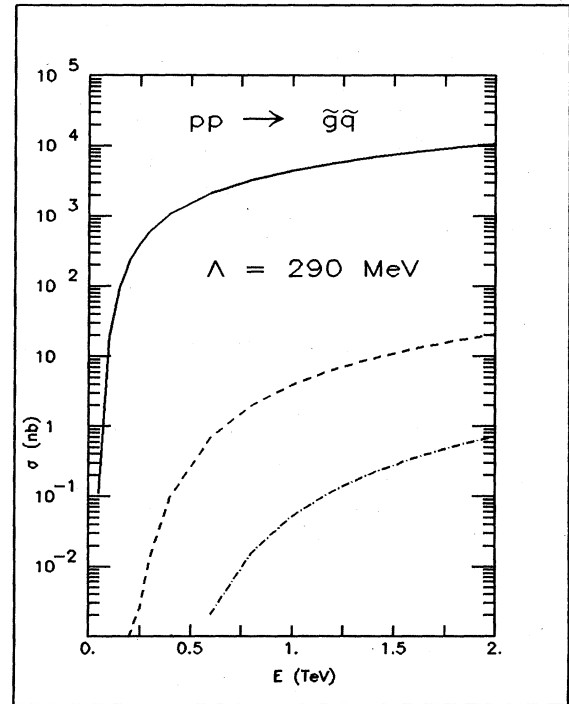

FIG. 58. Total cross section for pp (or $p\bar{p}$)$\rightarrow \tilde{g}\,\tilde{q}$ using parton distribution set 2. The cross sections are summed over up and down scalar quarks and scalar antiquarks. The supersymmetric-particle masses are as in Fig. 22. The scalar quarks $\tilde{q}_L$ and $\tilde{q}_R$ are assumed to be degenerate in mass but distinguishable.
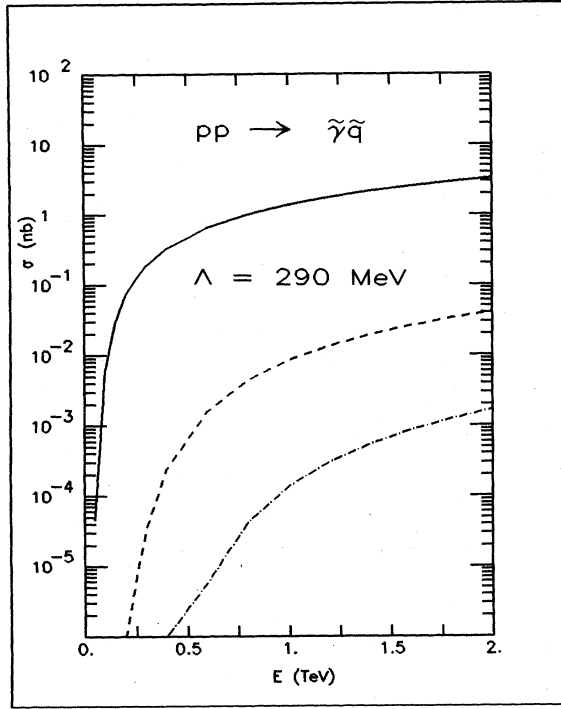
FIG. 59. Total cross section for pp (or $p\bar{p}$)$\to\tilde{\gamma}\,\tilde{q}$ using parton distribution set 2. The cross sections are summed over up and down scalar quarks and scalar antiquarks. The supersymmetric-particle masses are as in Fig. 22.
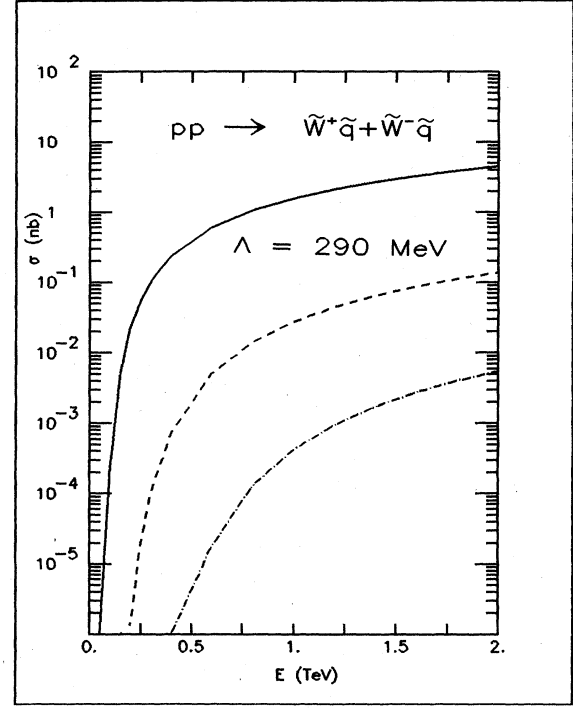

FIG. 61. Total cross section for pp (or $p\bar{p}$)$\to\tilde{W}^{+}\tilde{q}$ and $\tilde{W}^{-}\tilde{q}$ using parton distribution set 2. The cross sections are summed over up and down scalar quarks and scalar antiquarks. The supersymmetric-particle masses are as in Fig. 22.

FIG. 60. Total cross section for pp (or $p\bar{p}$)$\to\tilde{Z}\tilde{q}$ using parton distribution set 2. The cross sections are summed over up and down scalar quarks and scalar antiquarks. The supersymmetric-particle masses are as in Fig. 22.
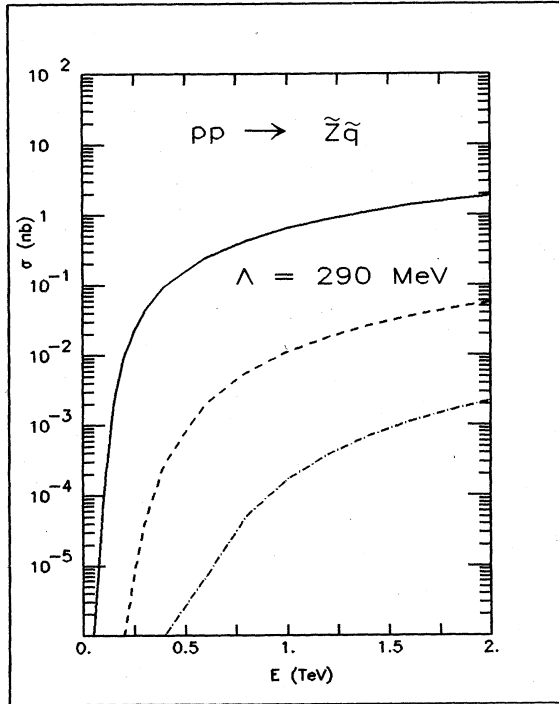
contributions, the pp and $p\bar{p}$ cross sections are the same. To obtain a measure of the uncertainty associated with initial distributions for gluons and quarks, we have also computed the cross sections using distribution set 1. These results are displayed in Figs. 62—65. Again, the differences are 10—20 % effects.

Probably the easiest process of this type to observe is scalar-quark—gluino production. For spectrum 3 ($m_{\tilde{q}}=m_{\tilde{g}}=100$ GeV/c^2), $\sigma(pp\to\tilde{q}+\tilde{g})=5.2\times10^{-2}$ nb at $\sqrt{s}=1000$ GeV, while for spectrum 2 ($m_{\tilde{q}}=m_{\tilde{g}}=50$ GeV/c^2), $\sigma(pp\to\tilde{q}+\tilde{g})=3.9$ nb at the same energy. The signature of these events is a jet in each hemisphere and missing $p_\perp$.

The cross section for $\tilde{\gamma}\,\tilde{q}$ production is 1.4 nb at $\sqrt{s}=1000$ GeV for spectrum 1 ($m_{\tilde{\gamma}}=100$ eV/c^2 and $m_{\tilde{q}}=20$ GeV/c^2). For spectrum 2 ($m_{\tilde{\gamma}}=m_{\tilde{q}}=50$ GeV/c^2), $\sigma(pp\to\tilde{\gamma}\,\tilde{q})=8.4\times10^{-3}$ nb at the same energy. If the gluino is light, the scalar quark will decay into a quark and gluino and the events will look similar to the $\tilde{\gamma}\,\tilde{g}$ events discussed in the previous section. If the photino decays to a photon and a light Goldstone fermion, then these events will have a hard photon in one hemisphere and a broad jet in the other with a $p_\perp$ imbalance due to the escaping Goldstone fermions. On the other hand, if the photino is stable, then there will be a jet in one hemisphere and nothing in the other.

Finally, consider the processes $pp\to(\tilde{W}^{+}+\tilde{W}^{-})\tilde{q}$ and
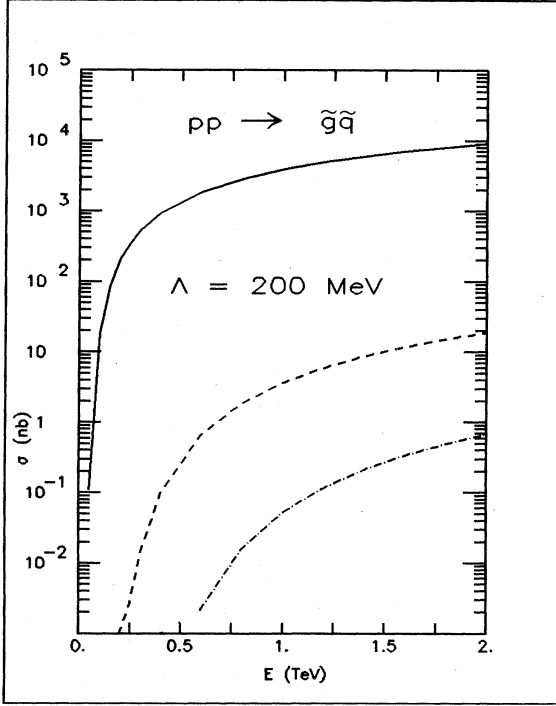
FIG. 62. Total cross section for pp (or $p\bar{p}$)$\rightarrow \tilde{g}\,\tilde{q}$ using parton distribution set 1. The cross sections are summed over up and down scalar quarks and scalar antiquarks. The supersymmetric-particle masses are as in Fig. 22.

FIG. 64. Total cross section for pp (or $p\bar{p}$)$\rightarrow \tilde{Z}\tilde{q}$ using parton distribution set 1. The cross sections are summed over up and down scalar quarks and scalar antiquarks. The supersymmetric-particle masses are as in Fig. 22.
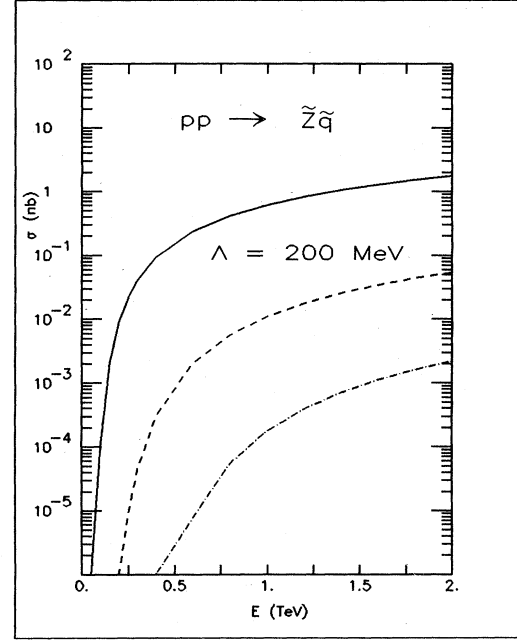

FIG. 63. Total cross section for pp (or $p\bar{p}$)$\rightarrow \tilde{\gamma}\tilde{q}$ using parton distribution set 1. The cross sections are summed over up and down scalar quarks and scalar antiquarks. The supersymmetric-particle masses are as in Fig. 22.
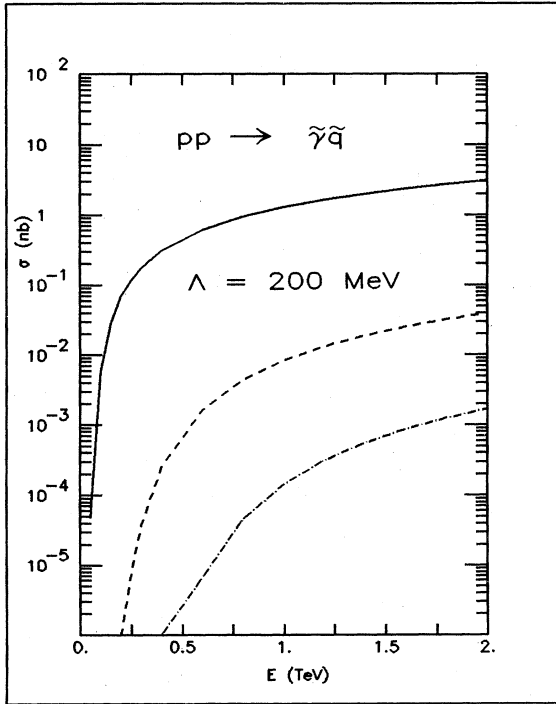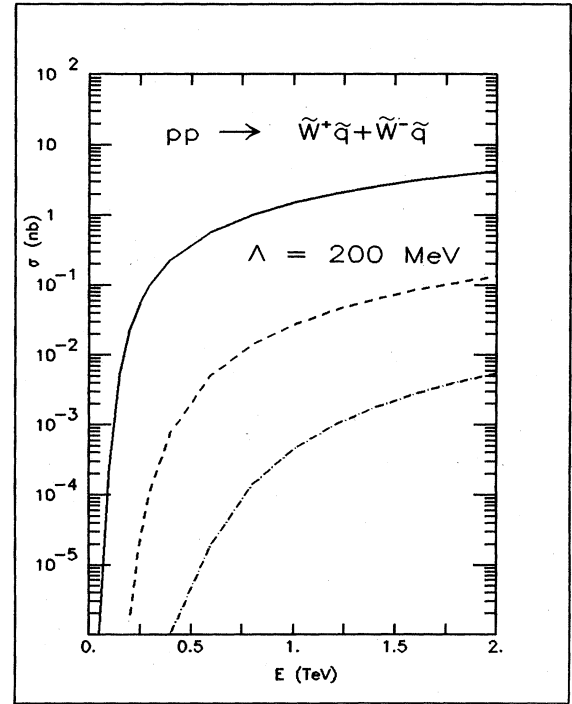

FIG. 65. Total cross section for pp (or $p\bar{p}$)$\rightarrow \tilde{W}^{+}\tilde{q}$ and $\tilde{W}^{-}\tilde{g}$ using parton distribution set 1. The cross sections are summed over up and down scalar quarks and scalar antiquarks and both W-gaugino charges. The supersymmetric-particle masses are as in Fig. 22.

$pp \rightarrow \tilde{Z}\,\tilde{q}$. The cross sections at $\sqrt{s} = 1000$ GeV are $\sigma(pp \rightarrow \tilde{Z}\tilde{q}) = 1.1 \times 10^{-2}$ nb and $\sigma(pp \rightarrow \tilde{W}\tilde{q}) = 2.7 \times 10^{-2}$ nb for spectrum 2 ($m_{\tilde{Z}} = m_{\tilde{W}} = m_{\tilde{q}} = 50$ GeV/c^2). The relatively small cross sections along with the lack of any clear experimental signature for the $\tilde{W}$ and $\tilde{Z}$ make these processes difficult to observe.

In Figs. 66—77, we present the differential cross sections for inclusive $\tilde{g}$, $\tilde{\gamma}$, and $\tilde{q}$ production in pp (or $p\bar{p}$) interactions at center-of-mass production angles of 90°, 45°, and 30°. We again make favorable assumptions (spectrum 1) about the masses of $\tilde{\gamma}$, $\tilde{g}$, and $\tilde{q}$.

E. Scalar-quark—scalar-quark production

Finally we turn to the pair production of two scalar superpartners of the quarks. Our results for pp collisions are shown in Figs. 78—84. The total cross section for production of up and down scalar quarks and scalar-antiquarks is given separately in Fig. 85. The results for $p\bar{p}$ collisions are shown in Figs. 86—93. Since the cross sections for pair production of identical-flavor scalar quarks are sensitive to the initial gluon distributions, we have also calculated the cross sections for $pp \rightarrow \tilde{q}_u^* \tilde{q}_u$ and $p\bar{p} \rightarrow \tilde{q}_u^* \tilde{q}_u$ using distribution set 1. These results are shown in Figs. 94 and 95. The total cross section for up
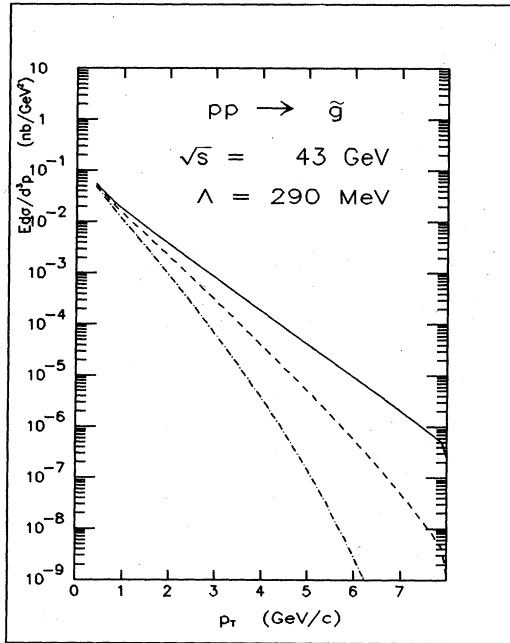

FIG. 67. Differential cross section $E\,d\sigma/d^3p$ for inclusive $\tilde{g}$ production for pp collisions at $\sqrt{s} = 53$ GeV. All other parameters are as in Fig. 66.

FIG. 66. Differential cross section $E\,d\sigma/d^3p$ for inclusive $\tilde{g}$ production at center-of-mass scattering angles $\theta = 90°$, 45°, and 30° for pp collisions at $\sqrt{s} = 43$ GeV. The supersymmetric-particle masses are those of spectrum 1. The parton distribution is set 2. We have only included the contribution when the other final-state superpartner is a scalar quark and have summed over all flavors of scalar quarks and scalar antiquarks. The production at center-of-mass angles 90°, 45°, and 30°, is represented by solid, dashed, and dot-dashed curves, respectively.
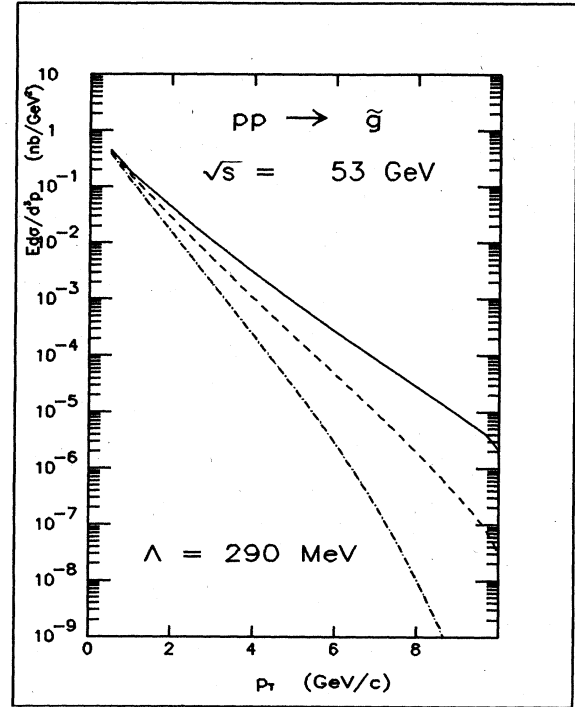

FIG. 68. Differential cross section $E\,d\sigma/d^3p$ for inclusive $\tilde{g}$ production for $p\bar{p}$ collisions at $\sqrt{s} = 540$ GeV. All other parameters are as in Fig. 66.

FIG. 69. Differential cross section $E \, d\sigma/d^3p$ for inclusive $\tilde{g}$ production for $p\bar{p}$ collisions at $\sqrt{s} = 2000$ GeV. All other parameters are as in Fig. 66.

FIG. 71. Differential cross section $E \, d\sigma/d^3p$ for inclusive $\tilde{\gamma}$ production for pp collisions at $\sqrt{s} = 53$ GeV. All other parameters are as in Fig. 66.

FIG. 70. Differential cross section $E \, d\sigma/d^3p$ for inclusive $\tilde{\gamma}$ production for pp collisions at $\sqrt{s} = 43$ GeV. All other parameters are as in Fig. 66.
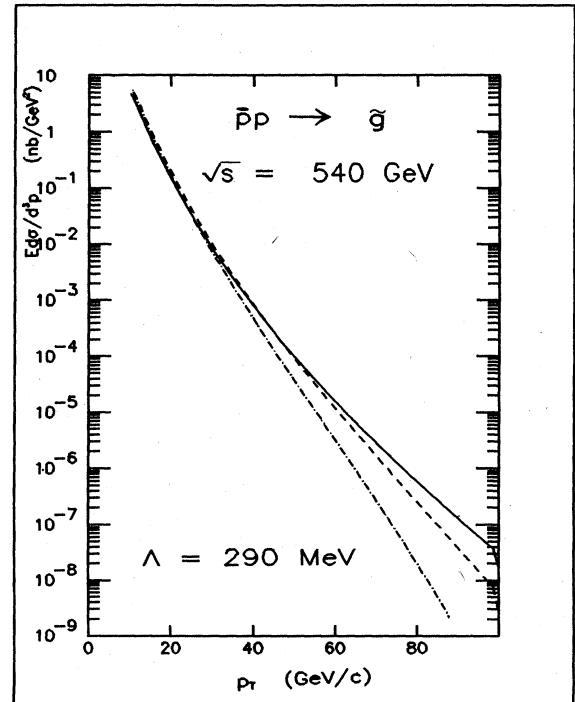

FIG. 72. Differential cross section $E \, d\sigma/d^3p$ for inclusive $\tilde{\gamma}$ production for $p\bar{p}$ collisions at $\sqrt{s} = 540$ GeV. All other parameters are as in Fig. 66.
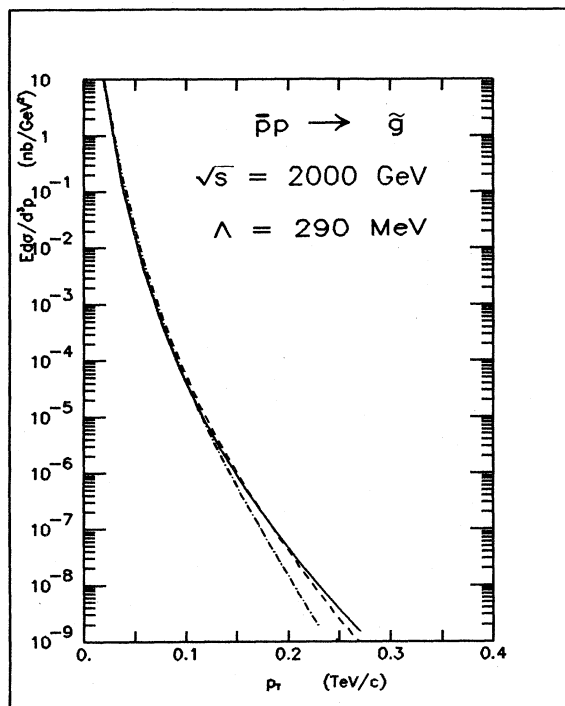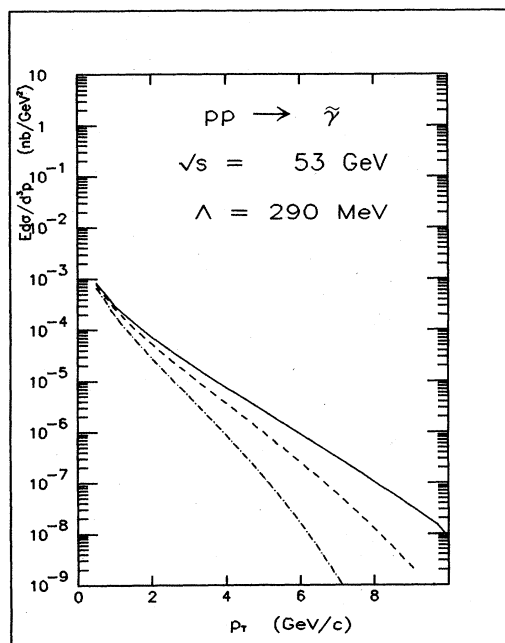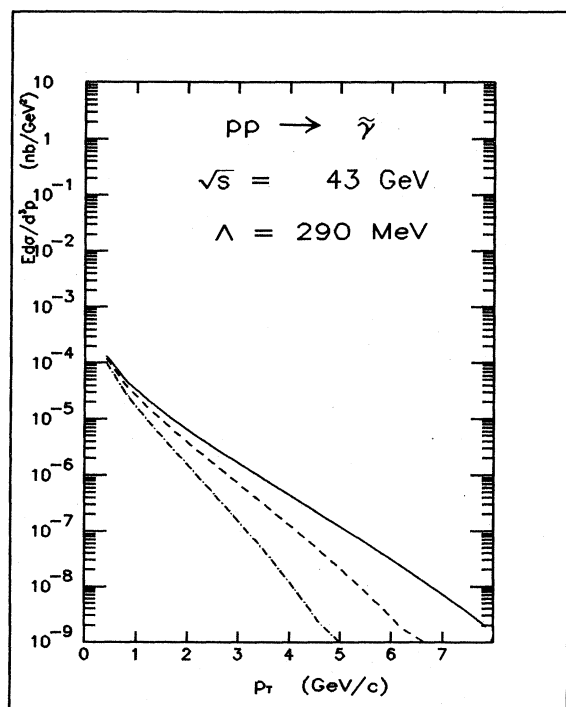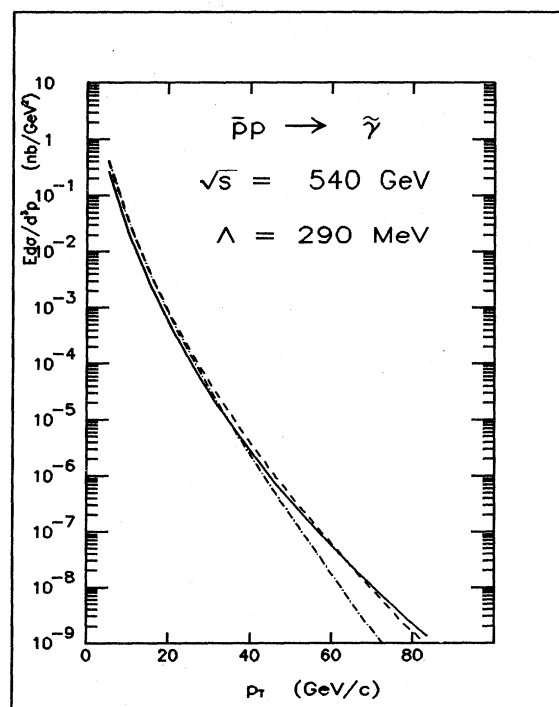
FIG. 73. Differential cross section $E \, d\sigma/d^3p$ for inclusive $\tilde{\gamma}$ production for $p\bar{p}$ collisions at $\sqrt{s} = 2000$ GeV. All other parameters are as in Fig. 66.
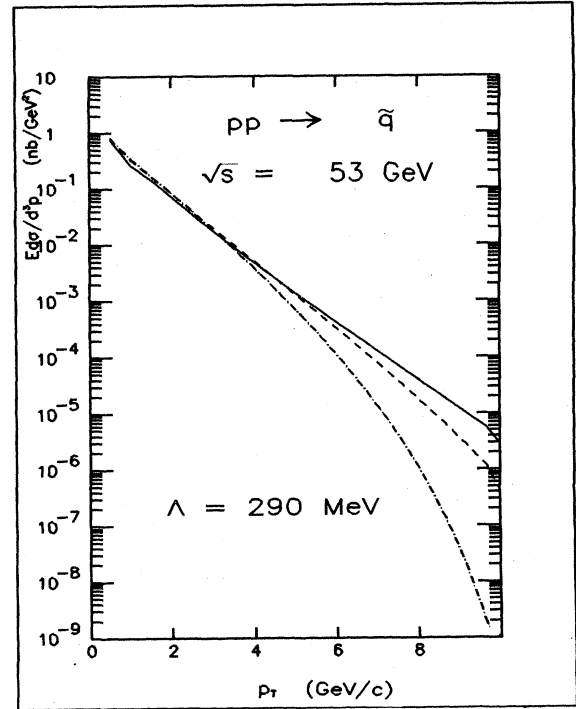
FIG. 75. Differential cross section $E \, d\sigma/d^3p$ for inclusive scalar-quark production for pp collisions at $\sqrt{s} = 53$ GeV. All other parameters are as in Fig. 66.
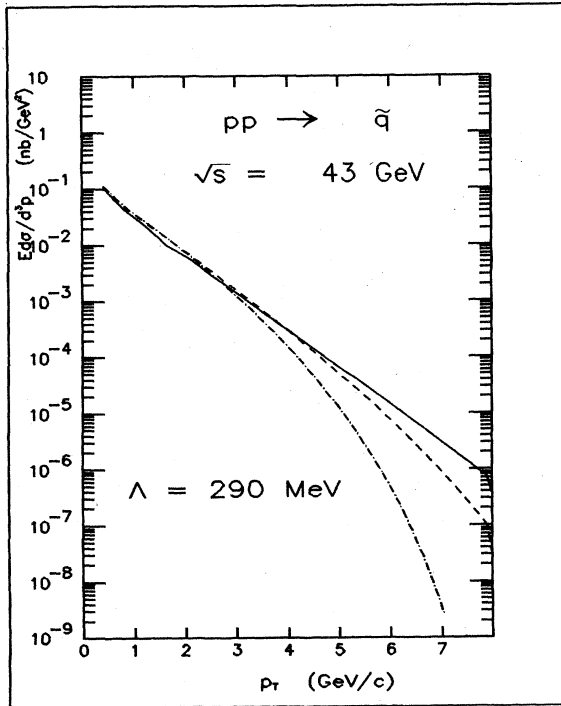
FIG. 74. Differential cross section $E \, d\sigma/d^3p$ for inclusive scalar-quark production for pp collisions at $\sqrt{s} = 43$ GeV. We have summed over scalar quarks, scalar antiquarks and scalar-quark flavors. We have included only the contribution when the other final-state superpartner is gaugino. All other parameters are as in Fig. 66.
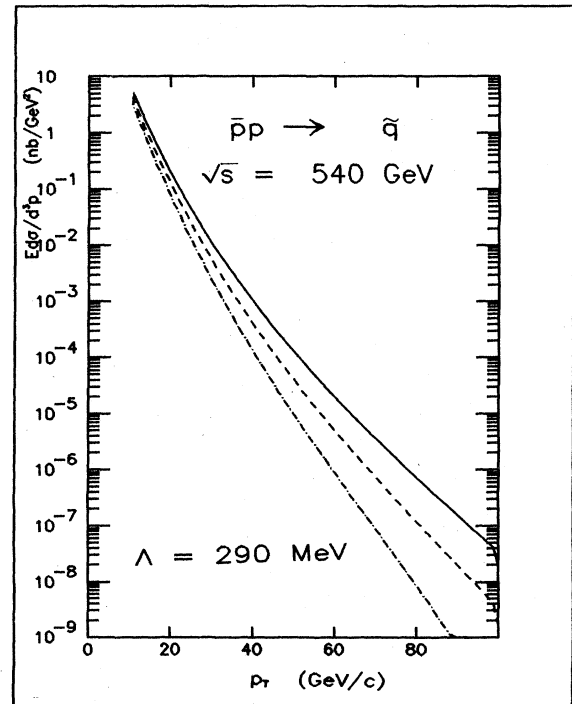
FIG. 76. Differential cross section $E \, d\sigma/d^3p$ for inclusive scalar-quark production for $p\bar{p}$ collisions at $\sqrt{s} = 540$ GeV. All other parameters are as in Fig. 66.
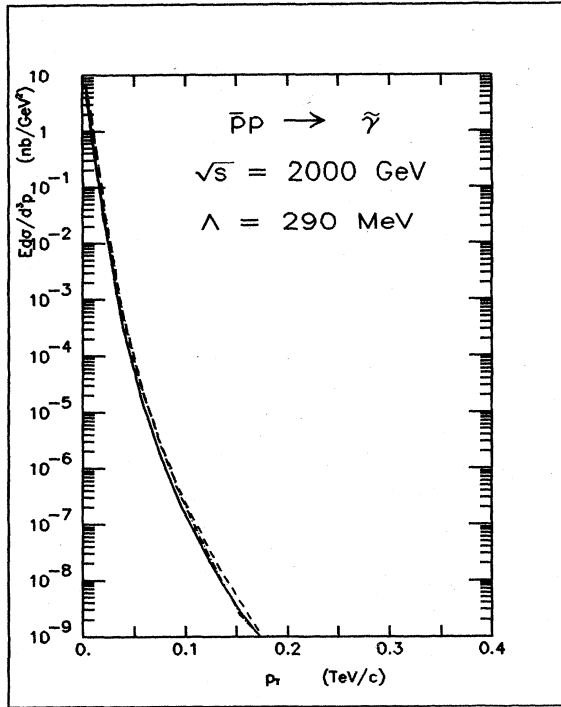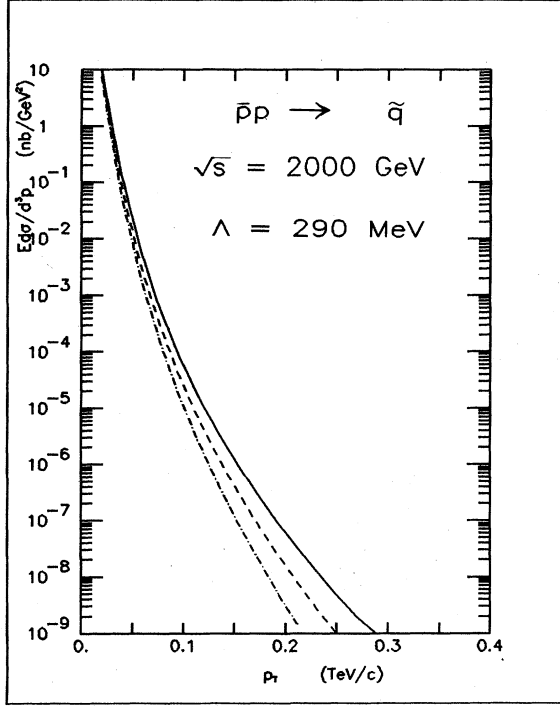
FIG. 77. Differential cross section $E\,d\sigma/d^3p$ for inclusive scalar-quark production for $p\bar{p}$ collisions at $\sqrt{s}=2000$ GeV. All other parameters are as in Fig. 66.


FIG. 79. Total cross section $pp\rightarrow\tilde{q}_u\tilde{q}_u+\tilde{q}_d\tilde{q}_d$. All other parameters are as in Fig. 78.
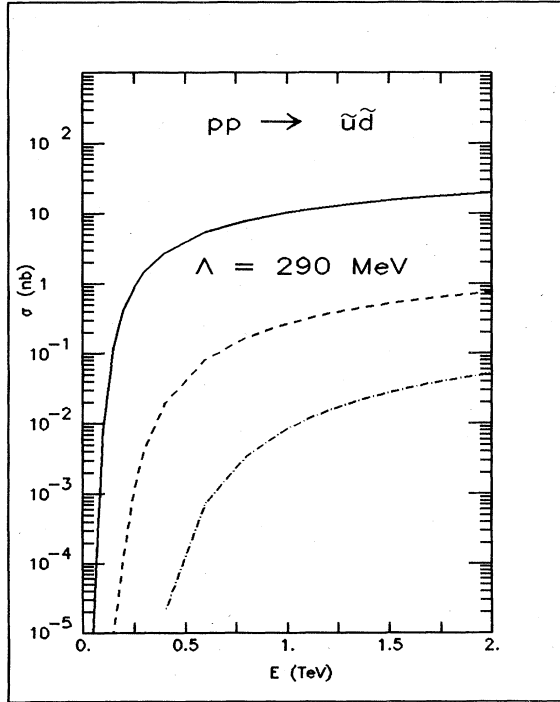
FIG. 78. Total cross section for $pp\rightarrow\tilde{q}_u\tilde{q}_d$. All scalar-quark production cross sections assume that $\tilde{q}_L$ and $\tilde{q}_R$ are degenerate in mass but distinguishable. The supersymmetric-particle masses are as in Fig. 22. We use parton distribution set 2.

FIG. 80. Total cross section for $pp\rightarrow\tilde{q}_u\tilde{q}_d^*+\tilde{q}_d\tilde{q}_u^*$. All other parameters are as in Fig. 78.

FIG. 81. Total cross section for $pp \to \tilde{q}_u \tilde{q}_u^*$. All other parameters are as in Fig. 78.
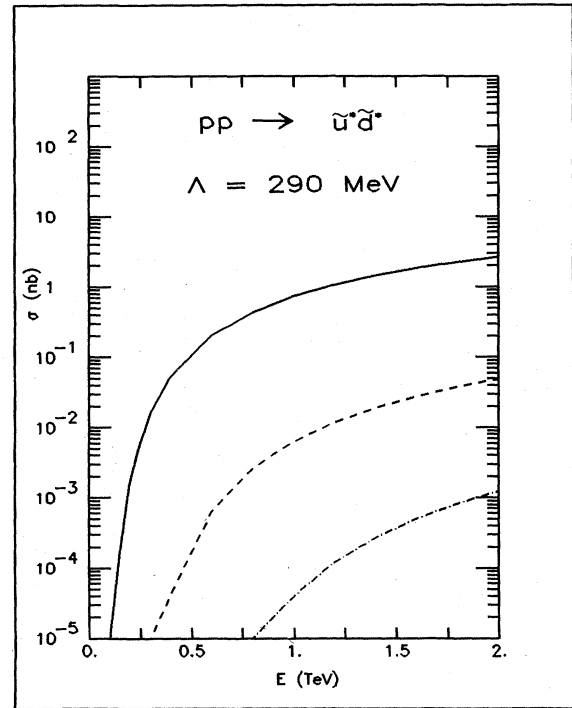
FIG. 83. Total cross section for $pp \to \tilde{q}_u^* \tilde{q}_d^*$. All other parameters are as in Fig. 78.
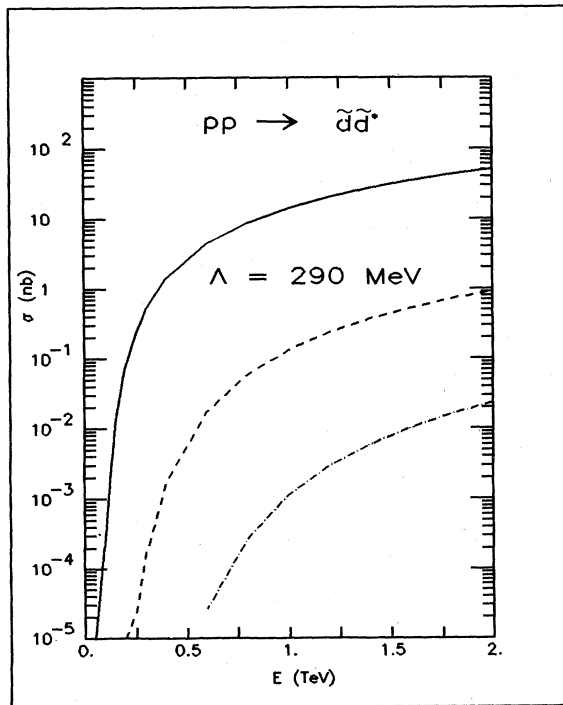
FIG. 82. Total cross section for $pp \to \tilde{q}_d \tilde{q}_d^*$. All other parameters are as in Fig. 78.

FIG. 84. Total cross section for $pp \to \tilde{q}_u^* \tilde{q}_u^* + \tilde{q}_d^* \tilde{q}_d^*$. All other parameters are as in Fig. 78.

FIG. 85. Total cross section for $pp \rightarrow (\tilde{q}_u$ or $\tilde{q}_d$ or $\tilde{q}_u^*$ or $\tilde{q}_d^*)+(\tilde{q}_u$ or $\tilde{q}_d$ or $\tilde{q}_u^*$ or $\tilde{q}_d^*)$. All other parameters are as in Fig. 78.

FIG. 87. Total cross section for $p\bar{p} \rightarrow \tilde{q}_u\tilde{q}_u+\tilde{q}_d\tilde{q}_d$. All other parameters are as in Fig. 78.

FIG. 86. Total cross section for $p\bar{p} \rightarrow \tilde{q}_u\tilde{q}_d$. All other parameters are as in Fig. 78.
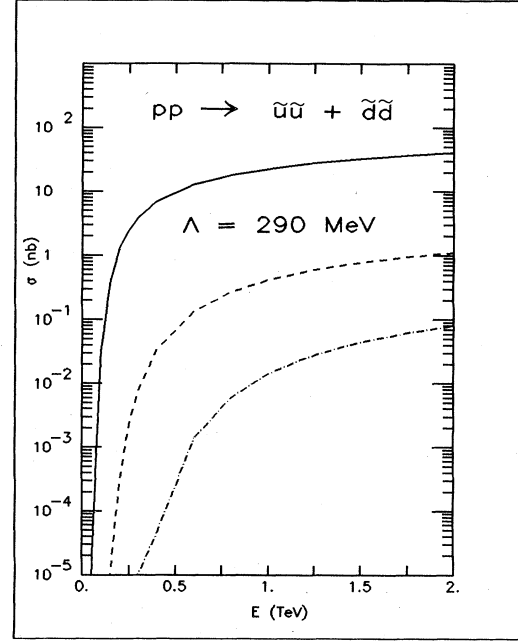
FIG. 88. Total cross section for $p\bar{p} \rightarrow \tilde{q}_u\tilde{q}_d^*+\tilde{q}_d\tilde{q}_u^*$. All other parameters are as in Fig. 78.
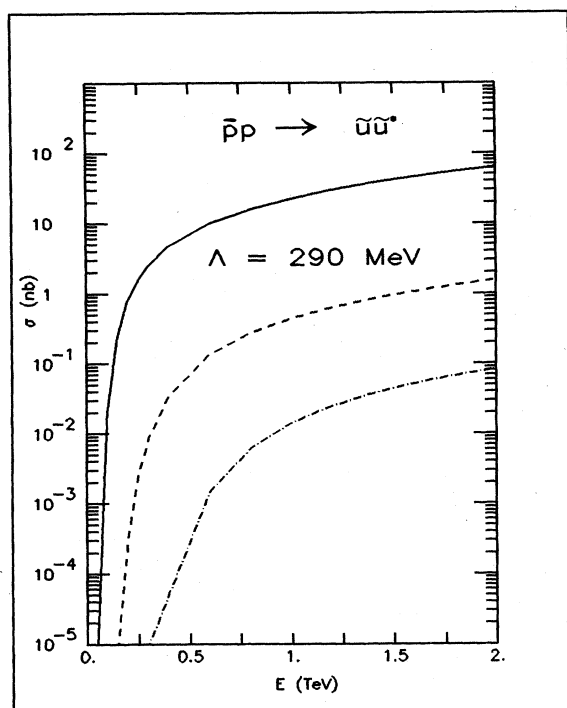
FIG. 89. Total cross section for $p\bar{p} \rightarrow \tilde{q}_u \tilde{q}_u^*$. All other parameters are as in Fig. 78.
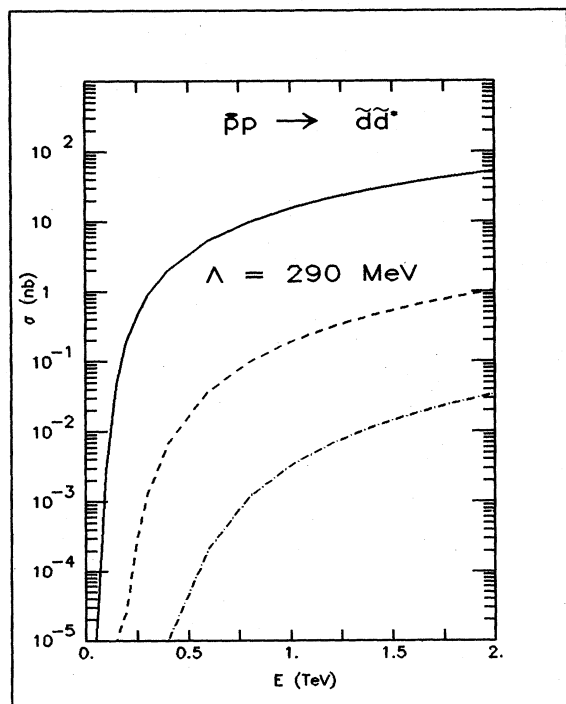
FIG. 90. Total cross section for $p\bar{p} \rightarrow \tilde{q}_d \tilde{q}_d^*$. All other parameters are as in Fig. 78.
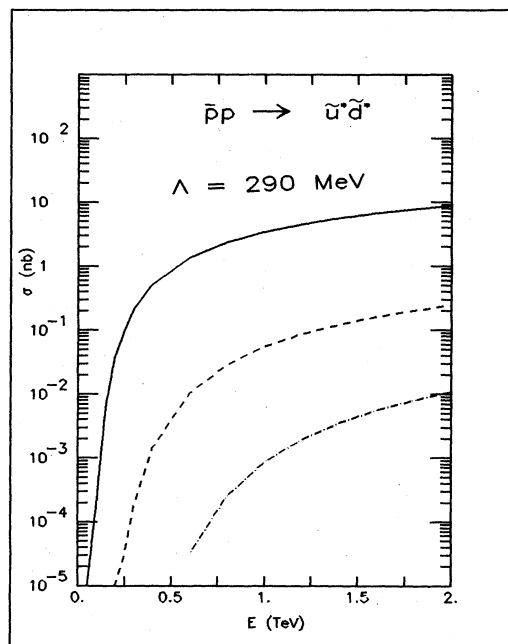
FIG. 91. Total cross section for $p\bar{p} \rightarrow \tilde{q}_u^* \tilde{q}_d^*$. All other parameters are as in Fig. 78.

and down scalar-quark and scalar-antiquark production at $\sqrt{s} = 1000$ GeV is $\sigma(pp \rightarrow \tilde{q}\tilde{q} + \tilde{q}^*\tilde{q} + \tilde{q}^*\tilde{q}^*) = 1.2$ nb for spectrum 2 ($m_{\tilde{q}_u} = m_{\tilde{q}_d} = 50$ GeV/c^2), using distribution set 2. If the scalar quark is lighter than the gluino, but heavier than the photino, then it will decay by $\tilde{q} \rightarrow q\tilde{\gamma}$ and the $\tilde{q}\tilde{q}^*$ final state will be $q\bar{q}\tilde{\gamma}\tilde{\gamma}$. If, instead, the scalar quark is heavier than the unstable gluino, so that $\tilde{q} \rightarrow q\tilde{g}$, the $\tilde{q}\tilde{q}^*$ final state will be $q\bar{q}q\bar{q}q\bar{q}\tilde{\gamma}\tilde{\gamma}$, which will con-
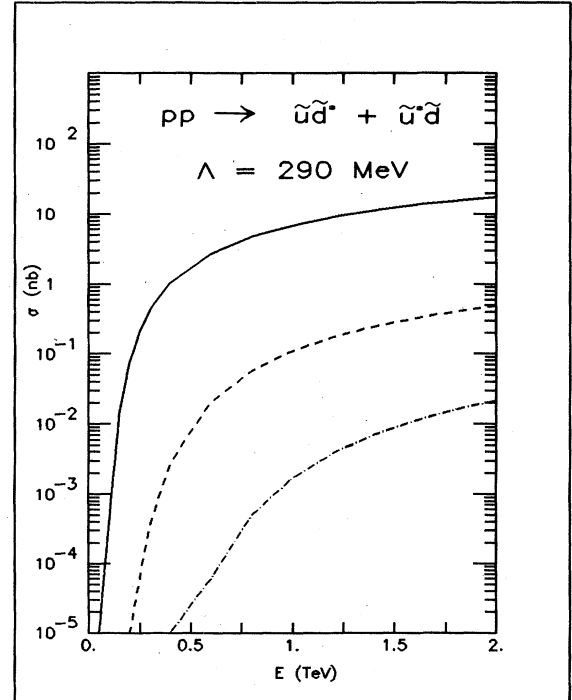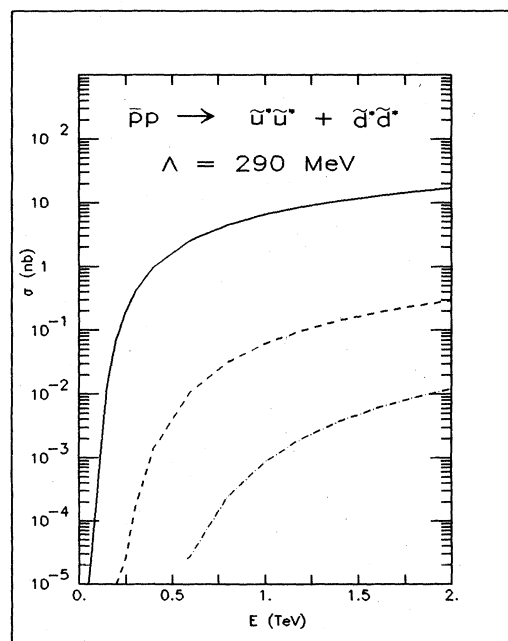

FIG. 92. Total cross section for $p\bar{p} \rightarrow \tilde{q}_u^* \tilde{q}_u^* + \tilde{q}_d^* \tilde{q}_d^*$. All other parameters are as in Fig. 78.
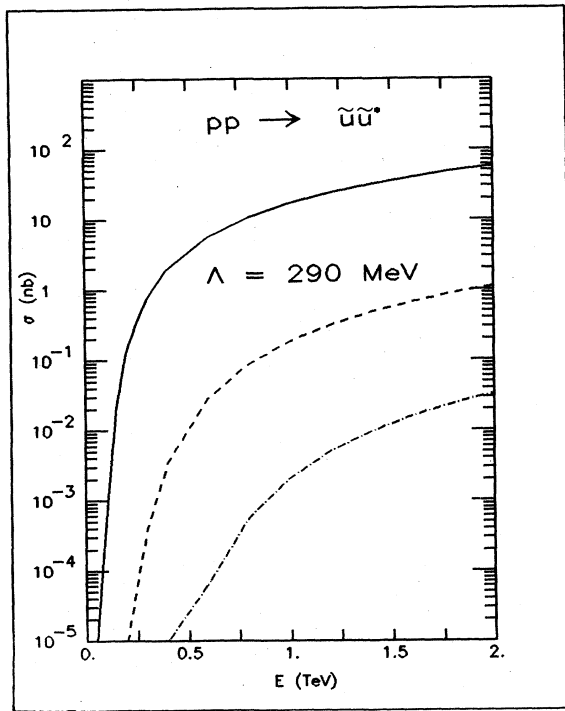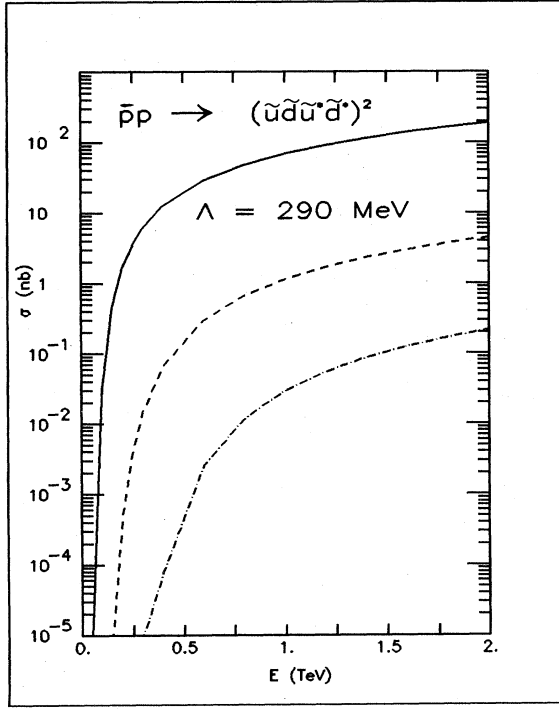
FIG. 93. Total cross section for $p\bar{p}\rightarrow(\tilde{q}_u$ or $\tilde{q}_d$ or $\tilde{q}^*_u$ or $\tilde{q}^*_d)+(\tilde{q}_u$ or $\tilde{q}_d$ or $\tilde{q}^*_u$ or $\tilde{q}^*_d)$. All other parameters are as in Fig. 78.
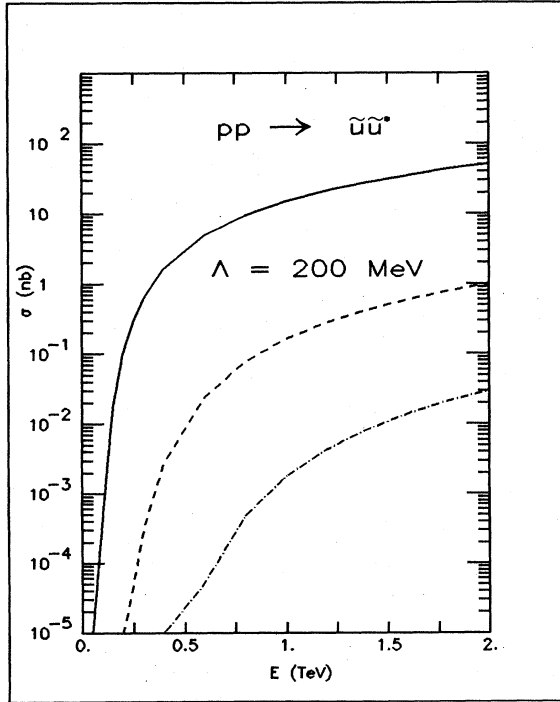
FIG. 94. Total cross section for $pp\rightarrow\tilde{q}_u\tilde{q}^*_u$ using parton distribution set 1. All other parameters are as in Fig. 78.
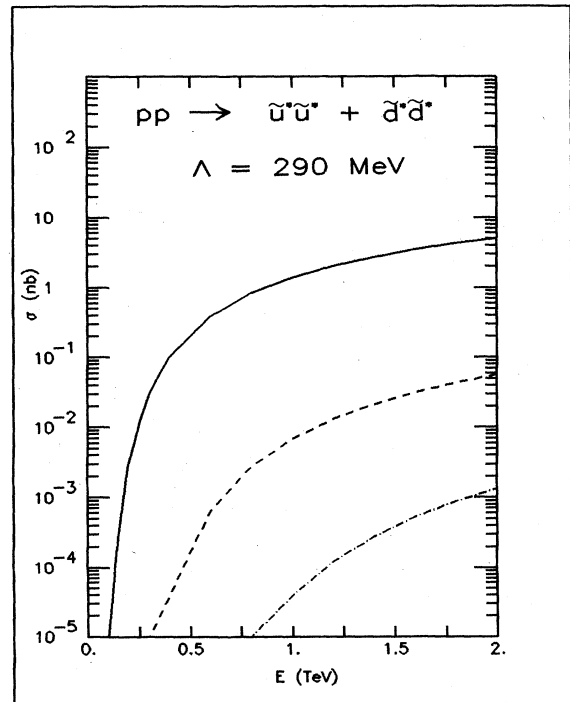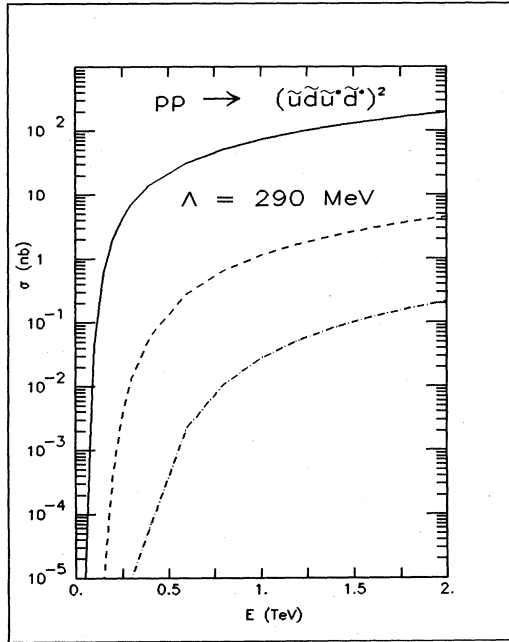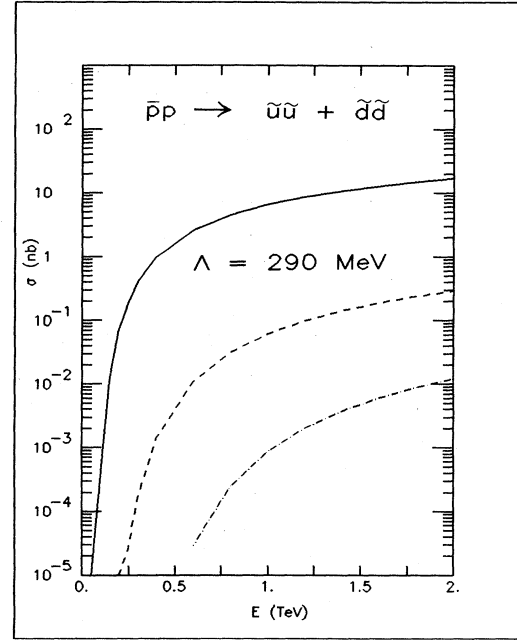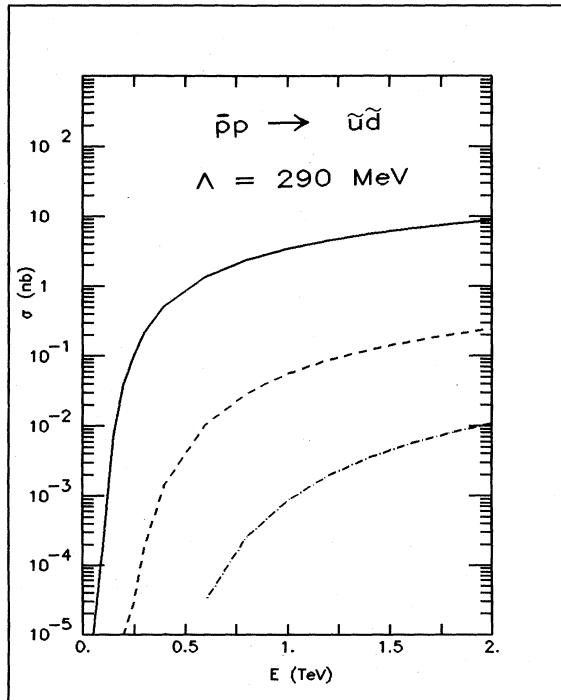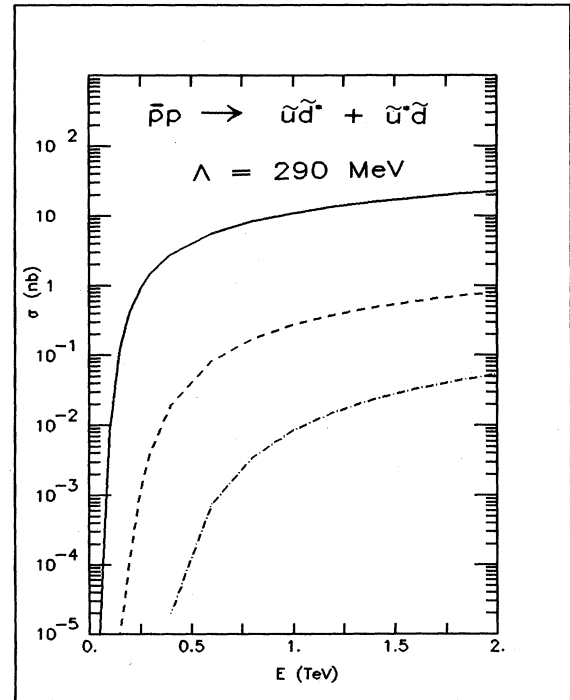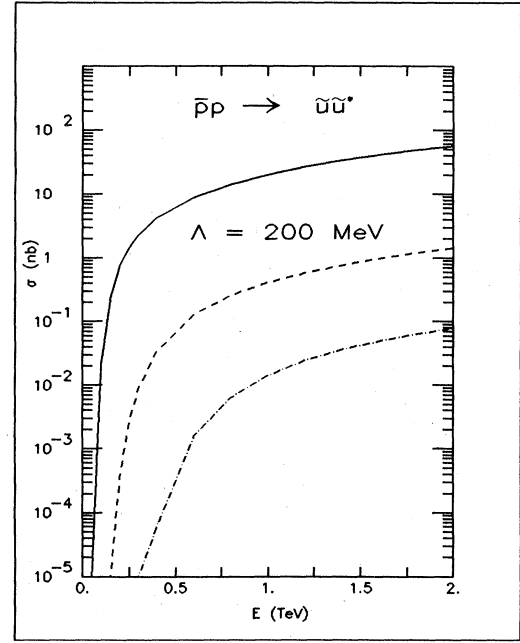

FIG. 95. Total cross section for $p\bar{p}\rightarrow\tilde{q}_u\tilde{q}^*_u$ using parton distribution set 1. All other parameters are as in Fig. 78.

siderably dilute the missing-transverse-momentum signature.

A special feature of some supersymmetric models is that the heaviest quark is associated with the lightest scalar quark.[66] In these models the lightest scalar quark would be the top scalar quark. The total cross section for this process is shown in Fig. 96 for pp and Fig. 97 for $p\bar{p}$ collisions. This scalar quark would then probably decay to a real or virtual top quark and a gluino which would give a good experimental signature.

The differential cross section $E\,d\sigma/d^3p$ for inclusive scalar-quark production in $p\bar{p}$ collisions is shown in Figs. 98 and 99 for production angles of 90°, 45°, and 30°. The differential cross section for inclusive top-scalar-quark production in $p\bar{p}$ collisions is shown in Figs. 100 and 101. The masses are those of spectrum 1.

In Fig. 102 we compare the production of scalar quarks and gluinos in the three processes $\tilde{q}\tilde{q}$, $\tilde{q}\tilde{g}$, and $\tilde{g}\tilde{g}$ for spectrum 2 ($m_{\tilde{q}}=m_{\tilde{g}}=50$ GeV/c^2). We see that at low energies the cross sections are in the order

$$\sigma(pp\rightarrow\tilde{q}\tilde{q})>\sigma(pp\rightarrow\tilde{q}\tilde{g})>\sigma(pp\rightarrow\tilde{g}\tilde{g})\ .$$

Hence the most likely way to see scalar quarks is in pair production and for gluinos is in associated production with a scalar quark. At high energies the order is inverted, so that scalar quarks are found mainly in associated production with gluinos.

F. Limits revisited

Here we use the results of Sec. III to derive the limits on gluinos and scalar quarks which are quoted in Sec. II.
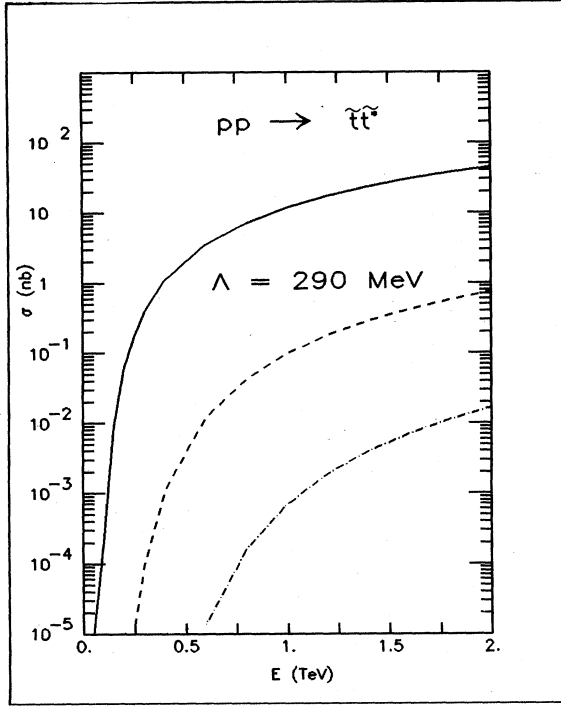
FIG. 96. Total cross section for $pp \to \tilde{t}\,\tilde{t}\,^*$, where $\tilde{t}$ is a top scalar quark. All other parameters are as in Fig. 78.
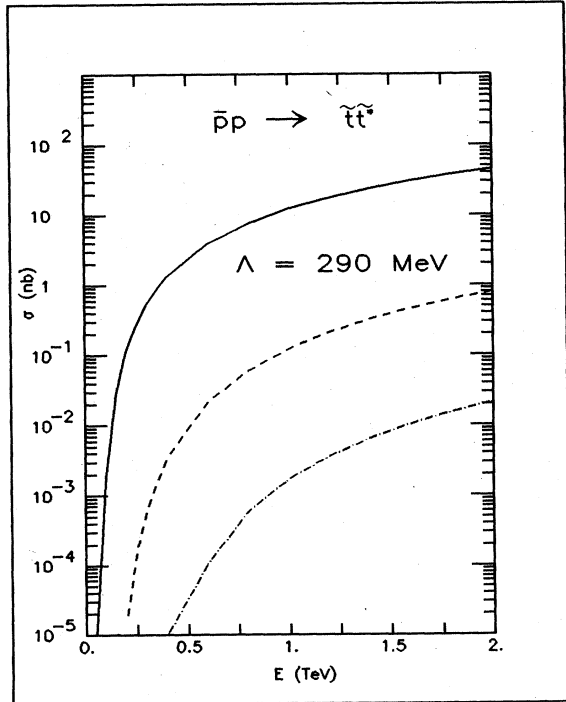
FIG. 97. Total cross section for $p\bar{p} \to \tilde{t}\,\tilde{t}\,^*$, where $\tilde{t}$ is a top scalar quark. All other parameters are as in Fig. 78.
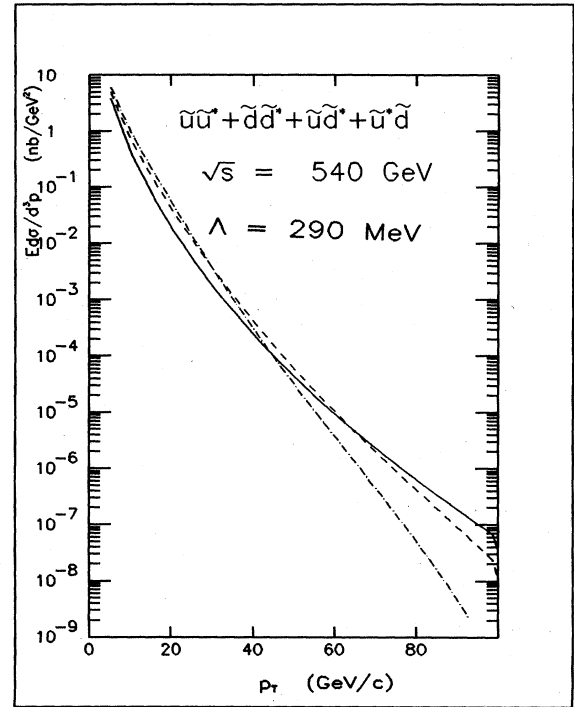
FIG. 98. Differential cross section section $E\,d\sigma/d^3p$ for inclusive scalar-quark production at center-of-mass scattering angles $\theta = 90°$, 45°, and 30° for $p\bar{p}$ collisions at $\sqrt{s} = 540$ GeV. We have summed over up and down scalar quarks and scalar anti quarks and used the supersymmetric-particle masses of spectrum 1. The contributions from all reactions leading to scalar-quark—scalar-antiquark pairs in the final states are included. The parton distribution of set 2 was used. The production at center-of-mass angles 90°, 45°, and 30° is represented by solid, dashed, and dot-dashed curves, respectively.

We consider three experiments here—Cutts et al.,[33] Alper et al.,[33] and Gustafson et al.[34]

The experiment of Cutts et al.[33] was a 400-GeV proton-nucleon experiment to search for massive long-lived particles. The experiment was performed at a laboratory angle of 2.5 mrad and was sensitive to charges greater than $2e/3$ and lifetimes greater than 5×10^{-8} sec. The limit they obtain is

$$E \frac{d\sigma}{d^3p} \bigg|_{p_\perp = 0.175 \text{ GeV}/c}$$

$$< 1.1 \times 10^{-37} \text{ cm}^2/\text{GeV}^2 \text{ per nucleon} \qquad (4.21)$$

for long-lived particles with masses between 4 and 10 GeV/c^2.

We reinterpret this result as a limit on stable charge 1 R hadrons (an example of such a state is $u\bar{d}\tilde{g}$). Using Eqs. (3.1) and (3.10), we find that at 400 GeV and 2.5 mrad, the differential cross section for pair-producing 9-GeV/c^2 gluinos is
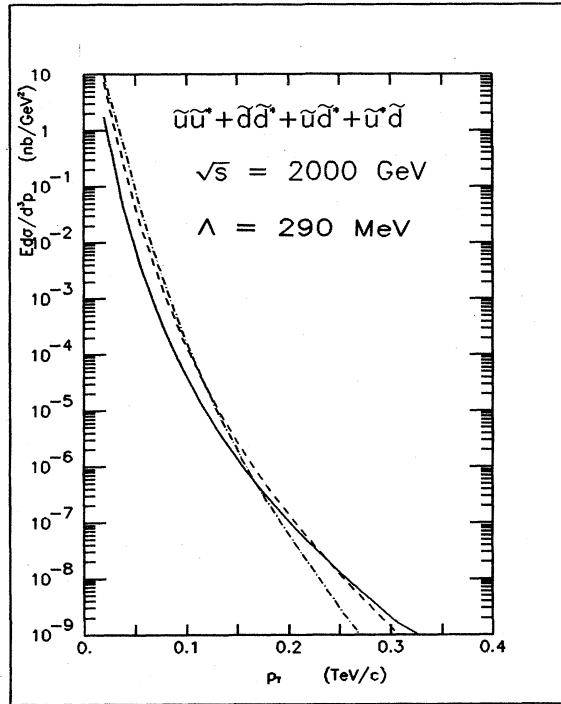
FIG. 99. Differential cross section $E\,d\sigma/d^3p$ for inclusive scalar-quark production for $p\bar{p}$ collisions at $\sqrt{s}=2000$ GeV. All other parameters are as in Fig. 98.
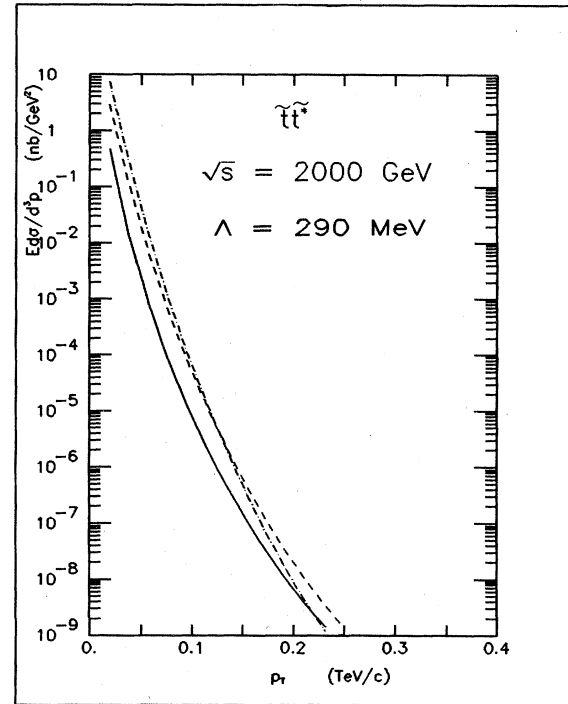
FIG. 101. Differential cross section $E\,d\sigma/d^3p$ for inclusive top-scalar-quark production for $p\bar{p}$ collisions at $\sqrt{s}=2000$ GeV. All other parameters are as in Fig. 100.
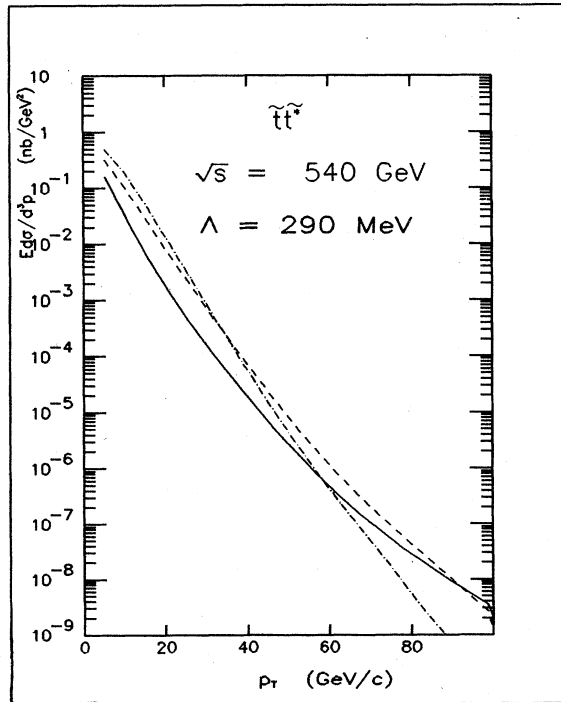
FIG. 100. Differential cross section $E\,d\sigma/d^3p$ for inclusive top-scalar-quark production for $p\bar{p}$ collisions at $\sqrt{s}=540$ GeV. All other parameters are as in Fig. 98.
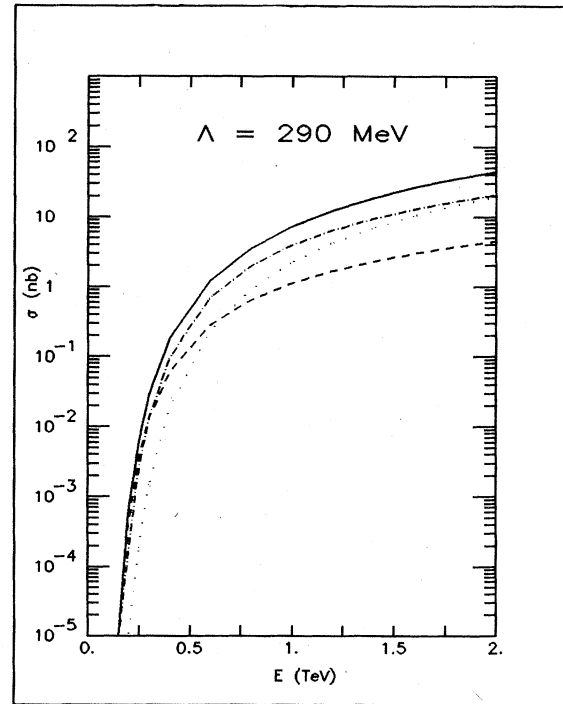
FIG. 102. Comparison of the total cross sections for $pp\rightarrow\tilde{g}\,\tilde{g}$ (dotted curve), $pp\rightarrow\tilde{g}\tilde{q}$ (dot-dashed curve), and $pp\rightarrow\tilde{q}\tilde{q}$ (dashed curve) for all supersymmetric-particle masses equal to 50 GeV/c^2. We have summed over up and down scalar quarks and scalar antiquarks. The total cross section for scalar-quark or gluino production is shown as the solid curve.

$$E\frac{d\sigma}{d^3p}(pp\rightarrow\tilde{g}\tilde{g})\Big|_{p_\perp=0.175\ \text{GeV}/c}$$

$$=1.4\times10^{-37}\ \text{cm}^2/\text{GeV}^2\ \text{per nucleon}\qquad(4.22)$$

according to the parton distributions of set 1.

We have chosen the up and down scalar-quark masses to be 20 GeV/c^2 in Eq. (4.22). However, since the dominant contribution to the gluino production cross section is from gluon fusion, the limit is essentially independent of the scalar-quark mass. We use this result to rule out charge 1 gluino-quark-antiquark bound states with masses between 4 and 9 GeV/c^2 and lifetimes greater than 10^{-8} sec.

The result of Cutts et al.[33] can also be interpreted as a limit on almost stable bound states of quarks and scalar quarks (e.g., $u\tilde{q}_d^*$). Using the parton distributions of set 1, we find that

$$E\frac{d\sigma}{d^3p}(pp\rightarrow\tilde{q}_i\,\tilde{q}_i^*)\Big|_{p_\perp=0.175\ \text{GeV}/c}$$

$$=9\times10^{-38}\ \text{cm}^2/\text{GeV}^2\ \text{per nucleon}\qquad(4.23)$$

at 400 GeV and 2.5 mrad for a scalar-quark mass of 7 GeV/c^2. Since the production of two scalar quarks of the same flavor proceeds primarily by gluon fusion, Eq. (4.23) holds for any flavor scalar quark. Charged scalar-quark—quark bound states are therefore prohibited in the mass range of 4 to 7 GeV/c^2.

To rule out R hadrons and scalar-quark—quark bound states with masses less than 4 GeV/c^2, we turn to the CERN ISR experiment of Alper et al.[33] This was a pp experiment at $\sqrt{s}=53$ GeV and was sensitive to lifetimes greater than 10^{-8} sec and charges greater than $\frac{2}{3}$. They obtain a limit $\sigma<7$ nb on the production of stable particles with masses between 1.5 and 24 GeV/c^2. From Eqs. (3.2) and (3.11), we find that this experiment rules out charge 1 gluino bound states with masses between 1.5 and

6 GeV/c^2 and $\tau>10^{-8}$ sec. Charge 1 scalar-quark—quark bound states with masses between 1.5 and 5 GeV/c^2 are also forbidden by this experiment. (At this point, it is necessary to add a caveat about interpreting the results of this experiment as a limit on scalar-quark and gluino production. The total-cross-section limit quoted by Alper et al. assumes proton-proton collisions producing two stable charged particles in an isotropic distribution. This is not the case for pair production of scalar quarks and gluinos. However, since we only use the results of this experiment to rule out scalar-quark and gluino masses between 1.5 and 4 GeV/c^2 where the Cutts experiment is not sensitive, it is presumably reliable.)

Finally, we consider the experiment of Gustafson et al.[34] This experiment is relevant for gluinos which are not bound into charged R hadrons. This was a neutral-particle search using 300-GeV proton-beryllium interactions. The experiment measured flight times of the produced particles and the energy deposited in the calorimeter in a search for neutral particles with lifetimes greater than 10^{-7} sec. Comparison of the predicted cross section for $pp\rightarrow\tilde{g}\tilde{g}$ [Eq. (3.11)], and the result of Gustafson et al. restricts the gluino mass to be greater than 4 GeV/c^2.

G. Experimental prospects

Hadron-hadron collisions, fixed-target stable-particle searches, beam-dump experiments, and short-lived particle searches all have some sensitivity to light superpartners, as we have discussed above. However, it is high-energy colliding beams that provide access to the greatest range of superparticle masses. The CERN SPS $\bar{p}p$ collider has operated at $\sqrt{s}=540$ GeV. With projected source improvements, the $\bar{p}p$ luminosity will approach $\mathcal{L}=10^{30}$ cm^{-2}sec^{-1}. The Tevatron collider at Fermilab, to be commissioned in 1985, will operate at $\sqrt{s}=2$ TeV with a $\bar{p}p$ luminosity that may eventually reach 10^{31} cm^{-2}sec^{-1}. To what masses can these machines extend the search for supersymmetry? (Projections for still higher energies have been given by Eichten, Hinchliffe, Lane, and Quigg in Ref. 62.)

TABLE IV. Expected discovery limits for superpartners at SPS $\bar{p}p$ and Tevatron colliders, based on associated production of scalar quarks and gauginos. All superpartner masses are set equal.

Superpartner (Events required for discovery)	Mass limit (GeV/c^2)					
	$\sqrt{s}=540$ GeV			$\sqrt{s}=2$ TeV		
			$\int dt\,\mathscr{L}$ (cm^{-2})			
	10^{36}	10^{37}	10^{38}	10^{36}	10^{37}	10^{38}
Gluino or scalar quark (1000 events)	40	55	70	85	130	165
Photino (100 events)	35	55	85	45	90	160
Z gaugino (1000 events)	17	30	50	22	50	95
W gaugino (1000 events)	20	35	55	32	60	110

To characterize the reach of the $\bar{p}p$ colliders we must make some assumptions about the observability of the superparticles. From the discussion of Secs. IV C–IV E, it is clear that because of the large backgrounds, many events will be required to establish the signals for gluinos and scalar quarks: we estimate the number of events needed at 10^3. The signal for photinos is, on the other hand, quite striking, and can perhaps be established with fewer than 100 events. The signals for W and Z gauginos are likely to be hard to separate from a variety of backgrounds, as discussed in Sec. IV C. We assume that 10^3 events would suffice for discovery. Under these assumptions, the mass limits which can be reached for associated production in a "standard run" of 10^7 sec are shown in Table IV, for the parton distributions of set 2. All of these projections can (and should) be sharpened with the aid of detailed Monte Carlo simulations for the signal, background, and detector response. For some range of $\widetilde{W}$, $\widetilde{Z}$, and $\widetilde{\gamma}$ masses, $W^{\pm}$ or Z^0 decays may provide a more copious source of superpartners.

Recently, a number of authors[67] have proposed supersymmetric interpretations of unusual events observed[68] in experiments at the CERN SPS $\bar{p}p$ collider. More data and more complete simulations are required to assess the merits of these suggestions.

V. CONCLUSIONS

In this article we have examined the consequences of a general class of supersymmetric theories which contain as an effective low-energy theory the supersymmetric extension of the Weinberg-Salam model. It is desirable that elements of this low-energy theory emerge from a more complete and more realistic supersymmetric model in the future. Such a model should predict the masses of the supersymmetric partners of the ordinary particles, which have been regarded as free parameters for the purposes of our analysis.

In reviewing the implications of existing experimental results, we have found low-energy supersymmetric models to be remarkably unconstrained. Within all the scenarios we have studied, photinos and gluinos as light as ~ 1 GeV/c^2 are allowed for some range of the other parameters of the theory. Interesting restrictions may be placed on the masses of stable scalar partners of quarks and leptons. What can be said about the masses of unstable scalar quarks and scalar leptons depends in an essential way upon the photino mass. Severe constraints apply only if the photino is approximately massless.

In the course of our survey we have suggested a few ways in which reanalysis of existing data might appreciably improve the limits on superparticle masses. Two examples are worth emphasizing here. (i) Reinterpreting heavy-lepton searches in e^+e^- collisions as searches for the supersymmetric partners of W and Z merely requires changing the acceptance calculations; this should clearly be done. (ii) A window exists in new-particle searches for lifetimes between 10^{-8} sec and 10^{-10} or 10^{-11} sec, in the range accessible neither to "stable"-particle searches nor to beam-dump calorimeter experiments. This is illustrated in Fig. 5, among others, for gluino searches. The

search for heavy particles with these intermediate lifetimes deserves some attention.

We have also presented a complete catalog of total and differential cross sections for the pair production of supersymmetric particles in $p^{\pm}p$ and e^+e^- interactions. These cross sections should be of value in the planning and analysis of future searches for these elusive particles.

At the energies accessible to the accelerators that exist or are under construction, a number of channels should have yields of supersymmetric particles of an interesting magnitude. What is needed is good signatures for superparticle production beyond the traditional "missing-energy" trigger. What seems to us a promising approach is to consider special topologies which have a characteristic appearance. An example is provided by the gluino-photino final state, which may lead to events with one broad jet at large transverse momentum opposite either the undetected stable photino or a hard photon from the unstable photino. Other mixed final states, such as $\widetilde{g}\,\widetilde{W}^{\pm}$ or $\widetilde{g}\widetilde{Z}$, may also have advantages for extracting signal from background. In emulsion searches for short-lived heavy quarks and leptons, scalar-quark and gluino decays may be recognized by a characteristic leptonless topology. This makes it important not to rely exclusively on a lepton tag in hadronic production experiments.

At the much larger energies which may become accessible in multi-TeV proton-(anti)proton colliders, the experimental possibilities are considerably broader because of the larger cross sections for superparticle production. Those possibilities are assessed in Ref. 62, using the results of the calculations presented here.

Regrettably, we have not devised any novel high-efficiency tags for superparticle production. The detection of these particles remains an outstanding challenge to experimental technique.

ACKNOWLEDGMENTS

APPENDIX A: SUPERPARTNER PRODUCTION IN ELECTRON-POSITRON COLLISIONS

In this appendix, we present the differential and total cross sections for the pair production of supersymmetric partners of the known particles in electron-positron interactions. The notation is that of Sec. III. As in the body of this paper, we neglect any mixing between the W and Z gauginos and various possible Higgs fermions. In the presence of such mixing, our results must be modified by the addition of the appropriate mixing angles and the

inclusion of contributions arising from Higgs-fermion exchange.[69] The resulting modifications are discussed in Appendix B. We also neglect the generalized Cabibbo mixing of Eq. (2.8). We continue to write cross sections in the form appropriate when the left-handed and right-handed charged scalar leptons are degenerate in mass.

1. Gaugino pair production

The possible final states are the neutral channels $\tilde{\gamma}\tilde{\gamma}$, $\tilde{\gamma}\tilde{Z}$, $\tilde{Z}\tilde{Z}$, and $\tilde{W}^+\tilde{W}^-$. As in the text, we allow for the possibility of an R' invariance. The differential cross section is given by

$$\frac{d\sigma}{dt}(e^+e^-\rightarrow\text{gauginos})=\frac{\pi\alpha^2}{s^2}\left[C_s\frac{[(t-m_1^2)(t-m_2^2)+(u-m_1^2)(u-m_2^2)+2m_1m_2s]}{(s-M_s^2)^2}\right.$$
$$+C_t\frac{(t-m_1^2)(t-m_2^2)}{(t-M_t^2)^2}+C_u\frac{(u-m_1^2)(u-m_2^2)}{(u-M_u^2)^2}+C_{st}\frac{[(t-m_1^2)(t-m_2^2)+m_1m_2s]}{(s-M_s^2)(t-M_t^2)}$$
$$\left.+C_{tu}\frac{m_1m_2s}{(t-M_t^2)(u-M_u^2)}+C_{su}\frac{[(u-m_1^2)(u-m_2^2)+m_1m_ss]}{(s-M_s^2)(u-M_u^2)}\right], \qquad (A1)$$

where m_1 and m_2 are the masses of the produced gauginos and M_s, M_t, and M_u are the masses of the particles exchanged in the s, t, and u channels, respectively. The coefficients C_x are collected in Table V for the four allowed channels. The total cross section is

$$\sigma(e^+e^-\rightarrow\text{gauginos})=\frac{\pi\alpha^2}{(1+I)s^2}\left[\frac{C_s\mathscr{S}}{3(s-M_s^2)^2}\{2s^2+s[6m_1m_2-(m_1^2+m_2^2)]-(m_1^2-m_2^2)^2\}\right.$$
$$+\left\{C_t\left[\mathscr{S}+(\Delta_{t1}+\Delta_{t2})\Lambda_t+\frac{\mathscr{S}\Delta_{t1}\Delta_{t2}}{M_t^4+m_1^2m_2^2+M_t^2(s-m_1^2-m_2^2)}\right]\right.$$
$$\left.+\frac{C_{st}}{(s-M_s^2)}\left[\mathscr{S}\left[M_t^2-\frac{(s+m_1^2+m_2^2)}{2}\right]+(\Delta_{t1}\Delta_{t2}+m_1m_2s)\Lambda_t\right]+(t\leftrightarrow u)\right\}$$

$$\left.-C_{tu}\frac{m_1m_2s(\Lambda_t+\Lambda_u)}{\Delta_{t1}+\Delta_{u2}+s}\right], \qquad (A2)$$

where $\mathscr{S}$, Δ_{ai}, and Λ_a are defined in Eqs. (3.3)—(3.5) and the statistical factor $1/(1+I)$ was introduced below (3.6).

If the scalar partners of the left-handed and right-handed electrons have unequal masses,

$$m_{\tilde{e}_L}\neq m_{\tilde{e}_R} . \qquad (A3)$$

Then the differential cross sections for $\tilde{\gamma}\tilde{\gamma}$, $\tilde{\gamma}\tilde{Z}$, and $\tilde{Z}\tilde{Z}$ production are modified as

$$\left.\frac{d\sigma}{dt}\right|_{m_{\tilde{e}_L}\neq m_{\tilde{e}_R}}=\frac{d\sigma}{dt}(C_L;M_t=m_{\tilde{e}_L},M_u=m_{\tilde{e}_L})$$
$$+\frac{d\sigma}{dt}(C_R;M_t=m_{\tilde{e}_R},M_u=m_{\tilde{e}_R}) . \qquad (A4)$$

TABLE V. Coefficients for the reaction $e^+e^-\rightarrow\text{gaugino}_1+\text{gaugino}_2$. We use the notation $x_W=\sin^2\theta_W$. The neutral-current couplings L_e and R_e are defined in Eq. (2.11b).

Gaugino$_1$	Gaugino$_2$	Exchanged particle s	t	u	C_s	C_t	C_u	C_{st}	C_{su}	C_{tu}
$\tilde{\gamma}$	$\tilde{\gamma}$		$\tilde{e}$	$\tilde{e}$	0	2	C_t	0	0	$-2C_t$
$\tilde{\gamma}$	$\tilde{Z}$		$\tilde{e}$	$\tilde{e}$	0	$\dfrac{(L_e^2+R_e^2)}{4x_W(1-x_W)}$	C_t	0	0	$-2C_t$
$\tilde{Z}$	$\tilde{Z}$		$\tilde{e}$	$\tilde{e}$	0	$\dfrac{(L_e^4+R_e^4)}{16x_W^2(1-x_W)^2}$	C_t	0	0	$-2C_t$
$\tilde{W}^+$	$\tilde{W}^-$	$\gamma(Z)$	$\tilde{\nu}_L$		$2-\dfrac{(L_e+R_e)}{x_W(1-M_Z^2/s)}+\dfrac{(L_e^2+R_e^2)}{4x_W^2(1-M_Z^2/s)^2}$	$\dfrac{1}{4x_W^2}$	0	$\dfrac{-1}{x_W}\left[1-\dfrac{L_e}{x_W(1-M_Z^2/s)}\right]$	0	0

where C_L and C_R are, respectively, the left-handed and right-handed contributions to the coefficients in Table V. For $\tilde{\gamma}\tilde{\gamma}$ production, $C_L = C_R = \frac{1}{2}C$. For $\tilde{\gamma}\tilde{Z}$ and $\tilde{Z}\tilde{Z}$ production, we define $C = C(L_e, R_e)$, whereupon $C_L = C(L_e, 0)$ and $C_R = C(0, R_e)$. For $\tilde{W}^+\tilde{W}^-$ production, the coefficients of the s-channel term are

$$C_L^{(s)} = 1 - \frac{L_e}{x_W(1 - M_Z^2/s)} + \frac{L_e^2}{4x_W^2(1 - M_Z^2/s)^2} \ ,$$

$$C_R^{(s)} = 1 - \frac{R_e}{x_W(1 - M_Z^2/s)} + \frac{R_e^2}{4x_W^2(1 - M_Z^2/s)^2} \ ,$$

while for all other channels $C_L = C, C_R = 0$. The total cross sections are modified similarly.

The cross section for $e^+e^- \to \tilde{\gamma}\tilde{\gamma}$ has been computed by Ellis and Hagelin.[70] We agree with their result. The cross section for $e^+e^- \to \tilde{\gamma}\tilde{Z}$ has been calculated by Dicus, Nandi, Repko, and Tata[71] for the case of massless photinos. We agree with their result.

2. Scalar-lepton pair production

Next we turn to the production of $\tilde{e}$, $\tilde{\mu}$, and $\tilde{\tau}$, which are always produced in particle-antiparticle pairs by s-channel γ or Z^0 exchange or, in the case of the selectron only, by t-channel $\tilde{\gamma}$ or $\tilde{Z}$ exchange. The differential cross section may be written as

$$\frac{d\sigma}{dt} = \frac{\pi\alpha^2}{s^2}\left[(ut - m^4)\left[\frac{D_s}{s^2} + \frac{D_{t\tilde{\gamma}}}{(t - m_{\tilde{\gamma}}^2)^2} + \frac{D_{t\tilde{Z}}}{(t - m_{\tilde{Z}}^2)^2}\right.\right.$$

$$\left.+ \frac{D_{tX}}{(t - m_{\tilde{\gamma}}^2)(t - m_{\tilde{Z}}^2)} + \frac{D_{st\tilde{\gamma}}}{s(t - m_{\tilde{\gamma}}^2)} + \frac{D_{st\tilde{Z}}}{s(t - m_{\tilde{Z}}^2)}\right]$$

$$\left.+ s\left[\frac{D'_{t\tilde{\gamma}}m_{\tilde{\gamma}}^2}{(t - m_{\tilde{\gamma}}^2)^2} + \frac{D'_{t\tilde{Z}}m_{\tilde{Z}}^2}{(t - m_{\tilde{Z}}^2)^2} + \frac{D'_{tX}m_{\tilde{\gamma}}m_{\tilde{Z}}}{(t - m_{\tilde{\gamma}}^2)(t - m_{\tilde{\gamma}}^2)}\right]\right] \ , \tag{A5}$$

where m is the mass of the produced scalar lepton $\tilde{l}$ and $m_{\tilde{\gamma}}$ and $m_{\tilde{Z}}$ are the mass of the photino and Z gaugino, respectively. The coefficients D_x are given in Table VI. In an R'-invariant theory (or for massless gauginos), the cross section for $e^+e^- \to \tilde{l}_L\tilde{l}_R^* + \tilde{l}_L^*\tilde{l}_R$ vanishes. The total cross section is

$$\sigma(e^+e^- \to \tilde{l}^+\tilde{l}^-) = \frac{\pi\alpha^2}{s^2}\left\{D_s\frac{\mathscr{S}^3}{6s^2} + D_{t\tilde{\gamma}}[-2\mathscr{S} + (s + 2\Delta_{\tilde{\gamma}})\Lambda_{\tilde{\gamma}}]\right.$$

$$+ D_{t\tilde{Z}}[-2\mathscr{S} + (s + 2\Delta_{\tilde{Z}})\Lambda_{\tilde{Z}}] + D_{tX}\left[-\mathscr{S} + \left[\frac{(sm_{\tilde{\gamma}}^2 + \Delta_{\tilde{\gamma}}^2)\Lambda_{\tilde{\gamma}} - (sm_{\tilde{Z}}^2 + \Delta_{\tilde{Z}}^2)\Lambda_{\tilde{Z}}}{(m_{\tilde{\gamma}}^2 - m_{\tilde{Z}}^2)}\right]\right]$$

$$+ D_{st\tilde{\gamma}}\left[-\frac{\mathscr{S}(1 + 2\Delta_{\tilde{\gamma}}/s)}{2} + (m_{\tilde{\gamma}}^2 + \Delta_{\tilde{\gamma}}^2/s)\Lambda_{\tilde{\gamma}}\right]$$

$$+ D_{st\tilde{Z}}\left[-\frac{\mathscr{S}(1 + 2\Delta_{\tilde{Z}}/s)}{2} + (m_{\tilde{Z}}^2 + \Delta_{\tilde{Z}}^2/s)\Lambda_{\tilde{Z}}\right]$$

$$+ D'_{t\tilde{\gamma}}\frac{\mathscr{S}sm_{\tilde{\gamma}}^2}{(sm_{\tilde{\gamma}}^2 + \Delta_{\tilde{\gamma}}^2)} + D'_{t\tilde{Z}}\frac{\mathscr{S}sm_{\tilde{Z}}^2}{(sm_{\tilde{Z}}^2 + \Delta_{\tilde{Z}}^2)} + D'_{tX}\frac{sm_{\tilde{Z}}m_{\tilde{\gamma}}}{(m_{\tilde{\gamma}}^2 - m_{\tilde{Z}}^2)}(\Lambda_{\tilde{\gamma}} - \Lambda_{\tilde{Z}})\right\} \ , \tag{A6}$$

where $\Delta_i = m_i^2 - m^2$ and Λ_i is defined in Eq. (3.5). The generalization to unequal-mass scalar quarks, $m_{\tilde{l}_L} \neq m_{\tilde{l}_R}$, follows the procedure given below Eq. (3.14).

The γ and $\tilde{\gamma}$ exchange contributions to $e^+e^- \to \tilde{e}\tilde{e}^*$ have been evaluated by Farrar and Fayet.[72] Our result agrees with theirs. Gluck and Reya have also considered $e^+e^- \to \tilde{e}\tilde{e}^*$.[73]

3. Scalar-neutrino pair production

Finally, we turn to the production of the scalar partners of the left-handed neutrinos. This cross section has contributions from s-channel Z^0 exchange and, for electron scalar neutrinos, t-channel $\tilde{W}$ exchange. The differential cross section is

TABLE VI. Coefficients for the reaction $e^+e^- \to \tilde{l}_i^+ \tilde{l}_i^-$. We write $x_W = \sin^2\theta_W$. The neutral-current couplings L_i and R_i are defined in Eq. (2.11b).

Scalar lepton	$\tilde{e}$	$\tilde{\mu}$ (or $\tilde{\tau}$)
D_s	$4 + \dfrac{(L_e^2 + R_e^2)^2}{16x_W^2(1-x_W)^2(1-M_Z^2/s)^2}$ $+ \dfrac{(L_e + R_e)^2}{2x_W(1-x_W)(1-M_Z^2/s)}$	$4 + \dfrac{(L_e^2 + R_e^2)(L_\mu^2 + R_\mu^2)}{16x_W^2(1-x_W)^2(1-M_Z^2/s)^2}$ $+ \dfrac{(L_e + R_e)(L_\mu + R_\mu)}{2x_W(1-x_W)(1-M_Z^2/s)}$
$D_{t\tilde{\gamma}} = D'_{t\tilde{\gamma}}$	2	0
$D_{t\tilde{Z}}$	$\dfrac{L_e^4 + R_e^4}{16x_W^2(1-x_W)^2}$	0
D_{tX}	$\dfrac{L_e^2 + R_e^2}{2x_W(1-x_W)}$	0
$D_{st\tilde{\gamma}}$	$4 + \dfrac{(L_e^2 + R_e^2)}{2x_W(1-x_W)(1-M_Z^2/s)}$	0
$D_{st\tilde{Z}}$	$\dfrac{(L_e^2 + R_e^2)}{2x_W(1-x_W)} + \dfrac{(L_e^4 + R_e^4)}{8x_W^2(1-x_W)^2(1-M_Z^2/s)}$	0
$D'_{t\tilde{Z}}$	$\dfrac{L_e^2 R_e^2}{8x_W^2(1-x_W)^2}$	0
D'_{tX}	$\dfrac{L_e R_e}{x_W(1-x_W)}$	0

$$\frac{d\sigma}{dt}(e^+e^- \to \tilde{\nu}_L \tilde{\nu}_L^*) = \frac{\pi\alpha^2}{4x_W^2 s^2}(ut - m^4)\left[\frac{E_s}{(s-m_Z^2)^2} + \frac{E_t}{(t-m_{\tilde{W}}^2)^2} + \frac{E_{st}}{(s-m_Z^2)(t-m_{\tilde{W}}^2)}\right], \qquad (A7)$$

where m is the (left-handed) scalar-neutrino mass, m_Z is the Z-boson mass, and $m_{\tilde{W}}$ is the W-gaugino mass. The coefficients E_x for this process are given in Table VII. The total cross section is

$$\sigma(e^+e^- \to \tilde{\nu}_L \tilde{\nu}_L^*) = \frac{\pi\alpha^2}{4x_W^2 s^2}\left[E_t[-2\mathcal{S} + (s+2\Delta)\Lambda] + E_s\left[\frac{\mathcal{S}^3}{6(s-M_Z^2)^2}\right]\right.$$
$$\left. + \frac{E_{st}}{(s-M_Z^2)}\left[-\frac{\mathcal{S}}{2}(s+2\Delta) + (\Delta^2 + m_{\tilde{W}}^2 s)\Lambda\right]\right], \qquad (A8)$$

where

$$\Delta = m_{\tilde{W}}^2 - m^2 \qquad (A9)$$

and

$$\Lambda = \ln\left[\frac{s + \mathcal{S} + 2\Delta}{s - \mathcal{S} + 2\Delta}\right].$$

This cross section has been computed by Barnett, Lackner, and Haber;[7] we confirm their result.

TABLE VII. Coefficients for the reaction $e^+e^- \to \tilde{\nu}_{iL} \tilde{\nu}_{iL}^*$. We use the shorthand $x_W = \sin^2\theta_W$. The neutral-current couplings L_e and R_e are defined in Eq. (2.11b).

Scalar neutrino	E_s	E_t	E_{st}
$\tilde{\nu}_e$	$\dfrac{(L_e^2 + R_e^2)}{4(1-x_W)^2}$	1	$\dfrac{L_e}{(1-x_W)}$
$\tilde{\nu}_\mu$ or $\tilde{\nu}_\tau$	$\dfrac{(L_e^2 + R_e^2)}{4(1-x_W)^2}$	0	0

APPENDIX B: MIXING BETWEEN GAUGINOS AND HIGGS FERMIONS

In this appendix we discuss the effects of mixing between the gauginos ($\tilde{W}$, $\tilde{Z}$, and $\tilde{\gamma}$) and the fermionic partners of the Higgs bosons. In the simplest supersymmetric extension of the Weinberg-Salam model, two SU(2)$_L$ Higgs doublets H and H' are required to give masses to the quarks. The fermionic partners of the Higgs scalars, the Higgs fermions,

$$\tilde{H} = \begin{bmatrix} \tilde{H}^+ \\ \tilde{H}^0 \end{bmatrix},$$

$$\tilde{H}' = \begin{bmatrix} \tilde{H}'^0 \\ \tilde{H}'^- \end{bmatrix}, \qquad (B1)$$

will in general mix with the gauginos to form the mass eigenstates. In computing the cross sections presented in Sec. III, we neglected the possible contributions of Higgs fermions on grounds of simplicity, and because no specific model has been singled out by experiment (or, for that

matter, by theory). In this appendix, we will remedy that omission. This is done not merely to present a more general formulation, but also to assess the model dependence of our cross-section estimates. We begin by discussing mixing between charged superpartners and then extend the analysis to include mixing in the neutral-fermion sector.

1. Higgs-fermion—W-gaugino mixing

The most general Lagrangian which can contribute to mass mixing in the W-gaugino—Higgs-fermion sector is

$$\mathcal{L}_M = \mu_1 \psi_{W^+} \psi_{W^-} - \mu_2 \psi_{H'^-} \psi_{H^+} + ig_W v_1 \psi_{W^-} \psi_{H^+}$$
$$+ ig_W v_2 \psi_{W^+} \psi_{H'^-} + \text{H.c.} , \quad \text{(B2)}$$

where the constants μ_1 and μ_2 can be calculated in specific models, $v_1 = \langle H^0 \rangle$, $v_2 = \langle H'^0 \rangle$, and all spinors are written in two-component notation. The terms in $\mathcal{L}_M$ proportional to μ_1 and μ_2 correspond to soft supersymmetry breaking.

When the supersymmetry is broken, it requires two unitary matrices to diagonalize the mass matrix. The mass eigenstates $\omega_{1,2}^{\pm}$ can be written as

$$\begin{pmatrix} \widetilde{\omega}_1^+ \\ \widetilde{\omega}_2^+ \end{pmatrix} = \begin{pmatrix} \cos\theta_+ & \sin\theta_+ \\ -\sin\theta_+ & \cos\theta_+ \end{pmatrix} \begin{pmatrix} -i\widetilde{W}^+ \\ \widetilde{H}^+ \end{pmatrix} \quad \text{(B3a)}$$

and

$$\begin{pmatrix} \widetilde{\omega}_1^- \\ \widetilde{\omega}_2^- \end{pmatrix} = \begin{pmatrix} \cos\theta_- & \sin\theta_- \\ -\sin\theta_- & \cos\theta_- \end{pmatrix} \begin{pmatrix} -i\widetilde{W}^- \\ \widetilde{H}'^- \end{pmatrix} , \quad \text{(B3b)}$$

where the mixing angles $\theta_\pm$ ($|\theta_\pm| \le \pi/2$) can be expressed in terms of $\mu_1, \mu_2,$ and v_1/v_2.

In terms of the mass eigenstates (B3), the Lagrangian of Eq. (B2) becomes

$$\mathcal{L}_M = -M_1 \psi_{\omega_1^+} \psi_{\omega_1^-} - M_2 \psi_{\omega_2^+} \psi_{\omega_2^-} + \text{H.c.} , \quad \text{(B4)}$$

where the mass eigenvalues are

$$M_{1,2} = \tfrac{1}{2}(\mu_1 + \mu_2) \pm \tfrac{1}{2}[(\mu_1 - \mu_2)^2 + 4g_W^2 v_1 v_2]^{1/2} . \quad \text{(B5)}$$

Because of the structure of the $SU(2)_L \otimes U(1)_Y$ symmetry breaking, $M_W^2 = g_W^2(v_1^2 + v_2^2)/2$. As a result, the masses of the physical eigenstates are related to the mixing angles $\theta_\pm$ of (B3) through the expression

$$4M_W^2 = (M_1 + M_2)^2 \sin^2(\theta_+ - \theta_-)$$
$$+ (M_1 - M_2)^2 \sin^2(\theta_+ + \theta_-) . \quad \text{(B6)}$$

Specifying the mass eigenvalues M_1 and M_2 and one of the mixing angles therefore completely determines the remaining mixing angle.

It is apparent that for some choices of the parameters μ_1 and μ_2 the mass matrix will have negative eigenvalues. This is easily accommodated by redefining the field $\widetilde{\omega}_i^-$ for which $M_i < 0$ so that the physical field is

$$(\widetilde{\omega}_i^-)' = -\widetilde{\omega}_i^- . \quad \text{(B7)}$$

In so doing, we take advantage of the freedom to rotate the phases of $\widetilde{\omega}_i^+$ and $\widetilde{\omega}_i^-$ independently.

If the supersymmetry is spontaneously broken, so that $\mu_1 = \mu_2 = 0$, the mass eigenstates are

$$\widetilde{\omega}_1^+ = \frac{-i\widetilde{W}^+ + \widetilde{H}^+}{\sqrt{2}} ,$$

$$\widetilde{\omega}_2^+ = \frac{-i\widetilde{W}^+ - \widetilde{H}^+}{\sqrt{2}} ,$$

$$\widetilde{\omega}_1^- = \frac{-i\widetilde{W}^- + \widetilde{H}'^-}{\sqrt{2}} , \quad \text{(B8)}$$

$$\widetilde{\omega}_2'^- = -\widetilde{\omega}_2^- = \frac{i\widetilde{W}^- + \widetilde{H}'^-}{\sqrt{2}} ,$$

with degenerate masses

$$M_1 = M_2 = g_W \sqrt{v_1 v_2} . \quad \text{(B9)}$$

For the special case $v_1 = v_2$, corresponding to unbroken supersymmetry, the common mass is

$$M_1 = M_2 = M_W . \quad \text{(B10)}$$

The Feynman rules for the interactions of the mass eigenstates $\widetilde{\omega}_i^\pm$ are easily found from Eqs. (B3) and (2.9). As an example, consider the couplings of the up and down quarks and scalar quarks to the charged-gaugino mass eigenstates, which are given by

$$\mathcal{L}_{\text{int}} = g_W \left[\left(-\psi_{\omega_1^+} \cos\theta_+ + \psi_{\omega_2^+} \sin\theta_+ \right) \psi_{Ld} \phi_{Lu}^* \right.$$
$$\left. + \left(\psi_{\omega_1^-} \cos\theta_- - \psi_{\omega_2^-} \sin\theta_- \right) \psi_{Lu} \phi_{Ld}^* \right]$$
$$+ \text{H.c.} , \quad \text{(B11)}$$

where we have neglected generalized Cabibbo mixing. The Higgs-fermion—quark—scalar-quark couplings are proportional to the quark masses, and will be neglected here. Thus the $\widetilde{\omega}_1^+ d_L \widetilde{u}_L^*$ coupling is proportional to $\cos\theta_+$, while the $\widetilde{\omega}_1^- u_L \widetilde{d}_L^*$ coupling is proportional to $\cos\theta_-$, etc. It is also straightforward to derive the $W^+ \widetilde{\omega}_i^- \widetilde{\gamma}$ and $W^+ \widetilde{\omega}_i^- \widetilde{Z}$ couplings because there is no Higgs-fermion—photino—W or Higgs-fermion—$\widetilde{Z}$—$\widetilde{W}$ vertex. The resulting interaction term is

$$\mathcal{L}_{\text{int}} = eW^{+\mu}(i\overline{\psi}_{\omega_1^+} \cos\theta_+ - i\overline{\psi}_{\omega_2^+} \sin\theta_+)\overline{\sigma}_\mu(\psi_A + \psi_Z \cot\theta_W)$$
$$- eW^{-\mu}(i\overline{\psi}_{\omega_1^-} \cos\theta_- - i\overline{\psi}_{\omega_2^-} \sin\theta_-)$$
$$\times \overline{\sigma}_\mu(\psi_A + \psi_Z \cot\theta_W) . \quad \text{(B12)}$$

The interaction Lagrangian of Eq. (B11) is all we require to derive the cross sections for $q\overline{q}' \to \widetilde{\omega}_i^\pm \widetilde{g}$. The differential cross section (3.1) becomes

$$\frac{d\sigma}{dt}(q\bar{q}\,'\rightarrow\widetilde{\omega}_1^+\widetilde{g})=\frac{\pi}{s^2}\left[A_tc_-^{\,2}\frac{(t-m_{\widetilde{\omega}}^2)(t-m_{\widetilde{g}}^2)}{(t-M_t^{\,2})^2}+A_uc_+^{\,2}\frac{(u-m_{\widetilde{\omega}}^2)(u-m_{\widetilde{g}}^2)}{(u-M_u^{\,2})^2}+A_{tu}\frac{m_{\widetilde{\omega}}m_{\widetilde{g}}sc_+c_-}{(t-M_t^{\,2})(u-M_u^{\,2})}\right],\quad\text{(B13)}$$

where $m_{\widetilde{\omega}}$ is the (positive or negative) mass eigenvalue M_1 of $\widetilde{\omega}_1^+$, $m_{\widetilde{g}}$ is the mass of the gluino, and M_t and M_u are the masses of the particles (scalar quarks) exchanged in the t and u channels. We have abbreviated $\cos\theta_\pm$ by $c_\pm$. The coefficients A_x are those of Table II in Sec. III.

The total cross section is

$$\sigma(q\bar{q}\,'\rightarrow\widetilde{\omega}_1^+\widetilde{g})=\frac{\pi}{s^2}\left\{A_tc_-^{\,2}\left[\mathscr{S}+(\Delta_{t\widetilde{\omega}}+\Delta_{t\widetilde{g}})\Lambda_t+\frac{\mathscr{S}\Delta_{t\widetilde{\omega}}\Delta_{t\widetilde{g}}}{M_t^{\,4}+m_{\widetilde{\omega}}^2m_{\widetilde{g}}^2+M_t^{\,2}(s-m_{\widetilde{\omega}}^2-m_{\widetilde{g}}^2)}\right]\right.$$
$$+A_uc_+^{\,2}\left[\mathscr{S}+(\Delta_{u\widetilde{\omega}}+\Delta_{u\widetilde{g}})\Lambda_u+\frac{\mathscr{S}\Delta_{u\widetilde{\omega}}\Delta_{u\widetilde{g}}}{M_u^{\,4}+m_{\widetilde{\omega}}^2m_{\widetilde{g}}^2+M_u^{\,2}(s-m_{\widetilde{\omega}}^2-m_{\widetilde{g}}^2)}\right]$$
$$\left.-A_{tu}\frac{m_{\widetilde{\omega}}m_{\widetilde{g}}sc_+c_-}{s+\Delta_{t\widetilde{\omega}}+\Delta_{u\widetilde{g}}}(\Lambda_t+\Lambda_u)\right\}.\quad\text{(B14)}$$

Here we have used the convenient quantities

$$\mathscr{S}=[s-(m_{\widetilde{\omega}}+m_{\widetilde{g}})^2]^{1/2}[s-(m_{\widetilde{\omega}}-m_{\widetilde{g}})^2]^{1/2},\quad\text{(B15)}$$

$$\Delta_{aj}=M_a^{\,2}-m_j^{\,2},\quad\text{(B16)}$$

and

$$\Lambda_a=\ln\left[\frac{s+\Delta_{a\widetilde{\omega}}+\Delta_{a\widetilde{g}}-\mathscr{S}}{s+\Delta_{a\widetilde{\omega}}+\Delta_{a\widetilde{g}}+\mathscr{S}}\right].$$

Cross sections for the reaction $q\bar{q}\,'\rightarrow\widetilde{\omega}_2^+\widetilde{g}$ are obtained from (B13) and (B14) by the replacements

$$\cos\theta_\pm\rightarrow\sin\theta_\pm,\quad\text{(B17)}$$

$$m_{\widetilde{\omega}}=M_1\rightarrow M_2.$$

For the production of $\widetilde{\omega}_i^-$, replace $\theta_+\leftrightarrow\theta_-$ in the corresponding $\widetilde{\omega}_i^+$ cross section.

In similar fashion we may calculate the effects of W-gaugino—Higgs-fermion mixing on the associated production of a charged gaugino and a scalar quark. The differential and total cross sections for the reaction

$$gq\rightarrow(\widetilde{\omega}_1^+\text{ or }\widetilde{\omega}_1^-)\widetilde{q}\quad\text{(summed)}\quad\text{(B18)}$$

are given by Eqs. (3.29) and (3.30) with the coefficients

$$B_s=B_u=-B_{su}=\frac{\alpha_s\alpha}{12x_W}|V_{q\bar{q}}|^2(\delta_{qu}c_-^{\,2}+\delta_{qd}c_+^{\,2})\quad\text{(B19)}$$

and $\mu=M_1$. The remaining coefficients B_t, B_{tu}, and B_{st} all vanish. The cross sections for $\widetilde{\omega}_2^\pm$ production are obtained by replacing

$$\cos\theta_\pm\rightarrow\sin\theta_\pm,\quad\text{(B20)}$$

$$\mu=M_1\rightarrow M_2.$$

We turn next to the calculation of the cross section for the reaction $q\bar{q}\,'\rightarrow\widetilde{\omega}_i^+\widetilde{\omega}_j^-$, for which we require the Higgs-fermion—Higgs-fermion—Z^0 couplings given by the interaction Lagrangian

$$\mathscr{L}_{\text{eff}}=e(A^\mu+Z^\mu\cot\theta_W)(\bar{\psi}_{W+}\bar{\sigma}_\mu\psi_{W+}-\bar{\psi}_{W-}\bar{\sigma}_\mu\psi_{W-})$$
$$+e(A^\mu+Z^\mu\cot2\theta_W)(\bar{\psi}_{H+}\bar{\sigma}_\mu\psi_{H+}-\bar{\psi}_{H'-}\bar{\sigma}_\mu\psi_{H'-}).$$
$$\text{(B21)}$$

It is apparent that the couplings of the photon to the charged gaugino mass eigenstates will be diagonal $(\gamma\widetilde{\omega}_i\widetilde{\omega}_i)$, whereas those of the Z^0 will include nondiagonal $(Z^0\widetilde{\omega}_1\widetilde{\omega}_2)$ terms as well. We first calculate the cross section for the reactions

$$q\bar{q}\rightarrow\widetilde{H}^+\widetilde{H}^{+*}\text{ or }\widetilde{H}'^-\widetilde{H}'^{-*},\quad\text{(B22)}$$

which proceed by direct-channel exchanges of γ and Z^0. The result is

$$\frac{d\sigma}{dt}(q\bar{q}\rightarrow\widetilde{H}^+\widetilde{H}^{+*})=\frac{d\sigma}{dt}(q\bar{q}\rightarrow\widetilde{H}'^-\widetilde{H}'^{-*})$$
$$=\frac{\pi\alpha^2}{3s^4}\left[2+\frac{(1-2x_W)(L_q+R_q)}{2x_W(1-x_W)(1-M_Z^2/s)}+\frac{(1-2x_W)^2(L_q^2+R_q^2)}{16x_W^2(1-x_W)^2(1-M_Z^2/s)^2}\right]$$
$$\times[(t-M_H^2)^2+(u-M_H^2)^2+2M_H^2s]\right],\quad\text{(B23)}$$

where M_H is the Higgs-fermion mass.

By combining (B23) and (3.1) according to the mixing of Eq. (B3), we obtain the cross sections for $q\bar{q}\rightarrow\widetilde{\omega}_i^+\widetilde{\omega}_j^-$. The differential cross section becomes

$$\frac{d\sigma}{dt}(q\bar{q}\rightarrow\widetilde{\omega}_i^+\widetilde{\omega}_j^-)=\frac{\pi}{s^2}\left[\frac{\mathscr{A}_s[(t-M_i^2)(t-M_j^2)+(u-M_i^2)(u-M_j^2)](c_+^2+c_-^2)/2+2\mathscr{A}_s'M_iM_jsc_+c_-}{s^2}\right.$$

$$+\mathscr{A}_tc_-^2\frac{(t-M_i^2)(t-M_j^2)}{(t-M_t^2)^2}+\mathscr{A}_uc_+^2\frac{(u-M_i^2)(u-M_j^2)}{(u-M_u^2)^2}$$

$$+\frac{\mathscr{A}_{st}(t-M_i^2)(t-M_j^2)c_-^2+\mathscr{A}_{st}'M_iM_jsc_+c_-}{s(t-M_t^2)}$$

$$\left.+\frac{\mathscr{A}_{su}(u-M_i^2)(u-M_j^2)c_+^2+\mathscr{A}_{su}'M_iM_jsc_+c_-}{s(u-M_u^2)}\right],\tag{B24}$$

where the coefficients $\mathscr{A}_x$ are listed in Table VIII for the $\widetilde{\omega}_1^+\widetilde{\omega}_1^-$ and $\widetilde{\omega}_1^+\widetilde{\omega}_2^-$ final states. There we have introduced the notation

$$\beta_\pm=\beta(\theta_\pm)=1-\frac{\sin^2\theta_\pm}{2(1-x_W)}.\tag{B25}$$

As in (B13) and (B14), M_i and M_j represent the (positive or negative) mass eigenvalues given by (B5), and M_t and M_u are the masses of the exchanged scalar quarks. The cross section for the $\widetilde{\omega}_2^+\widetilde{\omega}_2^-$ final state is obtained by replacing $\cos\theta_\pm\leftrightarrow\sin\theta_\pm$ in (B24) and Table VIII. The integrated cross section corresponding to (B24) is

$$\sigma(q\bar{q}\rightarrow\widetilde{\omega}_i^+\widetilde{\omega}_j^-)=\frac{\pi}{s^2}\left[\frac{\mathscr{S}}{3s^2}\{\mathscr{A}_s[2s^2-s(M_i^2+M_j^2)-(M_i^2-M_j^2)^2](c_+^2+c_-^2)/2+6\mathscr{A}_s'M_iM_jsc_+c_-)\}\right.$$

$$+\mathscr{A}_tc_-^2\left[\mathscr{S}+(\Delta_{ti}+\Delta_{tj})\Lambda_t+\frac{\mathscr{S}\Delta_{ti}\Delta_{tj}}{M_t^4+M_i^2M_j^2+M_t^2(s-M_i^2-M_j^2)}\right]$$

$$+\mathscr{A}_uc_+^2\left[\mathscr{S}+(\Delta_{ui}+\Delta_{uj})\Lambda_u+\frac{\mathscr{S}\Delta_{ui}\Delta_{uj}}{M_u^4+M_i^2M_j^2+M_u^2(s-M_i^2-M_j^2)}\right]$$

$$+\frac{\mathscr{A}_{st}c_-^2\{\mathscr{S}[M_t^2-(s+M_i^2+M_j^2)/2]+\Delta_{ti}\Delta_{tj}\Lambda_t\}+\mathscr{A}_{st}'M_iM_jsc_+c_-\Lambda_t}{s}$$

$$\left.+\frac{\mathscr{A}_{su}c_+^2\{\mathscr{S}[M_u^2-(s+M_i^2+M_j^2)/2]+\Delta_{ui}\Delta_{uj}\Lambda_u\}+\mathscr{A}_{su}'M_iM_jsc_+c_-\Lambda_u}{s}\right].\tag{B26}$$

Our calculations agree with those of Barger, Robinett, Keung, and Phillips.[57] To obtain the cross sections for $e^+e^-\rightarrow\widetilde{\omega}_i^+\widetilde{\omega}_j^-$, we replace q and q' by e in Table VIII, replace the flavor-mixing matrices V and V' by N and N', and replace $\delta_{qu}\rightarrow1,\delta_{qd}\rightarrow0$. The resulting cross sections must be multiplied by 3 to undo the color average. In (B24) and (B26), M_t is identified as the mass of the electron scalar neutrino.

The cross sections for $\widetilde{\omega}\widetilde{g}$ and $\widetilde{\omega}\widetilde{\omega}$ production are sensitive to the signs of the mass eigenvalues M_1 and M_2. In (B13) and (B14), the $t-u$ interference term is proportional to $m_{\widetilde{\omega}}m_{\widetilde{g}}/s$. In (B24) and (B26), the terms multiplying $\mathscr{A}_s'$, $\mathscr{A}_{st}'$, and $\mathscr{A}_{su}'$ all are proportional to M_iM_j/s, so the sensitivity to signs of the mass eigenvalues is limited to the $\widetilde{\omega}_1^+\widetilde{\omega}_2^-$ case.

To assess the resulting variability in reaction rates without committing ourselves to a particular model of mixing, we set $c_+=c_-=1$ in (B14) and compare the cross sections for

$$pp\rightarrow(\widetilde{\omega}_1^+\text{ or }\widetilde{\omega}_1^-)\widetilde{g}\text{ (summed)}\tag{B27}$$

that result when the charged-gaugino mass eigenvalue is positive or negative. Three cases are displayed in Fig. 103:

Spectrum $1^\pm$: $m_{\widetilde{g}}=3$ GeV/c^2 ,

$$m_{\widetilde{q}}=20\text{ GeV}/c^2=\pm m_{\widetilde{\omega}}\;;$$

Spectrum $2^\pm$: $m_{\widetilde{g}}=m_{\widetilde{q}}=50$ GeV/$c^2=\pm m_{\widetilde{\omega}}$;

Spectrum $3^\pm$: $m_{\widetilde{g}}=m_{\widetilde{q}}=100$ GeV/$c^2=\pm m_{\widetilde{\omega}}$.

The results for Spectra 1^+, 2^+, 3^+ are identical to those given in Fig. 25. The cross sections for Spectra 1^-, 2^-, 3^- with $m_{\widetilde{\omega}}<0$ are larger than for their counterparts, as expected from (B14). The differences are largest for large values of $m_{\widetilde{\omega}}m_{\widetilde{g}}/s$, and decrease as $s\rightarrow\infty$. We take these differences as guide to the uncertainty of the cross-section estimates that do not rely on detailed models of supersymmetry breaking.

2. Mixing in the neutral sector

In the neutral sector, mixing may occur between the photino, Z gaugino and two neutral Higgs fermions. The most general form of the Lagrangian which can give rise to mass mixing between the neutral gaugino and Higgs-fermion state is

TABLE VIII. Coefficients for the reaction $q\bar{q}\,' \to \tilde\omega_i^+\tilde\omega_j^-$. We write $x_W = \sin^2\theta_W$ and $c_\pm = \cos\theta_\pm$, $s_\pm = \sin\theta_\pm$; $\beta_\pm$ is defined in Eq. (B25). The neutral-current couplings are defined in Eq. (2.11b).

Final states	$\tilde\omega_1^+\tilde\omega_1^-$	$\tilde\omega_1^+\tilde\omega_2^-$
$\mathscr{A}_s$	$\dfrac{2\alpha^2}{3}\left[e_q^{\,2} + \dfrac{e_q(L_q+R_q)(\beta_+ + \beta_-)}{4x_W(1-M_Z^2/s)}\right.$ $\left. + \dfrac{(L_q^2+R_q^2)(\beta_+^2+\beta_-^2)}{16x_W^2(1-M_Z^2/s)^2}\right]$	$\dfrac{\alpha^2(L_q^2+R_q^2)(c_+^2 s_+^2 + c_-^2 s_-^2)}{48x_W^2(1-x_W)^2(1-M_Z^2/s)^2}$
$\mathscr{A}'_s$	$\dfrac{2\alpha^2}{3}\left[e_q^{\,2} + \dfrac{e_q(L_q+R_q)(\beta_+ + \beta_-)}{4x_W(1-M_Z^2/s)}\right.$ $\left. + \dfrac{(L_q^2+R_q^2)\beta_+\beta_-}{8x_W^2(1-M_Z^2/s)^2}\right]$	$\dfrac{\alpha^2(L_q^2+R_q^2)c_+^2 s_+^2 c_-^2 s_-^2}{6x_W^2(1-x_W)^2(1-M_Z^2/s)^2}$
$\mathscr{A}_t$	$\dfrac{\alpha^2 c_-^{\,4}\,\lvert V^*_{q\bar{q}''}V_{q'\bar{q}''}\rvert^2\delta_{qu}}{12x_W^2}$	$\dfrac{\alpha^2 c_-^{\,2}s_-^{\,2}\,\lvert V^*_{q\bar{q}''}V_{q'\bar{q}''}\rvert^2\delta_{qu}}{12x_W^2}$
$\mathscr{A}_u$	$\dfrac{\alpha^2 c_+^{\,4}\,\lvert V'_{\bar{q}''q}V'^{*}_{\bar{q}''q'}\rvert^2\delta_{qd}}{12x_W^2}$	$\dfrac{\alpha^2 c_+^{\,2}s_+^{\,2}\,\lvert V'_{\bar{q}''q}V'^{*}_{\bar{q}''q'}\rvert^2\delta_{qd}}{12x_W^2}$
$\mathscr{A}_{st}$	$\dfrac{\alpha^2 c_-^{\,2}}{3x_W}\left[e_q + \dfrac{L_q\beta_+}{2x_W(1-M_Z^2/s)}\right]\delta_{qu}$ $\times \mathrm{Re}(V^*_{q\bar{q}''}V_{q'\bar{q}''})$	$\dfrac{\alpha^2 c_-^{\,2}s_-^{\,2}L_q\delta_{qu}}{12x_W(1-x_W)(1-M_Z^2/s)}$ $\times \mathrm{Re}(V^*_{q\bar{q}''}V_{q'\bar{q}''})$
$\mathscr{A}'_{st}$	$\dfrac{\alpha^2 c_-^{\,2}}{3x_W}\left[e_q + \dfrac{L_q\beta_-}{2x_W(1-M_Z^2/s)}\right]\delta_{qu}$ $\times \mathrm{Re}(V^*_{q\bar{q}''}V_{q'\bar{q}''})$	$\dfrac{\alpha^2 c_+ s_+ c_- s_- L_q\delta_{qu}}{12x_W(1-x_W)(1-M_Z^2/s)}$ $\times \mathrm{Re}(V^*_{q\bar{q}''}V_{q'\bar{q}''})$
$\mathscr{A}_{su}$	$\dfrac{-\alpha^2 c_+^{\,2}}{3x_W}\left[e_q + \dfrac{L_q\beta_+}{2x_W(1-M_Z^2/s)}\right]\delta_{qd}$ $\times \mathrm{Re}(V'_{\bar{q}''q}V'^{*}_{\bar{q}''q'})$	$\dfrac{-\alpha^2 c_+^{\,2}s_+^{\,2}L_q\delta_{qd}}{12x_W(1-x_W)(1-M_Z^2/s)}$ $\times \mathrm{Re}(V'_{\bar{q}''q}V'^{*}_{\bar{q}''q'})$
$\mathscr{A}'_{su}$	$\dfrac{-\alpha^2 c_+^{\,2}}{3x_W}\left[e_q + \dfrac{L_q\beta_-}{2x_W(1-M_Z^2/s)}\right]\delta_{qd}$ $\times \mathrm{Re}(V'_{\bar{q}''q}V'^{*}_{\bar{q}''q'})$	$\dfrac{-\alpha^2 c_+ s_+ c_- s_- L_q\delta_{qd}}{12x_W(1-x_W)(1-M_Z^2/s)}$ $\times \mathrm{Re}(V'_{\bar{q}''q}V'^{*}_{\bar{q}''q'})$

$$\mathscr{L} = \frac{\mu_1}{2}\psi_{W_3}\psi_{W_3} - \mu_2\psi_{H^0}\psi_{H'^0} + \frac{\mu_3}{2}\psi_B\psi_B$$

$$-iM_Z\cos\theta\,\psi_Z\psi_{H^0} - iM_Z\sin\theta\,\psi_Z\psi_{H'^0} + \text{H.c.}\ , \qquad \text{(B28)}$$

where ψ_{W_3} and ψ_B are the $SU(2)_L$ and $U(1)_Y$ gauge fer-mions, and $\tan\theta = -v_2/v_1$. In constructing (B28) we have assumed that the soft supersymmetry-breaking terms do not break the electroweak gauge symmetry. The parameters μ_1 and μ_2 in (B28) are thus the same as those in (B2).

In the presence of the soft supersymmetry-breaking terms, the mass eigenstates are complicated linear com-
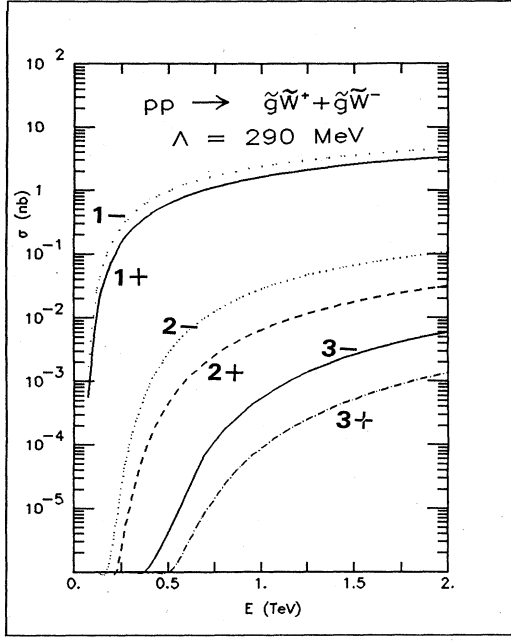
FIG. 103. Total cross section for $pp \to \tilde{g}\tilde{\omega}^+ + \tilde{g}\tilde{\omega}^-$. The supersymmetric-particle masses are given by spectra 1, 2, and 3 of Sec. IV C and Appendix B. The labels $\pm$ refer to the sign of the mass eigenvalue $m_{\tilde{\omega}}$.

binations of the neutral gaugino and Higgs-fermion fields. The analysis can be simplified by a convenient choice of basis fields. In terms of the combinations

$$\tilde{A} = \frac{g'\tilde{W}_3 + g\tilde{B}}{(g^2 + g'^2)^{1/2}}, \quad \tilde{Z} = \frac{g\tilde{W}_3 - g'\tilde{B}}{(g^2 + g'^2)^{1/2}},$$

$$\tilde{h} = \tilde{H}^0\cos\theta + \tilde{H}'^0\sin\theta, \quad \tilde{h}' = \tilde{H}'^0\cos\theta - \tilde{H}^0\sin\theta, \tag{B29}$$

the Lagrangian of (B28) can be rewritten as

$$\mathcal{L}_M = \tfrac{1}{2}\mathcal{M}_1\psi_A\psi_A + \mathcal{M}_2\psi_A\psi_Z + \tfrac{1}{2}\mathcal{M}_3\psi_Z\psi_Z - iM_Z\psi_Z\psi_h$$

$$-\mu_2\left[\sin2\theta\left[\frac{\psi_h\psi_h - \psi_{h'}\psi_{h'}}{2}\right] + \cos2\theta\psi_h\psi_{h'}\right] + \text{H.c.}, \tag{B30}$$

where

$$\mathcal{M}_1 = \frac{g'^2\mu_1 + g^2\mu_3}{g^2 + g'^2},$$

$$\mathcal{M}_2 = e(\mu_1 - \mu_3), \tag{B31}$$

$$\mathcal{M}_3 = \frac{g^2\mu_1 + g'^2\mu_3}{g^2 + g'^2}.$$

The resulting mass matrix is

$$\mathbf{M} = \begin{bmatrix} \mathcal{M}_1 & \mathcal{M}_2 & 0 & 0 \\ \mathcal{M}_2 & \mathcal{M}_3 & -M_Z & 0 \\ 0 & -M_Z & \mu_2\sin2\theta & \mu_2\cos2\theta \\ 0 & 0 & \mu_2\cos2\theta & -\mu_2\sin2\theta \end{bmatrix}. \tag{B32}$$

We next wish to rewrite the Lagrangian (B30) in terms of the mass eigenstates $\tilde{\chi}_p$, as

$$\mathcal{L}_M = -\tfrac{1}{2}\sum_{p=1}^{4} M_p\psi_{\chi_p}\psi_{\chi_p} + \text{H.c.} \tag{B33}$$

This is accomplished by diagonalizing the mass matrix (B32), for which the secular equation is

$$(\lambda^2 - \mu_2^2)[(\lambda - \mathcal{M}_1)(\lambda - \mathcal{M}_3) - \mathcal{M}_2^2]$$

$$- (\lambda - \mathcal{M}_1)(\lambda + \mu_2\sin2\theta)M_Z^2 = 0, \tag{B34}$$

or, in terms of the parameters of the original Lagrangian (B28) alone,

$$(\lambda^2 - \mu_2^2)(\lambda - \mu_1)(\lambda - \mu_3)$$

$$- \left[\lambda - \frac{g'^2\mu_1 + g^2\mu_3}{g^2 + g'^2}\right](\lambda + \mu_2\sin2\theta)M_Z^2 = 0. \tag{B35}$$

In the special case of the supersymmetric extension of the Weinberg-Salam model in which the supersymmetry is unbroken,

$$\mu_1 = \mu_2 = \mu_3 = 0, \tag{B36}$$

$$v_1 = v_2,$$

the eigenvalue equation reduces to

$$\lambda^4 - \lambda^2 M_Z^2 = 0, \tag{B37}$$

for which the eigenvalues are

$$M_1 = M_2 = 0, \quad M_3 = -M_4 = M_Z. \tag{B38}$$

The mass eigenstates $\tilde{\chi}_p$ with masses M_p are related to the basis states (B29) by a 4×4 orthogonal matrix $\mathcal{O}$, as

$$\begin{bmatrix} \tilde{\chi}_1 \\ \tilde{\chi}_2 \\ \tilde{\chi}_3 \\ \tilde{\chi}_4 \end{bmatrix} = \mathcal{O} \begin{bmatrix} -i\tilde{A} \\ -i\tilde{Z} \\ \tilde{h} \\ \tilde{h}' \end{bmatrix}, \tag{B39}$$

where M_p is determined by the eigenvalue conditions

$$(\mathbf{M} - M_p\mathbf{I})\tilde{\chi}_p = 0, \quad p = 1, \ldots, 4. \tag{B40}$$

For the special case of unbroken supersymmetry considered in the previous paragraph, we have

$$\tilde{\chi}_1 = -i\tilde{A}, \quad \tilde{\chi}_2 = \tilde{h}',$$

$$\tilde{\chi}_3 = \frac{-i\tilde{Z} - \tilde{h}}{\sqrt{2}}, \quad \tilde{\chi}_4 = \frac{-i\tilde{Z} + \tilde{h}}{\sqrt{2}}. \tag{B41}$$

The two massless fields $\tilde{\chi}_1$ and $\tilde{\chi}_2$ can be combined to make a massless Dirac photino. We redefine the physical field $\tilde{\chi}_4$ with negative eigenvalue $M_4 = -M_Z$ to be

$$\tilde{\chi}'_4 = i\tilde{\chi}_4 \tag{B42}$$

with physical mass M_Z. Then the states $\tilde{\chi}_3$ and $\tilde{\chi}'_4$ can be combined to form a four-component field of mass M_Z, a Dirac Z gaugino. As for the charged sector, it is the (positive or negative) mass eigenvalues M_p that enter the

Feynman rules.

To calculate cross sections, it is most convenient to work with the states $\widetilde{A}$, $\widetilde{Z}$, $\widetilde{H}^0$, and $\widetilde{H}'^0$. In this basis the mass eigenstates are

$$\widetilde{\chi}_p = -i\widetilde{A}a_p - i\widetilde{Z}b_p + \widetilde{H}^0 c_p + \widetilde{H}'^0 d_p , \qquad (B43)$$

where

$$a_p = \mathcal{O}_{p1}, \quad b_p = \mathcal{O}_{p2} ,$$

$$c_p = \mathcal{O}_{p3}\cos\theta - \mathcal{O}_{p4}\sin\theta , \qquad (B44)$$

$$d_p = \mathcal{O}_{p3}\sin\theta + \mathcal{O}_{p4}\cos\theta .$$

In spite of the large number of masses and mixing angles in the two-doublet model, there are only four independent parameters. If we choose these to be the four physical masses of the neutral states, we can determine the parameters μ_1, μ_2, μ_3 of the Lagrangian and the matrix $\mathcal{O}$ from Eq. (B39). Then Eq. (B44) fixes the mixing an-

gles in the neutral sector. Finally, we may use Eqs. (B2) and (B5) to compute the masses and mixing angles in the charged sector.

Because of the $Z^0\widetilde{H}^0\widetilde{H}^0$ and $Z^0\widetilde{H}'^0\widetilde{H}'^0$ couplings, the cross section for the reaction

$$q\bar{q} \to \chi_i\widetilde{\chi}_j \qquad (B45)$$

has an additional s-channel contribution which is not present in the pure $q\bar{q} \to \widetilde{\gamma}\widetilde{\gamma}$ cross section. The relevant couplings of the Z^0 boson to the neutral supersymmetric fermions are contained in the interaction Lagrangian

$$\mathcal{L} = -\frac{e}{\sin 2\theta_W} Z^\mu (\bar{\psi}_{H^0}\bar{\sigma}_\mu \psi_{H^0} - \bar{\psi}_{H'^0}\bar{\sigma}_\mu \psi_{H'^0}) . \qquad (B46)$$

When there is gaugino–Higgs-fermion mixing, it is appropriate to calculate the rate for reaction (B45) instead of the cross sections for $\widetilde{\gamma}\widetilde{\gamma}$ and $\widetilde{Z}\widetilde{Z}$ production. The differential cross section is

$$\frac{d\sigma}{dt}(q\bar{q}' \to \widetilde{\chi}_i\widetilde{\chi}_j) = \frac{\pi}{s^2}\left[\frac{\mathcal{A}_s[(t-M_i^2)(t-M_j^2)+(u-M_i^2)(u-M_j^2)]+2\mathcal{A}_s' M_i M_j s}{s^2} + \mathcal{A}_t \frac{(t-M_i^2)(t-M_j^2)}{(t-M_t^2)^2} \right.$$

$$+ \mathcal{A}_u \frac{(u-M_i^2)(u-M_j^2)}{(u-M_u^2)^2} + \frac{\mathcal{A}_{st}(t-M_i^2)(t-M_j^2)+\mathcal{A}_{st}' M_i M_j s}{s(t-M_t^2)}$$

$$\left. + \mathcal{A}_{tu}\frac{M_i M_j s}{(t-M_t^2)^2(u-M_u^2)} + \frac{\mathcal{A}_{su}(u-M_i^2)(u-M_j^2)+\mathcal{A}_{su}' M_i M_j s}{s(u-M_u^2)} \right] , \qquad (B47)$$

where the coefficients $\mathcal{A}_x$ are

$$\mathcal{A}_s = -\mathcal{A}_s' = \delta_{qq'}(c_i c_j - d_i d_j)^2 \frac{\alpha^2(L_q^2 + R_q^2)}{48 x_W^2(1-x_W)^2(1-M_Z^2/s)^2} ,$$

$$\mathcal{A}_t = \mathcal{A}_u = -\frac{1}{2}\mathcal{A}_{tu} = \delta_{qq'}\frac{\alpha^2}{12}(\mathcal{L}_{qi}^2\mathcal{L}_{q'j}^2 + \mathcal{R}_{qi}^2\mathcal{R}_{q'j}^2) , \qquad (B48)$$

$$\mathcal{A}_{st} = -\mathcal{A}_{st}' = \mathcal{A}_{su} = -\mathcal{A}_{su}' = \delta_{qq'}\frac{\alpha^2(d_i d_j - c_i c_j)}{12 x_W(1-x_W)(1-M_Z^2/s)}(L_q\mathcal{L}_{qi}\mathcal{L}_{q'j} - R_q\mathcal{R}_{qi}\mathcal{R}_{q'j}) ,$$

where

$$\mathcal{L}_{qi} = a_i e_q\sqrt{2} + \frac{b_i L_q}{\sqrt{2 x_W(1-x_W)}}, \quad \mathcal{R}_{qi} = a_i e_q\sqrt{2} + \frac{b_i R_q}{\sqrt{2 x_W(1-x_W)}} . \qquad (B49)$$

Our results for $\mathcal{A}_{st}$, $\mathcal{A}_{st}'$, $\mathcal{A}_{su}$, and $\mathcal{A}_{su}'$ disagrees with that of Ref. 69. The total cross section is

$$\sigma(q\bar{q}' \to \widetilde{\chi}_i\widetilde{\chi}_j) = \frac{1}{(1+\delta_{ij})}\frac{\pi}{s^2}\left[\frac{\mathcal{S}}{3s^2}(\mathcal{A}_s[2s^2 - s(M_i^2 + M_j^2) - (M_i^2 - M_j^2)^2] + 6\mathcal{A}_s' M_i M_j s) \right.$$

$$+ \mathcal{A}_t\left[\mathcal{S} + (\Delta_{ti} + \Delta_{tj})\Lambda_t + \frac{\mathcal{S}\Delta_{ti}\Delta_{tj}}{M_t^4 + M_i^2 M_j^2 + M_t^2(s - M_i^2 - M_j^2)}\right]$$

$$+ \mathcal{A}_u\left[\mathcal{S} + (\Delta_{ui} + \Delta_{uj})\Lambda_u + \frac{\mathcal{S}\Delta_{ui}\Delta_{uj}}{M_u^4 + M_i^2 M_j^2 + M_t^2(s - M_i^2 - M_j^2)}\right]$$

$$+ \frac{\mathcal{A}_{st}[\mathcal{S}(M_t^2 - (s + M_i^2 + M_j^2)/2) + \Delta_{ti}\Delta_{tj}\Lambda_t] + \mathcal{A}_{st}' M_i M_j s\Lambda_t}{s}$$

$$+ \frac{\mathcal{A}_{su}[\mathcal{S}(M_u^2 - (s + M_i^2 + M_j^2)/2) + \Delta_{ui}\Delta_{uj}\Lambda_u] + \mathcal{A}_{su}' M_i M_j s\Lambda_u}{s}$$

$$\left. + \mathcal{A}_{tu}M_i M_j s(\Lambda_t + \Lambda_u)/(s + \Delta_{ti} + \Delta_{uj}) \right] . \qquad (B50)$$

To obtain the cross sections for $e^+e^- \to \widetilde{X}_i \widetilde{X}_j$, we merely replace q and q' by e in Eqs. (B48) and (B49), multiply the cross sections by 3 to undo the color average, and identify M_t and M_u as the scalar-electron mass.

We now consider the effects of mixing in both the charged and neutral sectors. The cross sections for the reaction $q\bar{q}' \to \widetilde{\omega}_1^+ \widetilde{X}_j$ are given by (B47) and (B50), with the coefficients $\mathscr{A}_x$ given by

$$\mathscr{A}_s = \frac{\alpha^2(c_+{}^2 + c_-{}^2)}{12x_W} |U_{qq'}|^2 |N_j|^2, \quad \mathscr{A}'_s = \frac{\alpha^2 c_+ c_-}{6x_W} |U_{qq'}|^2 |N_j|^2,$$

$$\mathscr{A}_t = \frac{\alpha^2 c_-{}^2}{12x_W} |V_{q\bar{q}'}|^2 |\mathscr{L}_{q'j}|^2, \quad \mathscr{A}_u = \frac{\alpha^2 c_+{}^2}{12x_W} |V'_{\bar{q}q'}|^2 |\mathscr{L}_{qj}|^2,$$

$$\mathscr{A}_{tu} = -\frac{\alpha^2 c_+ c_-}{6x_W} \mathscr{L}_{qj}\mathscr{L}_{q'j} \mathrm{Re}(V^*_{q\bar{q}'} V'_{\bar{q}q'}), \quad \mathscr{A}_{st} = -\frac{\alpha^2 c_-{}^2}{3x_W\sqrt{2}} N_j \mathscr{L}_{q'j} \mathrm{Re}(U_{qq'} V^*_{q\bar{q}'}), \tag{B51}$$

$$\mathscr{A}'_{st} = -\frac{\alpha^2 c_+ c_-}{3x_W\sqrt{2}} N_j \mathscr{L}_{qj} \mathrm{Re}(U_{qq'} V^*_{q\bar{q}'}), \quad \mathscr{A}_{su} = \frac{\alpha^2 c_+{}^2}{3x_W\sqrt{2}} N_j \mathscr{L}_{qj} \mathrm{Re}(U^*_{qq'} V'_{\bar{q}q'}),$$

$$\mathscr{A}'_{su} = \frac{\alpha^2 c_+ c_-}{3x_W\sqrt{2}} N_j \mathscr{L}_{qj} \mathrm{Re}(U^*_{qq'} V'_{\bar{q}q'}),$$

where

$$N_j = a_j + b_j \left[\frac{1 - x_W}{x_W}\right]^{1/2}. \tag{B52}$$

The coefficients for the reaction $q\bar{q}' \to \widetilde{\omega}_2^+ \widetilde{X}_j$ are obtained from (B51) by the replacement $\cos\theta_\pm \to \sin\theta_\pm$. The coefficients for $\widetilde{\omega}_i^-$ production are obtained by making the substitution $\theta_+ \leftrightarrow \theta_-$ in the corresponding expressions for $\widetilde{\omega}_i^+$.

Finally, we examine the effects of mixing on the process $gq \to \widetilde{X}_i \widetilde{q}$. The coefficients B_x in Eqs. (3.29) and (3.30) become

$$B_s = B_u = -B_{su} = \frac{\alpha_s \alpha}{12x_W}(\mathscr{L}_{qi}{}^2 + \mathscr{R}_{qi}{}^2). \tag{B53}$$

[1]Yu. A. Gol'fand and E. P. Likhtman, Pis'ma Zh. Eksp. Teor. Fiz. **13**, 452 (1971) [JETP Lett. **13**, 323 (1971)]; D. V. Volkov and V. P. Akulov, Phys. Lett. **46B**, 109 (1973); J. Wess and B. Zumino, Nucl. Phys. **B70**, 39 (1974); Phys. Lett. **49B**, 52 (1974); Nucl. Phys. **B78**, 1 (1974); A. Salam and J. Strathdee, *ibid.* **B76**, 477 (1974); **B80**, 499 (1974).

[2]For an early review, see P. Fayet and S. Ferrara, Phys. Rep. **32C**, 249 (1977).

[3]A systematic development is given in J. Wess and J. Bagger, *Supersymmetry and Supergravity* (Princeton University Press, Princeton, New Jersey, 1983).

[4]This point of view is summarized, for example, in P. Fayet, in *Proceedings of the 21st International Conference on High Energy Physics, Paris, 1982*, edited by P. Petiau and M. Porneuf [J. Phys. (Paris) Colloq. 43, C3-673 (1982)].

[5]A fine survey of the quantum theory of gravitation before local supersymmetry appears in M. Veltman, in *Methods in Field Theory*, proceedings of Les Houches Summer School, 1975, edited by R. Balian and J. Zinn-Justin (North-Holland, Amsterdam, 1976; reprinted by World Scientific, Singapore, 1981), p. 265.

[6]S. Ferrara, D. Z. Freedman, and P. van Nieuwenhuizen, Phys. Rev. D **13**, 3214 (1976); S. Deser and B. Zumino, Phys. Lett. **62B**, 335 (1976); D. Z. Freedman and P. van Nieuwenhuizen, Phys. Rev. D **14**, 912 (1976); P. van Nieuwenhuizen, Phys. Rep. **68**, 189 (1981).

[7]S. Weinberg, Phys. Rev. Lett. **50**, 387 (1983); R. Arnowitt, A. H. Chamseddine, and P. Nath, Phys. Rev. Lett. **50**, 232 (1983); Phys. Lett. **129B**, 445 (1983); **132B**, 467 (1983); Nucl. Phys. **B227**, 121 (1983); L. Alvarez-Gaumé, J. Polchinski, and

M. B. Wise, Nucl. Phys. **B221**, 495 (1983); P. Fayet, Phys. Lett. **125B**, 178 (1983); R. M. Barnett, K. S. Lackner, and H. E. Haber, Phys. Rev. Lett. **51**, 176 (1983); Phys. Rev. D **29**, 1381 (1984); B. Grinstein, J. Polchinski, and M. Wise, Phys. Lett. **130B**, 285 (1983); R. Barbieri, N. Cabibbo, L. Maiani, and S. Petrarca, *ibid.* **127B**, 458 (1983); P. Fayet, *ibid.* **133B**, 363 (1983); D. Dicus, S. Nandi, W. Repko, and X. Tata, Phys. Rev. D **29**, 67 (1984).

[8]P. Fayet, Nucl. Phys. **B90**, 104 (1975); A. Salam and J. Strathdee, *ibid.* **B87**, 85 (1975).

[9]These matters are clearly explained in S. Weinberg, Phys. Rev. D **26**, 287 (1982).

[10]Higgs-fermion—gaugino mixing has been considered by J. Ellis and G. Ross, Phys. Lett. **117B**, 397 (1982); J.-M. Frère and G. L. Kane, Nucl. Phys. **B223**, 331 (1983); D. Dicus, S. Nandi, and X. Tata, Phys. Lett. **129B**, 451 (1983).

[11]See, for example, Refs. 2 and 18.

[12]P. Fayet, in *QCD and Lepton Physics*, edited by J. Tran Thanh Van (Editions Frontières, Dreux, France, 1981), p. 347.

[13]M. Dine and W. Fischler, Phys. Lett. **110B**, 227 (1982); L. Ibañez and G. G. Ross, *ibid.* **110B**, 215 (1982); C. Nappi and B. Ovrut, *ibid.* **113B**, 175 (1982).

[14]L. Hall, J. Lykken, and S. Weinberg, Phys. Rev. D **27**, 2359 (1983); L. Alvarez-Gaumé, J. Polchinski, and M. B. Wise, Nucl. Phys. **B221**, 495 (1983).

[15]S. S. Gershtein and Ya. B. Zeldovich, Pis'ma Zh. Eksp. Teor. Fiz. **4**, 174 (1966) [JETP Lett. **4**, 120 (1966)]; R. Cowsik and J. McClelland, Phys. Rev. Lett. **29**, 669 (1972).

[16]K. Freese and D. Schramm [Nucl. Phys. **B233**, 167 (1984)] review general cosmological constraints on weakly interacting

stable particles.

[17]H. Goldberg, Phys. Rev. Lett. **50**, 1419 (1983). The general strategy for dealing with heavy neutrinos was developed by B. W. Lee and S. Weinberg, Phys. Rev. Lett. **39**, 165 (1977).

[18]N. Cabibbo, G. Farrar, and L. Maiani, Phys. Lett. **105B**, 155 (1981).

[19]A convenient summary has been given by S. Yamada, in *Proceedings of the 1983 International Symposium on Lepton and Photon Interactions at High Energies, Ithaca, New York,* edited by D. G. Cassel and D. L. Kreinick (Newman Laboratory of Nuclear Studies, Cornell University, Ithaca, 1984), p. 525. See also H. Haber and G. L. Kane, Michigan Report No. UM HE TH 83-17 (unpublished).

[20]We thank George Snow for suggesting this possibility to us.

[21]H. J. Behrend *et al.* (CELLO Collobration) [Phys. Lett. **123B**, 127 (1983)], W. Bartel *et al.* (JADE Collaboration) [*ibid.* **139B**, 327 (1984)], and M. Althoff *et al.* (TASSO Collaboration) [DESY Report No. 84-072 (unpublished)] have studied high-energy e^+e^- collisions at PETRA.

[22]P. Fayet, Phys. Lett. **117B**, 460 (1982).

[23]P. Fayet, Phys. Lett. **84B**, 421 (1979).

[24]M. Fukugita and N. Sakai, Phys. Lett. **114B**, 23 (1982).

[25]J. Ellis and K. Olive, Nucl. Phys. **B223**, 252 (1983).

[26]A. Bouquet and C. E. Vayonakis, Phys. Lett. **116B**, 219 (1982).

[27]A similar bound, derived by S. Dimopoulos and M. Turner, in *The Birth of the Universe,* proceedings of the 2nd Moriond Astrophysics Meeting, Les Arcs, France, 1982, edited by J. Audouze and J. Tran Thanh Van (Editions Frontières, Gif-sur-Yvette, France, 1982), p. 113, from constraints on stellar energy loss through the process $\gamma e \rightarrow e \, \tilde{g} \, \tilde{g}$, would seem to be independent of the photino mass. However, the rate calculation overlooks a strong suppression due to the low-energy decoupling theorem discussed by W. A. Bardeen [report, 1974 (unpublished)] and B. de Wit and D. Z. Freedman [Phys. Rev. Lett. **35**, 827 (1975)].

[28]H. Pagels and J. Primack, Phys. Rev. Lett. **48**, 223 (1982).

[29]S. Deser and B. Zumino, Phys. Rev. Lett. **38**, 1433 (1977).

[30]S. Weinberg, Phys. Rev. Lett. **48**, 1303 (1982).

[31]G. Farrar and P. Fayet, Phys. Lett. **76B**, 575 (1978).

[32]M. Chanowitz and S. Sharpe, Phys. Lett. **126B**, 225 (1983).

[33]B. Alper *et al.*, Phys. Lett. **46B**, 265 (1973); D. Cutts *et al.*, Phys. Rev. Lett. **41**, 363 (1978).

[34]R. Gustafson *et al.*, Phys. Rev. Lett. **37**, 474 (1976).

[35]R. C. Ball *et al.*, Phys. Rev. Lett. **53**, 1314 (1984).

[36]F. Bergsma *et al.* (CHARM Collaboration), Phys. Lett. **121B**, 429 (1983).

[37]G. L. Kane and J. Leveille, Phys. Lett. **112B**, 227 (1982).

[38]G. Farrar and P. Fayet, Phys. Lett. **79B**, 442 (1978).

[39]P. Fayet, Phys. Lett. **86B**, 272 (1979).

[40]This possibility has also been noted by Chanowitz and Sharpe (Ref. 32).

[41]W. Bartel *et al.*, Phys. Lett. **123B**, 353 (1983).

[42]B. Adeva *et al.* (Mark J Collaboration), Phys. Rev. Lett. **53**, 1806 (1984).

[43]W. Bartel *et al.* (JADE Collaboration), Phys. Lett. **146B**, 126 (1984).

[44]W. Bartel *et al.*, Z. Phys. C **6**, 295 (1980).

[45]A. Marini *et al.*, Phys. Rev. Lett. **48**, 1649 (1982); M. C. Ross *et al.*, Phys. Lett. **118B**, 199 (1982).

[46]Preliminary results of the JADE Collaboration, presented by H. Takada at the International Eur021physics Conference on High Energy Physics, Brighton, 1983 (unpublished).

[47]C. Nappi, Phys. Rev. D **25**, 84 (1982).

[48]F. A. Heile *et al.*, Nucl. Phys. **B138**, 189 (1978).

[49]H. J. Behrend *et al.*, Phys. Lett. **114B**, 287 (1982); B. Adeva *et al.*, *ibid.* **115B**, 345 (1982); R. Brandelik *et al.*, *ibid.* **117B**, 345 (1982).

[50]E. Fernandez *et al.*, Phys. Rev. Lett. **52**, 22 (1984).

[51]M. K. Gaillard, L. Hall, and I. Hinchliffe, Phys. Lett. **116B**, 279 (1982).

[52]L. Gladney *et al.*, Phys. Rev. Lett. **51**, 2253 (1983).

[53]J. D. Bjorken and S. D. Drell, *Relativistic Quantum Mechanics* (McGraw-Hill, New York, 1964); *Relativistic Quantum Fields* (McGraw-Hill, New York, 1965).

[54]G. Farrar and S. Weinberg, Phys. Rev. D **27**, 2732 (1983).

[55]I. Hinchliffe and L. Littenberg, in *Proceedings of the 1982 DPF Summer Study on Elementary Particle Physics and Future Facilities, Snowmass, Colorado,* edited by R. Donaldson, R. Gustafson, and F. Paige (Fermilab, Batavia, Illinois, 1982), p. 242.

[56]P. R. Harrison and C. H. Llewellyn-Smith, Nucl. Phys. **B213**, 223 (1983); **B223**, 542E (1983).

[57]V. Barger, R. Robinett, W. Keung, and R. Phillips, Phys. Lett. **131B**, 375 (1983); Phys. Rev. D **28**, 2912 (1983).

[58]I. Antoniadis, L. Baulieu, and F. Delduc, Z. Phys. C **23**, 119 (1984).

[59]J. A. Grifols and A. Mendez, Phys. Rev. D **26**, 324 (1982).

[60]R. P. Feynman, *Photon-Hardon Interactions* (Benjamin, Reading, Mass., 1972).

[61]S. M. Berman, J. D. Bjorken, and J. B. Kogut, Phys. Rev. D **4**, 3388 (1971).

[62]E. Eichten, I. Hinchliffe, K. Lane, and C. Quigg, Rev. Mod. Phys. **56**, 579 (1984).

[63]G. Altarelli and G. Parisi, Nucl. Phys. **B126**, 298 (1977).

[64]S. H. Aronson, L. S. Littenberg, F. E. Paige, I. Stumer, and D. P. Weygand, in *Proceedings of the 1982 DPF Summer Study on Elementary Particle Physics and Future Facilities, Snowmass, Colorado* (Ref. 55), p. 505; A. Savoy-Navarro, Phys. Rep. **105**, 91 (1984).

[65]J. Ellis, J. S. Hagelin, D. V. Nanopoulos, and M. Srednicki, Phys. Lett. **127B**, 233 (1983); R. Barnett, H. Haber, and K. Lackner, *ibid.* **126B**, 64 (1983); H. Haber and G. L. Kane, Nucl. Phys. **B232**, 333 (1984).

[66]M. Claudson, L. Hall, and I. Hinchliffe, Nucl. Phys. **B228**, 501 (1983).

[67]V. Barger, K. Hagiwara, W.-Y. Keung, and J. Woodside, Phys. Rev. Lett. **53**, 641 (1984); Phys. Rev. D **31**, 528 (1985); V. Barger, K. Hagiwara, and W.-Y. Keung, Phys. Lett. **145B**, 147 (1984); J. Ellis and H. Kowalski, *ibid.* **142B**, 441 (1984); Nucl. Phys. **B246**, 189 (1984); J. Ellis and M. Sher, CERN Report No. TH. 3968/84 (unpublished); H. Haber and G. L. Kane, Phys. Lett. **142B**, 212 (1984); L. J. Hall and M. Suzuki, Nucl. Phys. **B231**, 419 (1984); P. G. Ratcliffe, Cavendish Laboratory Report No. HEP 84/4 (unpublished); E. Reya and D. P. Roy, Phys. Lett. **141B**, 442 (1984); Phys. Rev. Lett. **53**, 881 (1984).

[68]P. Bagnaia *et al.*, Phys. Lett. **139B**, 105 (1984); G. Arnison *et al.*, *ibid.* **139B**, 115 (1984).

[69]These questions have been addressed by J. Ellis, J.-M. Frère, J. S. Hagelin, G. L. Kane, and S. T. Petcov, Phys. Lett. **132B**, 436 (1983).

[70]J. Ellis and J. S. Hagelin, Phys. Lett. **122B**, 303 (1982).

[71]D. A. Dicus, S. Nandi, W. W. Repko, and X. Tata, Phys. Rev. Lett. **51**, 1030 (1983).

[72]G. Farrar and P. Fayet, Phys. Lett. **89B**, 191 (1980); Ellis *et al.* (Ref. 69).

[73]M. Glück and E. Reya, Phys. Lett. **130B**, 423 (1983).